

**VARICELLA-ZOSTER VIRUS ORF66 KINASE:
REVEALING CRITICAL CELL-SPECIFIC ROLES OF THE KINASE AND ITS
TARGETING OF THE NUCLEAR MATRIX PROTEIN, MATRIN 3**

by

Angela Erazo

B.S., Biology, Brooklyn College of the City University of New York, 2002

Submitted to the Graduate Faculty of
School of Medicine in partial fulfillment
of the requirements for the degree of
Doctor of Philosophy

University of Pittsburgh

2010

UNIVERSITY OF PITTSBURGH

SCHOOL OF MEDICINE

This dissertation was presented

by

Angela Erazo

It was defended on

May 26, 2010

and approved by

Donald B. DeFranco, Ph.D.

Professor, Department of Pharmacology and Chemical Biology

Frederick L. Homa, Ph.D.

Associate Professor, Department of Microbiology and Molecular Genetics

Thomas E. Smithgall, Ph.D.

Professor, Department of Microbiology and Molecular Genetics

Ora A. Weisz, Ph.D.

Professor, Departments of Medicine and Cell Biology and Physiology

Paul R. Kinchington, Ph.D.

Professor, Departments of Ophthalmology and Microbiology and Molecular Genetics

Copyright permission was granted for the use of parts of the following publications:

Erazo, A., M.B. Yee, N. Osterrieder, and P.R. Kinchington. 2008. Varicella-zoster virus open reading frame 66 protein kinase is required for efficient viral growth in primary human corneal stromal fibroblast cells. *J. Virol* 82: 7653-65

and

Erazo, A. and P.R. Kinchington. 2010. Varicella-Zoster Virus open reading frame 66 protein kinase and its relationship to alphaherpesvirus US3 kinases. *Curr Top Microbiol Immunol. In Press.*

**VARICELLA-ZOSTER VIRUS ORF66 KINASE:
REVEALING CRITICAL CELL-SPECIFIC ROLES OF THE KINASE AND ITS
TARGETING OF THE NUCLEAR MATRIX PROTEIN, MATRIN 3**

Angela Erazo, Ph.D

University of Pittsburgh, 2010

Varicella-Zoster Virus (VZV) is the causative agent of chickenpox during primary infection and herpes-zoster or shingles following reactivation from neuronal latency. The VZV ORF66 protein kinase is a serine/threonine kinase and one of two VZV protein kinases. Its homologue in the alphaherpesviruses are termed the US3 kinases, and through phosphorylation of targets affect many events in infection, influencing processes such as survival of the infected cell to apoptosis, the state of permissivity to gene expression, avoidance of immunity, modulating cellular pathways affecting host actin dynamics, and influencing the nuclear structure and nuclear membrane to enable assembly of virus components. ORF66 is not essential in most cell culture but important for viral replication in T cells. In this work, we have found the ORF66 is critical for viral growth in primary corneal fibroblasts and thus established a model for further investigation of cell-type dependent functions for ORF66. This finding may have important applications for viral pathogenesis as VZV reactivates and causes infection of the eye in herpes zoster ophthalmicus disease. Here we also describe a novel ORF66 cellular target, the nuclear matrix protein, matrin 3. Specific matrin 3 phosphorylation is conserved for herpes simplex virus - type 1 and pseudorabies virus US3 kinases. Thus, this finding may have important implications for the role of ORF66/US3 function in common alphaherpesvirus strategies to utilize host cell machinery in establishing a host cell environment conducive to viral replication. ORF66/US3-induced phosphorylation of matrin 3 was needed for matrin nuclear retainment late

in viral infection, suggesting that ORF66/US3 may have a role in modulating matrix 3 nuclear functions needed for viral replication. The ORF66 kinase is clearly important for VZV growth in certain cell types relevant to human disease and our studies underscore the diverse roles of this protein in VZV infection.

TABLE OF CONTENTS

PREFACE.....	XIII
1.0 INTRODUCTION.....	1
1.1 VARICELLA-ZOSTER VIRUS DISEASE	1
1.1.1 Clinical Presentation & Complications.....	1
1.1.2 Prevention & Treatment Strategies: Impact on VZV Epidemiology.....	3
1.2 VZV VIROLOGY.....	5
1.2.1 Classification	5
1.2.2 Physical & Molecular Properties.....	8
1.2.3 VZV Life cycle.....	11
1.3 VZV TROPISM & PATHOGENESIS	17
1.4 VZV ORF66 KINASE	19
1.4.1 Introduction.....	19
1.4.2 Genetics.....	20
1.4.3 ORF66 Structure & Characteristics	21
1.4.4 ORF66 targets	26
1.4.4.1 Autophosphorylation.....	26
1.4.4.2 IE62	27
1.4.4.3 HDACS	29

1.4.5	Additional cellular activities modulated by the ORF66 protein kinase.	31
1.4.5.1	MHC-1 surface presentation	31
1.4.5.2	IFN Signaling	33
1.4.5.3	Apoptosis	33
1.4.6	Alphaherpesvirus US3 kinase studies that guide the search for roles of ORF66	34
1.4.6.1	US3 Kinases and Inhibition of Apoptosis	34
1.4.6.2	US3 Modulation of HDAC	35
1.4.6.3	Nucleocapsid Egress	36
1.4.6.4	Alteration of the host cytoskeleton	38
1.4.6.5	Concluding Remarks	39
1.5	STATEMENT OF GOALS.....	41
2.0	VARICELLA-ZOSTER VIRUS ORF66 PROTEIN KINASE IS REQUIRED FOR EFFICIENT VIRAL GROWTH IN PRIMARY HUMAN CORNEAL FIBROBLASTS.....	43
2.1	ABSTRACT.....	44
2.2	INTRODUCTION	45
2.3	MATERIALS & METHODS	48
2.3.1	Cells.....	48
2.3.2	VZV and derivation of rVZV.....	49
2.3.3	Antibodies & Immunological Procedures.....	51
2.3.4	Analaysis of viral growth.....	52
2.3.5	Virion purification and characterization.....	53

2.3.6	Apoptosis Assay.....	54
2.4	RESULTS	54
2.4.1	ORF66 is required for efficient growth in PCF cells.....	54
2.4.2	Derivation of VZV expressing IE62 protein mutated at the critical ORF66 phosphorylation site.	59
2.4.3	VZV.IE62(S686A) ² IE62 remains nuclear in the presence of functional ORF66. 62	
2.4.4	Tegument proteins of VZV.IE62(S686A) ²	64
2.4.5	Growth comparisons of VZV.IE62(S686A) ² and rVZV lacking functional ORF66 in PCF cells	67
2.4.6	Detection of apoptosis levels in recombinant VZV-infected corneal fibroblasts	68
2.5	DISCUSSION.....	71
3.0	THE ALPHAHERPESVIRUS ORF66/US3 KINASES DIRECT SPECIFIC PHOSPHORYLATION OF THE NUCLEAR MATRIX PROTEIN, MATRIN 3	77
3.1	ABSTRACT.....	78
3.2	INTRODUCTION	79
3.3	MATERIALS & METHODS	83
3.3.1	Cell culture	83
3.3.2	Viruses.....	83
3.3.3	Protein identification by MALDI TOF	86
3.3.4	Plasmid construction	87
3.3.5	Drug treatments	88

3.3.6	Transfections & Infections	89
3.3.7	Antibodies & Immunological Procedures.....	89
3.3.8	Immunoblot analysis & Immunoprecipitation.....	91
3.3.9	GST fusion protein purification & <i>In vitro</i> kinase assay.....	92
3.4	RESULTS	93
3.4.1	PKA-substrate profiles show drastic differences between VZV, HSV, &PRV	93
3.4.2	The 125 kDa protein represents a host cell target	96
3.4.3	Matrin 3 is a conserved phosphorylation target for the alphaherpesvirus ORF66/US3 kinases.....	97
3.4.4	Identification of matrin 3 target residues for the ORF66/US3 kinases	101
3.4.5	ORF66-induced matrin 3 phosphorylation is through a non-PKA dependent pathway	104
3.4.6	Matrin 3 localization in VZV-infected cells.....	109
3.4.7	Matrin 3 efficient nuclear retention is dependent on US3 kinase expression.....	111
3.5	DISCUSSION.....	113
4.0	FUTURE DIRECTIONS & GENERAL SUMMARY	122
	APPENDIX.....	135
	REFERENCES.....	136

LIST OF TABLES

Table 1. Human Herpesviruses	7
Table 2. Mammalian alphaherpesviruses.....	8
Table 3. <i>In vivo</i> and <i>in vitro</i> protein substrates of the ORF66/US3 kinases	40

LIST OF FIGURES

Figure 1-1. VZV genome.....	9
Figure 1-2. VZV ORF66 kinase putative catalytic subdomains.....	23
Figure 1-3. Alphaherpesvirus ORF66/US3 putative catalytic subdomains.....	24
Figure 2-1. IE62 cellular distribution and GFP expression in VZV-infected cells.....	57
Figure 2-2. Progeny virus growth curves reveal a requirement for ORF66 for VZV growth in PCFs.....	58
Figure 2-3. DNA characterization of BAC DNA and of VZV-infected cell of the recombinants VZV.71.S686A and VZV.IE62(S686A) ²	61
Figure 2-4. IE62 localizes to the nucleus in VZV.IE62(S686A) ² - infected cells.....	63
Figure 2-5. VZV.IE62(S686A) ² does not incorporate IE62 into the virion tegument.....	66
Figure 2-6. Progeny growth curves of VZV.IE62(S686A) ² , VZV-66, and ORF66 mutants in PCFs.....	68
Figure 2-7. Apoptosis in PCF and MRC-5 cells infected with VZV and kinase negative mutants.....	70
Figure 3-1. Conserved ORF66/US3-dependent phosphorylation of a 125kDa protein by alphaherpesviruses displaying different PKA-substrate profiles.....	95
Figure 3-2. The 125 kDa 66-specific PKA-substrate is a host cell protein.....	97

Figure 3-3. VZV ORF66 kinase activity induces specific matrin 3 phosphorylation	100
Figure 3-4. Matrin 3 is a conserved phosphorylation target for the US3 kinases during infection	101
Figure 3-5. Matrin 3 a.a. T150 is the major phosphorylation site for VZV ORF66 and HSV-1 US3 kinase	103
Figure 3-6. The 125kDa PKA-substrate protein is phosphorylated through a non-PKA pathway	107
Figure 3-7. ORF66 does not target matrin 3 under the conditions required for IE62.....	108
Figure 3-8. VZV infection leads to subtle differences in matrin 3 cellular localization	110
Figure 3-9. HSV-1 and PRV US3 kinase expression leads to matrin 3 nuclear retention or shuttling to the nucleus during infection.....	112
Figure 4-1. List of candidate VZV ORF66 targets	126
Figure 4-2. VZV ORF66 targets ORF 4 & ORF9 <i>in vitro</i>	127
Figure 4-3. VZV ORF66 kinase activity induces actin rearrangement in infected cells.....	129
Figure 4-4. VZV ORF66 kinase activity induces greater phosphorylation of nuclear PKA-substrate proteins.	131
Figure 4-5. GST66 is detected by PKA-substrate antibody.....	132

PREFACE

I have many people to thank for having reached this point in my education. First, I would like to thank my thesis advisor, Dr. Paul Kip Kinchington. I am very fortunate to have had him as my mentor; his guidance, flexibility, good nature, and enthusiasm for science has played a large part in my growth as a scientist that I did not know I was capable of. I also thank my past mentors, whom have provided key lessons that I will continue to use as I develop in my career. I sincerely thank my committee members Dr. Homa, Dr. Smithgall, Dr. Weisz, & Dr. Defranco for their support, & recommendations throughout the years. I also thank members of the Kinchington lab – Amie Eisfeld, Srividya Ramachandran, Michael Yee, and JP Vergnes for their friendship and assistance. You have been wonderful people to work with & I will miss you very much. Last, but very importantly, I would like to thank my family - especially my mother & father. I am very lucky to have been raised by them and their model of incredible work ethic. My father has always been proud of me & taught me the importance of reading very early on. My mother, whom I can only aspire to become a person of her character, thank you for loving me so much and never hesitating to listen to me & support me. Thanks to my sisters, Kathy & Vanessa for their support and for keeping my life interesting. I am grateful for my niece Sarah who doesn't know yet how important she is, and for being my ray of sunshine on the best and worst of days, & my grandmother Clotilde for her love and for starting everything.

1.0 INTRODUCTION

1.1 VARICELLA-ZOSTER VIRUS DISEASE

1.1.1 Clinical Presentation & Complications

Varicella-Zoster Virus (VZV) is the causative agent of chickenpox during primary infection and herpes-zoster or shingles following reactivation. VZV is a highly communicable agent, spread through respiratory aerosols or direct contact with vesicular lesions (140). In healthy children, the virus typically is a benign disease, affecting those between 1-9 years of age. VZV in adults is often a more severe disease including complications such as interstitial pneumonia (140). Following an incubation period of 14-15 days, symptoms first appear as fever, headache, and general malaise concurrent with an itchy rash that progresses from a macular rash to a vesicular lesion that eventually crusts over 1-2 weeks later (67, 140). In immunocompromised patients (e.g. bone marrow, liver, or renal transplant patients) varicella infection is more likely to cause severe disseminated disease (67). The virus then undergoes latency within neurons of the cranial nerve ganglia & dorsal root ganglia - potentially along any level of the neuraxis (140). Complications associated with chickenpox are serious bacterial infections (40) as well as central nervous system complications such as cerebellar ataxia, meningitis, and meningoencephalitis. Importantly, VZV can also lead to vasculopathies which can present as a stroke. Furthermore,

untreated vasculopathies which result from productive VZV replication in small and/or large cerebral arteries can lead to mortality in 25% of untreated patients (140).

VZV then enters sensory nerve fibers innervating the skin and travels retrogradely up the nerve to sensory ganglia to undergo neuronal latency usually for decades in its host, and reactivates in the form of herpes zoster (“shingles”). During reactivation, the virus travels in an anteretrograde direction from the sensory ganglia to the nerves of the skin leading to a localized dermatomal rash. Zoster symptoms are characterized by unilateral radicular pain, itching, numbness, or hypersensitivity to touch (allodynia). Days later a vesicular rash develops in the area (usually 1-3 dermatomes) and persists for 7-10 days, followed crusting of lesions which usually heal within 4 weeks of rash onset (140, 153). Zoster is also infectious till the point where the lesion is crusted over. Systematic dissemination can occur in immunocompromised patients (e.g. hematologic malignancy or iatrogenic immunosuppression), leading to multidermatomal involvement (140).

Zoster has the potential to be a serious, morbid, debilitating disease. Zoster incidence & severity increases with advancing age and/or immunosuppression. A serious neurological complication of herpes zoster (HZ) is postherpetic neuralgia (PHN) which affects 10-30 % of zoster patients (214) and can range from mild to excruciating pain. PHN is characterized by constant severe stabbing or burning pain, as well as allodynia in a majority of affected patients (153) that persists for 3 months and potentially years after resolution of rash. Thoracic zoster is the most common form followed by ophthalmic zoster which follows VZV reactivation from the trigeminal ganglia. Other rare complications have been reported including VZV myelitis which can be fatal in immunocompromised patients such as AIDS patients, VZV vasculopathy, and zoster sin herpete (reactivation without rash) (63, 140).

Herpes zoster ophthalmicus (HZO) occurs when reactivation occurs from the ophthalmic (V-1) division of the trigeminal nerve, which is affected approximately 20 times more often than other divisions of the TG (156). Keratitis most often occurs in HZO patients, potentially leading to blindness if untreated. An indicator of involvement of the eye during reactivation is *Hutchinson's sign*, where rash develops on the tip of the nose. Other ophthalmic complications include VZV acute retinal necrosis and progressive outer retinal necrosis, which is the second most common opportunistic retinal infection in AIDS patients in North America (140).

1.1.2 Prevention & Treatment Strategies: Impact on VZV Epidemiology

Treatment for varicella infection depends on stage of infection, patients' age and immune status. Chickenpox is usually a mild disease in children and there is usually no specific therapy required. Antiviral agents used for the treatment of VZV infections are nucleoside analogues that require phosphorylation by a viral thymidine kinase (TK) that act as viral DNA synthesis inhibitors, such as acyclovir (ACV) and related drugs exhibiting higher bioavailability. In cases where varicella symptoms are more serious, ACV is suggested 24h following appearance of skin lesions, while intravenous ACV is effective in immunosuppressed patients even 72 hrs after appearance of lesions. Foscarnet, also a viral DNA synthesis inhibitor, acts independently of TK and can be used in cases of ACV-resistant VZV (145).

The aim of treatment for shingles is to reduce the acute symptoms of pain and limit spread and duration of lesions, as well as prevent complications like PHN and HZO. In shingles patients over the age of 50 or immunosuppressed patients, antiviral therapy (ACV, valacyclovir, famciclovir) must be quickly started within 72 hrs after onset of skin lesions. Treatments for PHN are varied and rarely lead to complete pain relief. Recommendations depend on harshness

of pain, patient mental status and preference. Treatments include topical analgesics, anticonvulsants (e.g. gabapentin), tricyclic antidepressants (e.g. amitriptyline), opioids, and other treatments (e.g. N-methyl-D aspartate receptor antagonists, intrathecal corticosteroid injection, spinal stimulation and surgical removal of the painful skin area) whose efficacy are questionable (145).

Fortunately, a varicella vaccine and zoster vaccine are available & aimed to prevent disease and/or severity of disease. Before introduction of the VZV vaccine, virtually every child in the US was afflicted with chickenpox usually between the 1 and 9 years of age. Varicella infection was responsible for on average, 10,632 hospitalizations and 105 deaths per year (125). In 1995, a live attenuated Oka/Merck VZV vaccine (Varivax, Merck) was approved in the US as part of universal childhood varicella vaccination program (117). The vaccine is safe, effective, and has high acceptance rates, reported to prevent varicella of any severity by 80-85%, hospitalizations by 75-88%, and deaths by 74% (125). Approximately 2-3% of children and 30-40% of adults experienced breakthrough varicella - infection after exposure to wild type VZV in a vaccinee. Consequently, in 2006 a two-dose vaccine regimen was adopted (117).

The lifetime risk for having HZ is 30%, or approximately one million cases per year in the US (117). In 2006, a new live attenuated VZV zoster vaccine (Zostavax, Merck & Co became available as a result of the US Shingles Prevention Study (154). The aim of the vaccine was to boost VZV cell-mediated immunity (CMI) which according to the Hope-Simpson model, maintains protection from HZ. The vaccine was found to reduced the burden of illness from HZ by 61.1% and reduce incidence of HZ and PHN by 51.3% and 66.5% respectively (117, 154). Currently it is recommended for people over the age of 60, including those who already have had an episode of zoster or have chronic medical conditions. It is not yet recommended for

immunosuppressed patients, children, & pregnant women (117) as safety & effectiveness are unknown. Furthermore, risk-benefit ratio is unknown for moderately immunosuppressed patients. Hence, there are still concerns with the effects of VZV vaccinations. Duration of protection by the varicella vaccine is also unknown. Additionally, because the VZV vaccine is so effective, it is hypothesized that the general population is not receiving VZV CMI “boosters” stemming from exposure to WT VZV. This may result in an increase of HZ in those under 50 yrs of age (117).

1.2 VZV VIROLOGY

1.2.1 Classification

VZV is a member of the family *Herpesviridae* which divides into three subfamilies, the alpha-, beta-, and gamma- herpesviruses. VZV is an alphaherpesvirus and one of eight human herpesviruses which span all three subfamilies (Table 1). While some herpesviruses have a broad host range, most display a high degree of host specificity which has aided in their ability to coevolve with their host. It is thought that herpesviruses infected an ancient host progenitor and subsequent viruses underwent cospeciation within their host. Estimates indicate that the three subfamilies diverged 180 to 220 million years ago, yet still there are 43 genes common to the subfamilies. A fundamental biological feature of herpesviruses is their ability to establish inapparent lifelong latent infection which can reactivate once or multiple times to cause and transmit disease (43, 57). Characteristics of most herpesviruses also include viral replication and

capsid assembly occurring in the nucleus, and expression of a large number of proteins involved in nucleic acid metabolism (e.g. thymidine kinase), DNA replication (e.g. DNA polymerase, helicase/primase), and protein modification (e.g. kinases).

The α herpesviruses are characterized as neurotrophic during their latency stage, & exhibit a short replication cycle (~18hrs), efficient cell destruction & variable host range *in vitro* and *in vivo* (135). In contrast to HSV-1, VZV is highly host-restricted in cell culture yet displays broad tissue tropism in humans for reasons unknown (135). Mammalian α herpesviruses are further subdivided into the genera Simplexvirus (α_1 -herpesviruses) & Varicellovirus (α_2 -herpesviruses) (Table 2) (135). The simplexviruses have primates as their natural hosts, yet the varicelloviruses infect a variety of mammals. Members of two other lineages in the α herpesviruses are Marek's disease virus (MDV) and infectious laryngotracheitis virus, both avian viruses (43).

Table 1. Human Herpesviruses

<i>Human Herpesvirus</i>	<i>Synonym</i>	<i>Subfamily</i>	<i>Latency</i>	<i>Disease</i>
HHV-1	Herpes simplex virus type 1	α	Neuron	facial & labial lesions, HSK
HHV-2	Herpes simplex virus type 2	α	Neuron	genital lesions
HHV-3	Varicella-Zoster Virus	α	Neuron	chickenpox & shingles
HHV-5	Human cytomegalovirus	β	Monocytes, lymphocytes & others	birth defects, retinitis, pneumonia
HHV-6	HHV-6	β	T lymphocytes & others	childhood roseola
HHV-7	HHV-7	β	T lymphocytes & others	childhood roseola
HHV-4	Esptein-Barr virus	γ	B lymphocytes	Burkitt's lymphoma, nasal pharyngeal carcinoma, infectious mononucleosis
HHV-8	Kaposi's Sarcoma- Associated herpesvirus	γ	Unknown	Kaposi's Sarcoma, primary effusion lymphoma, multicentric Castleman disease

Table 2. Examples of mammalian alphaherpesviruses

Lineage	Virus	Natural Host	Disease in natural host
$\alpha 1$	HSV-1	Humans	Generally asymptomatic
	HSV-2	Humans	Generally asymptomatic
	B virus	Macaques	Generally asymptomatic
	SA8	Baboons	Generally asymptomatic
$\alpha 2$	VZV	Humans	Varicella/Herpes zoster
	SVV	Old world monkeys	Varicella-like disease
	EHV-1	Horses	Abortion
	EHV-4	Horses	Rhinopneumonitis
	BHV-1	Cattle	Rhinotracheitis/vulvovaginitis
	BHV-5	Cattle	Meningoencephalitis
	PRV	Pigs	Aujeszky's disease

1.2.2 Physical & Molecular Properties

Morphologically, the VZV virion is indistinguishable from HSV (prototypic α herpesvirus). The virion is 150-200-nm in diameter and is pleiomorphic. VZV is a linear double-stranded DNA virus that is encapsidated by an icosohedral nucleocapsid which consists of 162 capsomeres. Capsids, in turn, are surrounded by a proteinaceous tegument layer and cell-derived lipid envelope. The VZV genome is approximately 125 kbp nucleotides in length (44), and is closely homologous to HSV-1, with an overall genome structure that is similar to other alphaherpesvirus (α herpesvirus) members. Specifically, the VZV genome consists of a covalently linked unique long (U_L) and unique short (U_S) regions bounded by inverted repeat sequences IR_L/TR_L and

IR_S/TR_S. The U_L is 104,836bp long and flanked by 88bp inverted repeats, while the U_S is 5232bp long flanked by 7320 bp inverted repeats (Figure 1-1).



Figure 1-1. VZV genome

The VZV genome consists of 125 kbp double-stranded DNA, made up of a U_L and U_S region (shown as black bars), bounded by internal and terminal repeats (TR_L and IR_L – red, IR_S and TR_S – yellow). ORF62 location is depicted within the IR_S and TR_S regions. ORF66 location within the unique short region (U_S) is indicated by the black arrow.

The VZV genome contains two origins of replication, Ori_s sites, in the IR_S/TR_S region. Concatameric DNA contains one cleavage site as typical of some α2 viruses - as opposed to two sites in the α1 (HSV), thus leading to one cleavage site per VZV genome length. The U_S region is directed in one of two directions 50% of the time, and the U_L region exists in one direction 95% of the time and 5% in the opposite direction, therefore two VZV genomic isomers predominate (177). The genome encodes 71 predicted open reading frames (ORF), and at least 68 unique VZV genes. Five of these genes (ORFs 1, 2, 13, 32, 57) have no HSV homolog, yet some are found in EHV-1. ORFs 62, 63, and 64 are found within the IR_S region, and are duplicated as ORFs 71, 70, and 69, respectively, in the opposite direction within the TR_S region.

ORF42 and ORF45 are the only two known splicing products from the same 5.7kbp primary transcript.

The tegument layer connects the nucleocapsid and lipid envelope and holds a cargo of several VZV proteins, including ORFs 4, 9, 10, 47, 62, and 63 (54, 97, 100, 200). There is also evidence for cellular proteins CDK1 & cyclin B1 in the VZV tegument (112), which is not unprecedented as cellular proteins in the tegument have been reported for other herpesviruses (6, 47). Mostly through studies in HSV & PRV, functions attributed to the tegument include targeting the virion to and from the nucleus during entry and egress, recruiting of molecular motors utilized in virion transport, regulation of cell & viral gene and protein expression, and directing virion assembly during egress (91).

Lastly like other fusogenic viruses, herpesviruses encode for an array of glycoproteins involved in the fusion process. VZV encodes for eight envelope proteins that are glycosylated: gB, gC, gE, gH, gI, gK, gL, and gM (96, 224). It is unknown if gN is glycosylated. All of these are conserved in HSV-1 in the U_L region, yet VZV lacks many glycoproteins found in the HSV-1 U_S region. Notably, VZV does not encode a gD homolog which is essential for HSV-1 replication (135). Five glycoproteins are conserved amongst all herpesviruses gB, gH, gL, gM, and gN suggesting that they provide critical functions for their respective viruses. Consequently, in transient expression systems, a minimum combination of VZV gH and gL or gB and gE are required for cell-cell fusion (39). Additionally, gE is conserved in all α herpesviruses, yet is only essential for VZV replication and important for cell-cell spread and fusion (39, 122, 124). VZV is highly cell-associated *in vitro*, and unlike HSV and PRV, VZV does not spontaneously release infectious virions from cultured cells (215). Differences in use of glycoproteins during viral fusion, the fact that VZV causes syncytia within vesicles of infected skin, and its cell-associated

nature *in vitro* suggests that the VZV envelope machinery is more geared to accommodate cell-cell fusion than HSV.

1.2.3 VZV Life cycle

Entry. The mechanism for VZV entry is not well understood but advances in our understanding of VZV receptors have been made in recent years. In HSV, four cellular proteins - Herpesvirus entry mediator A, nectin-1, nectin-2, and 3-O-sulfated heparan sulfate, are established receptors involved in entry. This does not directly translate to VZV as these receptors all have been found to interact with HSV gD, of which there is no VZV homologue (29, 134). However, similarly to other herpesviruses, heparan sulfate proteoglycan is involved in the initial attachment of VZV virions (232). Thus far, two host cell receptors have been implicated in mediating VZV entry. Cation-independent mannose 6-phosphate receptors (MPR^{ci}) receptors have been implicated in cell-free but not cell-associated VZV entry spread, since MPR^{ci} – deficient cells do not restrict entry of cell-associated VZV. Four viral glycoproteins (gB, gE, gH, and gI) contain N-linked oligosaccharides with mannose 6-phosphate groups (25). MPR^{ci} receptors are acquired during virion trafficking on the convex face of the *trans*-Golgi network (TGN) that become transport vesicles directed to late endosomes. In late endosomes, acidification leads to degradation of VZV particles. This process is held responsible for the lack of efficient release of infectious particles in cell culture and cell-to-cell VZV dissemination in the body. Interestingly, this process is thought to occur in all VZV-infected cells excepted for cells of the suprabasal epidermis (corneocytes) which downregulate expression of MPR^{ci} (61). It is at the outer epidermis where infectious cell free VZV is secreted in lesions. The second receptor, Insulin

Degrading Enzyme (IDE), mediates cell-to-cell spread in VZV. IDE is a zinc metalloproteinase that bind various ligands such as glucagon and insulin-like growth factor II, without activation of its hydrolyzing activity. Moreover, IDE has a wide tissue distribution, and is present in the cytoplasm as well as plasma membranes, including the surface of differentiated neurons (115). Studies do indicate that other receptors may be involved in VZV entry since blocking of IDE did not completely block VZV infection (115).

VZV DNA Replication & Regulatory Proteins. Investigating the kinetics of VZV transcription has been difficult because low amounts of cell-free VZV prevent high multiplicity synchronized infections. Nevertheless, VZV transcription likely follows the temporally-controlled transcription cascade found in other herpesviruses (78), where genes are designated as immediate early (IE), early (E), or late (L). It is thought that upon entry, tegument proteins - of which three are IE proteins - are released and enter the nucleus with the nucleocapsid to activate viral genes. IE gene transcription occurs first without the need for prior *de novo* protein synthesis. These are transcribed in the nucleus, then translated in the cytoplasm and transported back to the nucleus. This cycle repeats with E and L genes. VZV E gene transcription requires IE proteins, and function in facilitating DNA replication and metabolism. Once DNA replication ensues, VZV late proteins are made and locate to the nucleus for capsid assembly. Nucleocapsids will then commence nuclear egress. VZV encodes homologues of the seven viral proteins required for origin-dependent DNA synthesis in HSV. These include a viral DNA polymerase catalytic subunit (ORF28) and accessory factor (ORF16), major DNA binding protein (ORF29), a putative heterotrimeric helicase/priamse complex encoded by ORFs 6, 52, and 55, as well as an origin binding protein ORF 51. Most α herpesvirus genes are expressed from their own promoters. The model for VZV DNA replication posits that linear DNA from an infecting virion

circularizes in the nucleus prior to the initiation of replication. In the case of closed circular DNA this would have happened just prior or post-packaging of DNA (177). DNA replication then begins at one of the two *Oris*, where unwinding of the origin is likely facilitated by ORF29 enabling the recruitment of proteins involved in VZV DNA synthesis and a nick is introduced in the replicating DNA and shifts to a rolling circle mechanism resulting in head to tail concatemers that are cleaved at the novel L-S joint created during circularization (177). VZV encodes homologues to four of five HSV IE genes, ORFs 4, 61, 62, and 63, yet only ORFs 4 (46), 62 (58), and 63 (150) have found to be expressed under IE conditions. ORF 61 is potentially an IE protein as it is expressed very early in infection (1 hr PI) (174). Only ORF62 contains an upstream TAATGARAT-like sequence, which in HSV is important for responsiveness to the transcriptional activator VP16. Analysis of single human fibroblasts has demonstrated that a productive cycle of VZV infection occurs between 9 and 12 hours, with viral DNA and formation of replication compartments visible by 4 hours (174).

VZV transcription depends on host cell RNA polymerase and transcription factors, in addition to several VZV proteins that have transactivating functions, many of which are tegument proteins. Regulatory proteins include ORFs 4, 10, 61, 62/71, 63/70 (100). VZV also encodes for two kinases ORFs 47 and 66, and as well as functional thymidine kinase. ORF 4 is a transcriptional activator of all gene classes as well as a co-activator of IE62-mediated transactivation in transient expression (4, 96). VZV ORF 10 is the homologue of the essential HSV VP16 protein, and shares some of its properties such as its tegument incorporation, transactivating property, and binding to TAATGARAT motifs and cell proteins HCF-1 and Oct-1. Unlike VP16, VZV ORF10 is a non-essential protein in cultured cells (32) and it

transactivates IE62 and not other IE genes (136). However, ORF10 is important for VZV replication in skin xenografts *in vivo* (24).

ORF61 is the homologue of the multifunctional protein HSV-1 ICP0. In transient expression assays the protein transactivated several viral and cell promoters, and repressed or enhanced the promoters of ORF4 and IE62 (136, 146, 158). The transcription factor, specificity protein 1 (Sp1), binds to the ORF61 promoter, and these sites have been found to be important for ORF61 contributions to VZV virulence in severe combined immunodeficiency (SCID-hu skin) xenografts. Additionally, ORF61 may be involved in inhibiting the chromatin silencing effects of histone deacetylases, an important function of ICP0 (28, 211).

IE62 is a major tegument protein and is the key transcriptional activator of all VZV genes and some cellular promoters. It is divided into 5 regions (I to V) based on alignments with other α herpesvirus homologs. IE62 interacts with several cell transcription factors including Sp1, upstream stimulatory factor (USF), TATA binding protein (TBP), TFIIB, human mediator complex and upstream cis-activating elements in VZV promoters (157, 178, 225, 227). IE62 can also directly bind DNA in region II through the DNA binding domain. This region is highly conserved and responsible for IE62 homodimerization and repressor activities (218). Region III contains the nuclear localization phosphorylation, and also sites for phosphorylation by VZV kinases (99, 102). Region IV functions are unknown and Region V is the site of many mutations in VZV vaccine strains (65).

ORF63 is a tegument protein that is the most abundantly found VZV transcript expressed in latently infected human ganglia (34, 38). The protein has been reported to bind IE62 (119). Additionally, ORF63 has been reported to act as a transcriptional repressor for VZV and cell promoters (18, 50) and involved in inhibiting innate immune responses (2).

ORF 47 is a serine/threonine kinase that is conserved amongst all three herpesvirus subfamilies & displays homology to HSV-1 UL 13 kinase and casein kinase II (152, 198). This tegument protein is dispensable for VZV replication in fibroblasts and melanoma cells but is important for replication in human T cells and skin xenografts in the SCID-hu mouse model cells (73, 133, 199). ORF 47 autophosphorylates and phosphorylates gE, gI, ORF 62, 63, and 32 (73, 95, 148, 173, 184). Although the function of ORF47 kinase activity on IE62 is not well delineated, ORF47 N-terminal binding to IE62 contribute to VZV replication in skin xenografts (15).

VZV Egress. For all α -herpesviruses, nucleocapsids are assembled in the nucleus and during egress an envelope is acquired as capsids pass through the inner nuclear envelope and into the perinuclear space which is continuous with the lumen of the rough endoplasmic reticulum (RER). VZV is thought to then undergo the de-envelopment – re-envelopment process where nucleocapsids acquire a primary envelope at the the inner nuclear membrane, enter the perinuclear space/RER lumen, and lose the envelope as it crosses the RER membrane - as opposed to acquiring its final envelope at the inner nuclear membrane. Most VZV glycoproteins tested sort to the TGN, supporting this model (212). In the TGN, tegument proteins interact with the cytoplasmic domains of glycoproteins. During invagination of the nucleocapsid with the TGN, the nucleocapsid then undergoes final envelopment, acquiring tegument and glycoproteins. In cell culture, newly synthesized VZV are diverted to the MPR-mediated endosomal pathway and eventually the transport vesicles become late endosomes, which then through exocytosis release degraded noninfectious virions (70). Infectious virions are thought to be the result of vesicles that have escaped this pathway, with most infection depending on cell to cell fusion.

VZV Latency. VZV establishes a latent infection in neurons of sensory ganglia (93), where it assumes a circular or concatameric state (27). Here VZV is present as 2-9 copies in 1 to 7% of individual neurons, therefore viral burden is predicted to be 30 to 3500 VZV DNA copies per 100 ng of total ganglionic DNA (37-38, 93, 159), likely depending on the severity of primary infection. Several transcripts corresponding to ORF 4, 21, 29, 62, 63, 66 have been found in latently infected human ganglia, with the most predominant being ORF63 (36, 38, 92) as well proteins encoded by these genes (36, 92, 118, 120). These proteins exhibit a cytoplasmic localization in neurons, as compared to nuclear localization for most of these proteins during lytic infection – this is thought to be a mechanism to regulate nuclear transcriptional activator activities and thus maintain latency. ORF66 functions may be critical in maintenance of latency, as during VZV infection it functions in regulating IE62 localization and causes a dramatic IE62 nuclear exclusion late in infection (35, 52, 54). In contrast, HSV gene expression is tightly regulated with silencing of most lytic expression concomitant with expression of latency associated transcript (LAT) gene which encodes a 8.3 kb primary transcript and two stable introns (2.0 kb and 1.5 kb) (94), whereas apparently VZV does not encode a LAT homologue. While the molecular mechanisms of VZV reactivation are largely unknown, immune responses also seem to play a more critical role in control of VZV reactivation compared to HSV (135). According to the Hope-Simpson model reported in 1965, Hope-Simpson postulated that following chickenpox infection, VZV elicits an immune response that impedes future VZV reactivations from progressing to zoster. This level of immunity over time declines but is boosted through subclinical infections stemming from exogenous exposures to VZV in the environment (chickenpox or zoster patients) (79, 153). These boosts help slow the age-related

decline in immune responses to VZV, yet eventually the patients' immune response declines to a critical level where previously "contained reversions" now advanced to cause herpes-zoster.

1.3 VZV TROPISM & PATHOGENESIS

VZV has a highly restricted host range and host-cell range in experimental settings, yet exhibits broad tissue tropism in humans, its only natural reservoir. Primary VZV infection begins with inoculation of the respiratory mucosal epithelium, and subsequent events have been based on a mousepox model. This Fenner-Groze model dictates that during the first replication or primary phase, VZV infects mononuclear cells in regional lymph nodes bringing the virus to reticuloendothelial organs, e.g. liver. Here a second replication occurs leading to a second viremia that brings the virus to the skin (68, 106). However, work by the Arvin group using the SCID-hu mouse support a model where infected T cells mediate the transfer to the skin during primary viremia, and the VZV incubation period reflects the time it takes to overcome innate immune system barriers, e.g. IFN α , at the skin before a chickenpox lesion presents. VZV infects the upper respiratory tract and regional lymph node where the virus targets peripheral blood mononuclear cells (PBMC) (121, 219), particularly lymphocytes (105) although all subpopulations have been found to be susceptible to infection (82). Dendritic cells are also susceptible to infection and can mediate the transfer to T lymphocytes (1). Using the SCID-hu mouse model VZV possessed a tropism for CD4 and CD8 T cells within thymus/liver xenografts. Specifically tonsil CD4 T cells with activated memory subpopulations are highly permissive for VZV infection *in vitro* (107), as well as those with skin homing markers

cutaneous leukocyte antigen (CLA) and chemokine receptor 4 (CCR4). Interestingly, more than 20% of mononuclear cells in the tonsils are CD3 T cells, and although B cells are also present, VZV infection of B cells induces their apoptosis (105-106). Hence, this model holds that VZV preferentially targets this cell type that is programmed for immune surveillance as a means of VZV transmission to the skin. Interestingly, VZV infection of T cells did not trigger their fusion in contrast to the cell-to-cell spread and polykaryocyte formation that is seen in skin cells, suggesting T cells depend on infectious cell-free VZV during transfer to the skin (132). Through studies in skin-xenografts, it was found that once VZV reaches the skin there is a progressive lesion that eventually extends up to surface keratinocytes.

Further studies in the SCID-hu mouse model using dorsal root ganglia xenografts (230) have contributed to the understanding of herpes zoster neuropathogenesis (230). VZV reactivation is characterized by a lesion involving the dermatome innervated by the successfully reactivating sensory ganglia. This is in contrast to HSV, where reactivation usually presents as a more focal region of the affected skin innervated by the reactivating neuron. In the SCID DRG xenografts, VZV genomic DNA, proteins, and virions were found both in neurons and satellite cells of the DRG. Furthermore, VZV infection induced cell-cell fusion and polykaryon formation between these two cell types. It is postulated that VZV reactivation may begin with replication in one neuron which spreads through cell-to-cell fusion to neighboring satellite cells. Subsequently, satellite cells would spread VZV to adjacent satellite cells surrounding a separate neuron within the ganglion, and thus increase the likelihood for VZV to gain access to more neurons within the ganglion and thus affect a large region within the dermatome. Past studies have supported VZV infection within the ganglia prior to involvement in the skin, as patients often present with neuralgia several days before the zoster rash appears.

1.4 VZV ORF66 KINASE

1.4.1 Introduction

The ORF66 protein kinase is one of two VZV protein kinases initially identified based on genomic position and homology to herpes simplex virus (HSV) kinases and the presence of classical structural motifs found common to all ser/thr kinases. Homologs of ORF66 are often termed the US3 kinases, since they are found in the unique short region of the genome of all sequenced neurotrophic α herpesviruses (and probably all α herpesviruses), but are absent in members of beta and gamma herpesviruses. By influencing phosphorylation states, the key means of reversible protein functional modulation, the US3 kinase family affect many events in infection, such as resistance of the infected cell to apoptosis, the state of permissivity to gene expression, avoidance of immunity, modulating cellular pathways affecting host actin dynamics, and influencing the nuclear structure and nuclear membrane to enable assembly of virus components. The ORF66 kinase is clearly important for VZV growth in certain cell types relevant to human disease. Thus, interest in the ORF66 kinase and the search for its targets continues.

1.4.2 Genetics

VZV ORF66 lies in the unique short region of the VZV genome (nucleotides 113,037 to 114218 in VZV Dumas, 113142 – 114323 in POka). Its genetic disruption in VZV, first reported by Heineman et al 1995, established it as not required for growth in cell cultures used for VZV propagation. In this regard, ORF66 mirrors similar US3 mutants of HSV, pseudorabiesvirus (PRV) and marek's disease virus (MDV). In the vaccine Oka background, ORF66 disruption had no effect on viral growth rates, but in the parent Oka VZV background, disruption causes 3-20 fold drop in peak growth levels compared to parental virus, depending on host cell type. As the gI gene lies immediately downstream of ORF66, the complete ORF66 gene cannot be deleted entirely without affecting gI expression, as ORF66 contains control elements in the gI promoter.

VZV mutants lacking ORF66 kinase activity do show more impaired growth in certain cell types or in organ culture models, suggesting that the host cell dictates the importance of the kinase to infection. VZV lacking ORF66 grow poorly in cultured T cells (199) and in human thymus/liver xenografts in SCID-hu mice (133, 185-186). This has relevance to human disease, since current models of VZV infection propose that tonsillar T cells transport VZV from the tonsillar respiratory epithelium to the skin (106). In T cells, VZV lacking ORF66 kinase show greater sensitivity to IFN- γ treatment, and increased levels of apoptosis. Electron microscopic examination of such cells reveals an apparent defect in the formation of nucleocapsids, but do not show the accumulation of abundant nucleocapsids at invaginations of the inner nuclear membrane, as seen for US3 kinase-deficient HSV-1 and PRV (see section 1.4.6.3). Although we have noted accumulation of major capsid protein at the nuclear membrane

in VZV-infected cells expressing kinase dead ORF66 kinase (Eisfeld, A. unpublished results). The molecular basis for the VZV phenotypes is not yet understood.

VZV without functional ORF66 also replicate poorly in primary corneal fibroblasts obtained from human corneal stroma donor rims (54). This is significant to human disease, as the cornea is often infected during zoster reactivating from the fifth cranial nerve. Corneal fibroblasts were initially evaluated to investigate possible roles of the ORF66 kinase on actin dynamics, as they develop prominent stress fibers when cultured on plastic support. Using recombinant VZV in which GFP was tagged N-terminally to ORF66 kinase, a truncated form or a kinase-inactive form, it was found that VZV without kinase were blocked for replication at a stage following the initial round of replication following infection with infected human MRC-5 cells. VZV lacking ORF66 formed microfoci of GFP positive cells that subsequently fail to expand over time. The basis for growth impairment is not yet known, but data suggested it was not a result of differential regulation of apoptosis or regulation of cellular localization of IE62 (54).

1.4.3 ORF66 Structure & Characteristics

The ORF66 protein kinase, at 393 residues, has a predicted molecular weight of 44 kDa. It is a phosphoprotein (202) that migrates at 55kDa as two forms which appear to be differentially phosphorylated. There is no evidence to suggest alternative forms initiating at alternative ATG residues, as seen for US3 kinases of HSV and PRV (164, 209). ORF66 has a conserved 286 residue kinase (catalytic) domain spanning amino acids 93 to 378 that has homology to all Ser/Thr kinases, which consists of 12 subdomains that fold into a characteristic 3-dimensional active core structure to transfer a γ -phosphate from ATP to the hydroxyl group of a specific S/T

residue within its protein substrate. These subdomains are remarkably invariant within the eukaryotic protein kinase superfamily (71). A constraint-based multiple alignment tool illustrates the putative 12 kinase subdomains in ORF66 using known subdomains (71) in cellular eukaryotic kinases in (Figure 1-2). As shown in figure 1-3, these subdomains account for most of the homology between α herpesviruses and as expected, kinase invariant residues are preserved for those viruses listed. Conservative mutations (D206E and/or K208R) in the central catalytic domain spans residues 203-211 disrupt kinase activity (99). Comparing ORF66 to the cellular Ser/Thr kinases predicts the ATP binding residue is likely K122: a K122A mutation also abrogates kinase activity (99). Using the entire gene in blast searches, the closest cellular homologs are human serine/threonine kinase 9 (also known as cyclin dependent kinase –like 5) and the yeast the cell cycle regulator cdc28 (127, 186). However, the amino terminal region of the protein has a high ratio of acidic residues, as found in all US3 kinases and also in the p21-activated kinases upstream of Cdc42/Rac pathways. The precise role of the acidic domain is not clear.

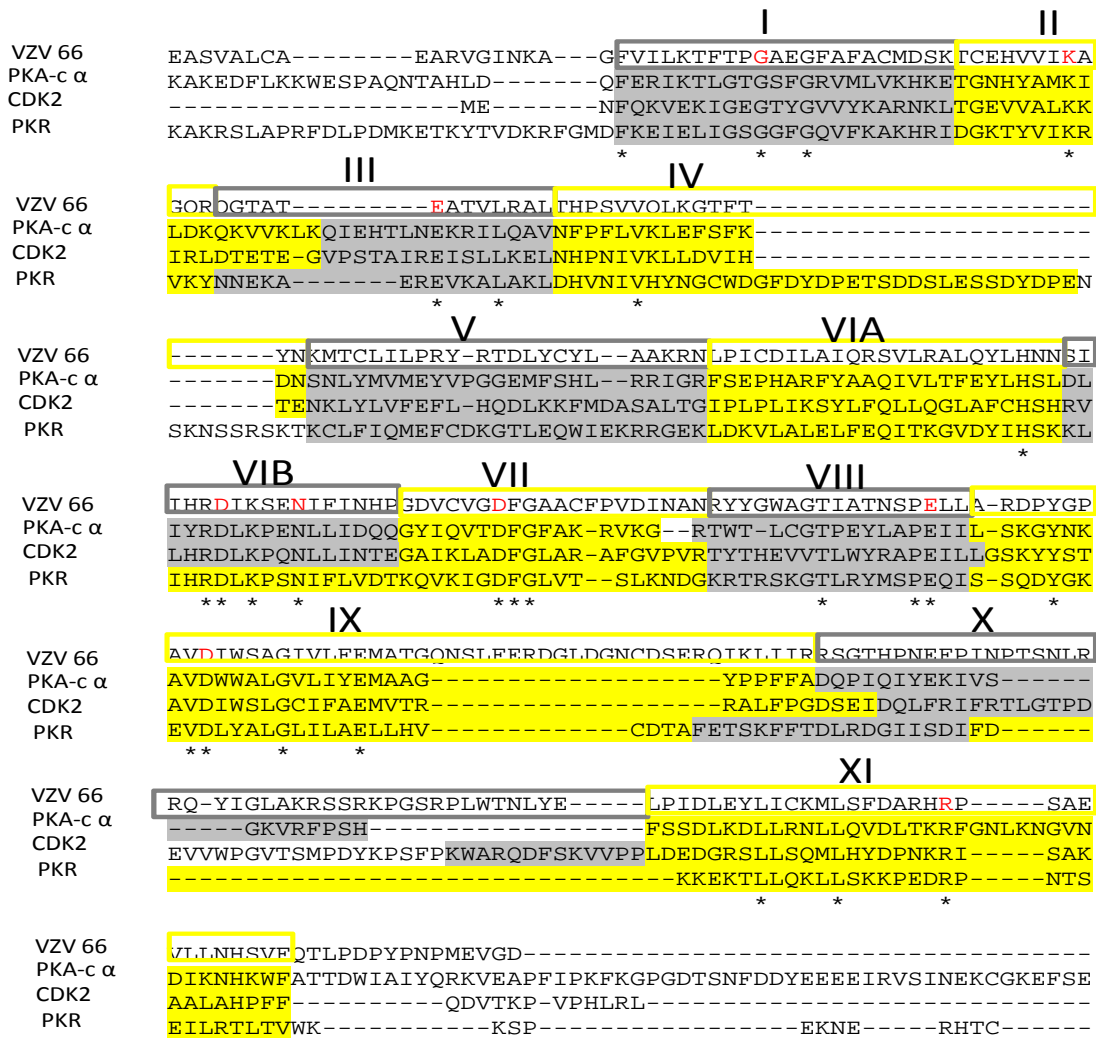


Figure 1-2. VZV ORF66 kinase putative catalytic subdomains

A constraint based multiple alignment tool (COBALT) was used to perform an alignment of VZV ORF66 kinase with Protein Kinase A catalytic subunit alpha (PKA-c α), cyclic-dependent kinase 2 (CDK2), and Protein Kinase R (PKR – Eukaryotic translation initiation factor 2- α kinase). Known catalytic subdomains for these cellular kinases (filled yellow/gray boxes), domain boundaries were extended to a best fit for ORF66 kinase (grey/yellow-outlined boxes). Stars denote shared residues. Invariant catalytic subdomain residues are shown in red. Subdomains regions are denoted by roman numerals above alignments.

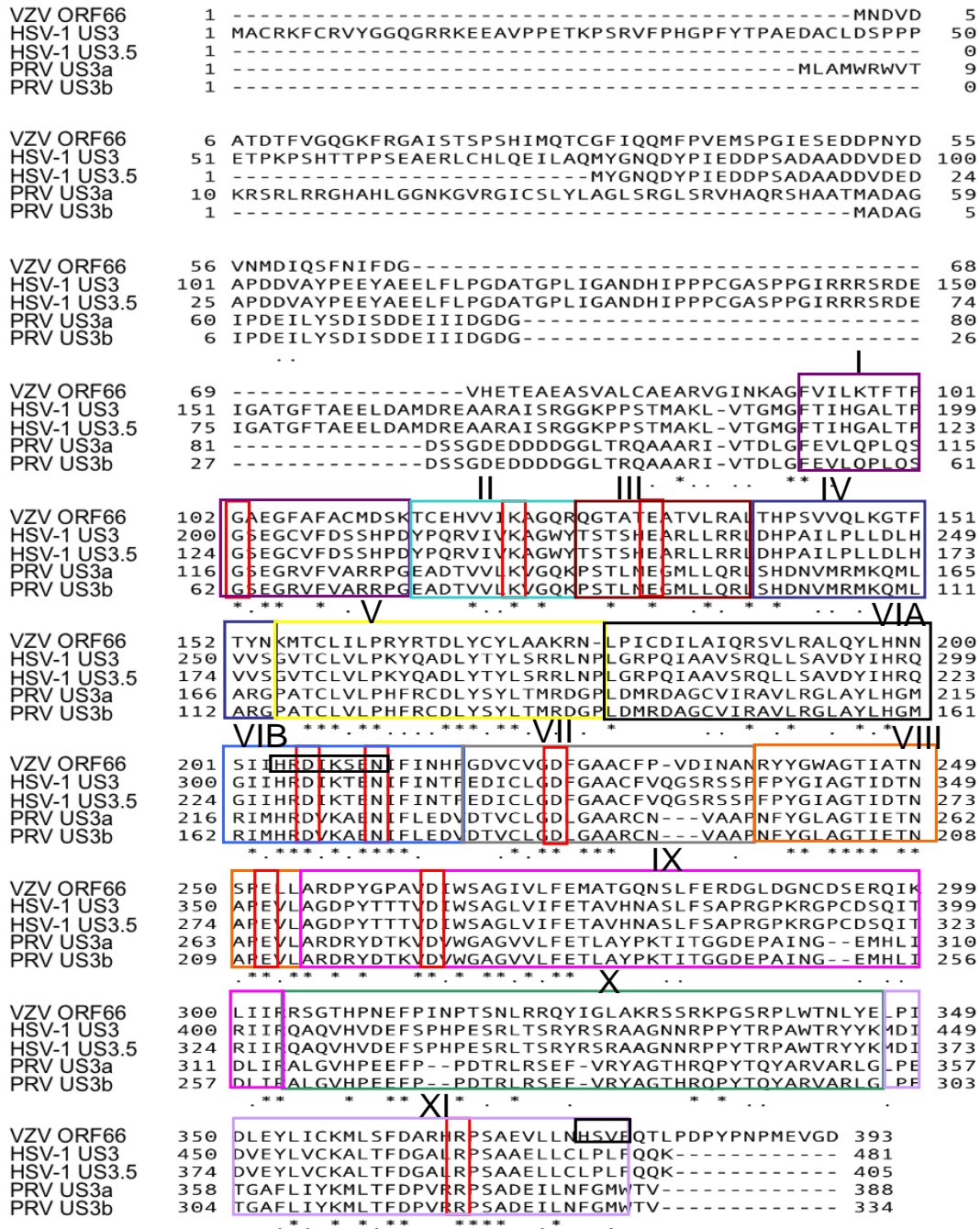


Figure 1-3. Alphaherpesvirus ORF66/US3 putative catalytic subdomains

Illustration of kinase catalytic subdomains in the HSV and PRV US3 kinases (colored boxes – denoted above by roman numerals) based on the putative ORF66 kinase catalytic subdomains outlined in figure 1-2. The red vertical boxes highlight invariant residues conserved in all kinases. The horizontal black box in region VIB is the catalytic loop region of the kinase. The vertical box in region XI is the likely consensus motif (his-x-Aromatic-hydrophobic) that is found 9-13 residues downstream from the invariant arginine of this subdomain.

A significant fraction of ORF66 kinase is insoluble in most buffers designed to solubilize the protein without disturbing its kinase activity. ORF66 solubility is increased in higher pH buffers, as found for HSV-1 US3 kinase, and our optimal buffer used to solubilize GST-tagged ORF66 from baculovirus-infected cells contains 20mM Tris-HCl pH 8.5, 50mM KCL, 1mM EDTA, 1mM DTT, 1%NP40, and 0.5% DOC. Kinase activity in vitro is optimal in 20mM Hepes pH 7.5, 50mM Mn^{2+} , and 50mM KCl. ORF66 is not inhibited by 10 μ g/ml heparin (which effectively block casein kinase II activity), so this is included in assays. 10mM Mg^{2+} can also be used as the cation in the ORF66 in vitro kinase assay (52).

The cellular localization of ORF66 protein has an unusual distribution. While initial studies using ORF66 specific antibodies first indicated ORF66 as a cytoplasmic protein (202), studies from our lab using epitope tagged or functional GFP-ORF66 fusions indicate both nuclear and cytoplasmic distribution in VZV-infected cells and in cells expressing the kinase autonomously, with nuclear forms predominating (53, 99, 185). Nuclear ORF66 shows a discrete and distinct punctate nuclear accumulation, forming rings of puncta surrounding the infected cell nucleolus (53, 99). Characterization of these ORF66 speckles is in progress, and these appear dynamic (Eisfeld, A., and P.R. Kinchington manuscript in preparation). Functional ORF66 also associates with replication compartments early in infection in MRC-5 cells, whereas kinase dead (kd) forms (D206E, K208R) accumulate in both nuclear replication compartments and nuclear rim of late stage VZV-infected cells, colocalizing with major capsid protein (MCP) (Eisfeld, A. and P.R. Kinchington manuscript in preparation). This suggests that ORF66 kinase activity influences its own cellular distribution, and may be associated with capsid assembly and/or egress.

1.4.4 ORF66 targets

Only one target of ORF66 has been extensively characterized – IE62. The two sites targeted strongly suggest ORF66 is a basophilic kinase that phosphorylates ser/thr residues preceded by multiple arginine or lysine residues, particularly at -2 and -3 positions. This is consistent with target motifs of PRV and HSV US3 kinases determined by in vitro peptide substrates, and are optimal at $(R)_nX-(S/T)-Y-Y$, where n is >2 , S/T is the target site where either serine or threonine is phosphorylated, X can be absent or any amino acid but preferably Arg, Ala, Val, Pro, or Ser, and Y is similar to X except that it cannot be an absent amino acid, proline, or an acidic residue. The optimal consensus sequence is similar except that X is not absent and n is ≥ 3 (9). However, studies on the US3 kinase suggest the optimal motif is overly restrictive, and sites of phosphorylation with much lower matches to the consensus have been reported on lamin C (138). Of particular note is that both VZV ORF66 and HSV-1 US3 kinase target motifs overlap that targeted by Protein kinase A (PKA). Using antibodies to the phosphorylated serine/threonine in the PKA target motif, we will show that novel substrates are detected in extracts of VZV-infected cells that are not found in VZV kinase-deficient infected cells, suggesting the kinase targets multiple cellular proteins or induces activation of cellular kinases that target phospho-PKA motifs. Interestingly, by western blot the antibody identifies radically different protein profiles in the same cell type infected with VZV, HSV and PRV (Section 3.0).

1.4.4.1 Autophosphorylation

Protein kinase autophosphorylation is frequently employed to uphold the specificity of kinase functions, thus it is not surprising that ORF66 autophosphorylates. Disruption of the kinase

catalytic domain or the ATP binding residue result in a poor ^{32}P - incorporation into the protein within VZV-infected cells and in *in vitro* reactions with purified kinase. The sites of phosphorylation remains to be determined. Assuming kinase targeting of serines preceded by basic residues, likely candidate sites are located at KRS₃₃₁SRK and RHRPS₃₆₈. However, mutagenesis studies indicate that the S₃₃₁ residue is not required for kinase activity (186). VZV ORF66 has no obvious equivalent to the S147 autophosphorylation residue found to be the site of HSV-1 US3 autophosphorylation (87), and it is not yet known if ORF66 is phosphorylated by ORF47. The US3 kinase is phosphorylated by the UL13 kinase (89) in HSV-1 infected cells.

1.4.4.2 IE62

ORF66 kinase targets IE62, the major regulatory protein of VZV. IE62 is a nuclear transcriptional regulatory protein that drives VZV transcription by interacting with transcriptional activators, components of the mediator complex and members of the general factors involved in recruitment of RNA pol II complex (178). While the underlying mechanisms by which IE62 acts are not resolved, its ability to partly substitute for HSV ICP4 infers that both IE62 and ICP4 act in a similar manner. The targeting of IE62 by the VZV ORF66 kinase was serendipitously discovered in studies to examine the influence of ORF47 kinase on IE62 functions, which had previously been shown (148). Cells transfected to express IE62 with or without the ORF47 kinase showed IE62 as a predominantly nuclear protein. The IE62 nuclear localization signal (NLS) is a classical SV40-like signal high in arg/lys rich residues mapping to residues 677-85 (102). However, IE62 coexpressed with the ORF66 kinase showed accumulation of abundant cytoplasmic forms of IE62, mirroring that seen in late stage VZV-infected cells. While IE62 is nuclear early in VZV infection before ORF66 is expressed, IE62 levels build in the cytoplasmic compartment as ORF66 accumulates, until some infected cell nuclei appear

devoid of IE62. Cytoplasmic IE62 does not form in cells infected with VZV lacking functional ORF66 kinase, establishing that kinase activity was required. The sites of phosphorylation on IE62, mapped using plasmids expressing IE62 peptides in ORF66 transfected and VZV-infected cells, are predominantly restricted to IE62 residues S686 and S722 (52). ORF66 directly phosphorylated IE62 *in vitro*, and bacterially expressed IE62 peptides with both or one serine intact remained a target for purified VZV ORF66 kinase *in vitro*, whereas loss of both serines abrogated the ability of IE62 to be an ORF66 target.

The ORF66 kinase-mediated regulation of IE62 has not been reported for the corresponding proteins of other alphaherpesviruses, but it reflects the regulated nuclear import of many cellular proteins through phosphorylation (72, 85). As phosphorylation is reversible, it can enable multifunctional proteins to be controlled by their relocation to different cellular compartments. The nuclear exclusion of IE62 in VZV infection enables the packaging of abundant levels of IE62 into VZV virions, at about 50% of the level of the major capsid protein. Virions obtained from VZV-infected cells lacking kinase show virtually no structural forms of IE62 (98). It was concluded that nuclear exclusion of IE62 allows it to relocate to the *trans*-Golgi network, where VZV tegument is added to the egressing nucleocapsid. Virion packaging of IE62 may allow the introduction of preformed IE62 into the newly infected cell to promote the first events of infection, although this remains to be formally shown. We will show the importance of the targeting of S686 in the ORF66 driven relocation of IE62 using a VZV recombinant containing S686A changes in both copies of IE62 in the VZV genome (Section 2.0). Such virus expressed IE62 protein which did not relocate to cytoplasm or become packaged during infection, despite the presence of a functional ORF66 kinase (54).

We postulate that this interaction may come to play during VZV latency. VZV infects

sensory nerve endings during varicella and establishes latency in neural nuclei in dorsal root ganglia (DRG). In contrast to HSV-1, where there is predominant silencing of protein expression and expression of non-coding latency associated RNA transcripts (LATs), VZV latency is characterized by expression of several lytic mRNAs and some regulatory proteins which show nuclear exclusion. Transcripts and proteins of ORF62 and the ORF66 kinase have been reported in human latently infected tissue (34-35), and IE62 shows predominantly cytoplasmic distribution (35, 118). It has been proposed that VZV latency is maintained by preventing nuclear functions of the regulatory proteins through nuclear exclusion. Our discovery may mechanistically explain IE62 nuclear exclusion during latency.

Interestingly S686 in IE62, which immediately follows the nuclear import signal, is highly conserved in virtually all the alphaherpesvirus ICP4/IE62 homologs. This suggests that their cellular localization may also be regulated by phosphorylation. Indeed, cotransfection studies suggest US3 kinases reduce nuclear import of the corresponding IE62/ ICP4 homolog (Yee and Kinchington, in preparation). However, HSV-1 ICP4 shows cytoplasmic forms as infection progresses, but these are more reliant upon the functionality of the HSV ICP27 protein (191).

1.4.4.3 HDACS

Transcription is strongly influenced by the chromatin state of the template DNA that, in turn, is under an elaborate control system that modulates histone binding and condensation. A key component is the reversible post translational modification of histones through the addition and subtraction of acetyl groups to their lysine tails. In general, permissive gene expression is promoted by histone acetyl transferases which acetylate histones to lessen DNA binding and

condensation. Silencing of expression is partly driven by their deacetylation, mediated by histone deacetylases (HDACS). HDACs are an ancient family of enzymes that have a major role in numerous biological processes. Eleven different HDAC isoforms have been identified in mammalian genomes and these are classified into four different families: class I (HDAC1, 2, 3 and 8), class II, (HDAC4, 5, 6, 7, 9 and 10), sirtuin class III and class IV (HDAC11) (69, 190). Because HDACs lack intrinsic DNA-binding activity, they are recruited to target genes through direct association with transcription regulatory proteins. HDAC activity is controlled by phosphorylation by numerous cellular kinases (160). This blocks their deacetylase functions and promotes a cellular permissive state of transcription. The herpesviral infected cell is favored by a pro-active transcriptional state in which deacetylation is inhibited. In HSV-1 infected cells, multiple mechanisms are involved in the inactivation of HDAC activity, for example HSV-1 ICP0 dislodges the LSD1/CoREST/REST complex from HDAC1 and HDAC2, disrupting the silencing effects of this repressor complex on viral promoters. More recently, it was reported that HDAC-1 and 2 showed novel forms which were induced by the US3 kinase, and that cells expressing the US3 kinase showed a more activated transcriptional state (162-163).

We have been part of the recent work suggesting that HDAC-1 and 2 are also modulated in VZV-infected cells in an ORF66-dependent manner (213). HDAC-1 and 2 show novel slower mobility forms in SDS-PAGE gels of VZV-infected cell extracts that are not apparent if the ORF66 kinase is deleted. The slower form is differentially phosphorylated and is also seen in cells expressing the ORF66 protein kinase autonomously by transfection or by transduction with ORF66 expressing adenoviruses. Mapping of the sites of HDAC phosphorylation identified a specific phosphorylated residue in the C terminal domain of both proteins which are preceded by basic residues at -2 and -3 positions, consistent with PKA target motifs.

Functional consequences of ORF66 activity affecting HDACs has been suggested from studies using the HDAC inhibitors sodium butyrate. At 1mM, this inhibitor relieves some of the attenuation of the ORF66 negative VZV as compared to parental virus. Thus it seems that a prime function of the kinase is to regulate cell permissivity at the transcriptional level through interactions with HDAC-1 and 2 and possibly other HDACs.

1.4.5 Additional cellular activities modulated by the ORF66 protein kinase

1.4.5.1 MHC-1 surface presentation

The ORF66 protein kinase appears to mediate VZV-encoded immune evasion strategies. In the host, viral and cellular antigenic peptides are presented on the cell surface for CD8⁺ T cell recognition in conjunction with the major histocompatibility complex type I or MHC-I. Most herpesviruses have mechanisms to reduce surface presentation of MHC-I coupled viral antigens, presumably to allow prolonged survival of the cell in the presence of a developed immune system. In MHC biogenesis, antigenic peptides generated by the host 26S proteasome are actively transported to the ER lumen by the Transporter of Antigen Presentation (TAP), composed of a heterodimer of TAP-1 and TAP-2. TAP is inhibited by many viruses, because its inhibition affects MHC-I A and B, the main antigen presenters, but not MHC-I types that are needed to signal to natural killer (NK) cells. TAP is blocked in HSV-1 infected cells by the immediate early protein ICP47 (76), of which there is no homolog in VZV. Varicelloviruses are reported to have a second gene that blocks TAP, of which the bovine herpesvirus UL49.5 is the most well characterized (104). However, we and others have not seen evidence that VZV ORF 9.5 has similar activities (53). In the ER lumen, MHC-I heavy chain (Hc) bound to beta 2-microglobulin is stabilized by several chaperones (tapasin, ERp57 and calreticulin) until it

couples with TAP and the antigenic peptide. The peptide loading complex can be disrupted or actively inhibited by some viral MHC-I modulators (e.g. human Cytomagalovirus US2) (62). Once loaded, the antigenic peptide is processed to high affinity forms, which mature through the secretory pathway via the Golgi to the cell surface. *Cis- to medial-* Golgi transport is concurrent with conversion of high mannose glycan side chains to complex endoglycosidase-H (endo H) resistant forms.

It is not surprising that VZV downmodulates surface antigen presentation, as first reported by Abendroth et al (1). VZV has lymphotropic parameter in its human pathogenesis, and can sustain infection in multiple cell types over a prolonged period, including professional antigen presenting cells and chronic antigen-expressing neurons during latency. The lack of an ICP47 homolog suggests VZV uses novel mechanisms to mediate this block. Following an initial report by Abendroth et al in which reduced MHC-I expression in ORF66 expressing cells, we reported that surface MHC-I was reduced in ORF66 expressing cells mediated by transfection, adenovirus mediated transduction or in recombinant viruses expressing GFP tagged forms of ORF66, but were not downregulated to the same extent in the corresponding conditions when the expressed kinase was disrupted or abrogated (53). In both adenovirus transduced and in VZV-infected cells, the ORF66 kinase delays Golgi-processing of MHC-I and induces the accumulation of endoglycosidase H sensitive MHC-1 forms, suggesting that it blocks either at the assembly stage or the Golgi maturation step prior to *cis to medial* Golgi processing. In VZV infections without ORF66 kinase, MHC-1 processing is still partly blocked as compared to control cells, suggesting that additional mechanisms exist for VZV to block surface MHC-I . In this respect, VZV is like many herpesviruses, and employs overlapping mechanisms. This is currently under further study.

1.4.5.2 IFN Signaling

Schaap et al demonstrated that expression of ORF66 correlated with a differential level of signaling following IFN γ treatment of VZV-infected T cells. Specifically, the formation of phospho-Stat in T cells following IFN γ binding to its receptor was significantly diminished with ORF66 expression as compared to VZV infections lacking functional ORF66 (186). It is not yet resolved as to how ORF66 blocks this activity, but it is notable that Roizman and colleagues have recently indicated that the HSV-1 US3 kinase may phosphorylate IFN- γ R α to prevent its signaling (116).

1.4.5.3 Apoptosis

Arvin and colleagues also demonstrated that ORF66 protein kinase modulates the apoptosis of T cells that mediate dissemination of VZV from respiratory sites of infection to skin (106). VZV lacking ORF66 grew to levels 2 logs lower than parental virus in cultured human T cells but not in MeWo cells, and the expression of the kinase conferred a marginal growth advantage in skin xenografts . T cells infected with a kinase-inactive G102A mutant showed increased levels of active caspase 3, the executioner protease in apoptosis, suggesting that loss of the ORF66 kinase correlated with VZV inability to check the development of apoptosis from VZV infection in this cell type (186). These findings imply that ORF66 has an important function in extending the survival of infected T cells until they are able to home in on the skin (185). Therefore, inhibition of apoptosis may be the contributing function or the defining function of ORF66 needed for VZV propagation in T cells. It has also been reported that VZV modulates the PI3K/Akt pathway, involved in regulation of apoptosis. Expression of ORF66 transiently or by VZV-infected MeWo cells is involved in a pro-survival signaling by activation of Akt, indicated by

the increase of Akt phosphorylation at serine 473, that decreased when 66 was not expressed (171). This may also partly explain the growth deficit of VZV in this cell type (133). However results from studies of ORF66 kinase deficient infections in human corneal fibroblasts, which are very restrictive for such mutants, indicated no significantly increased levels of apoptosis. Recent work has revealed that the role of apoptosis in HSV-1 infection is more important in highly replicating or transformed cells than in primary cell lines (149).

1.4.6 Alphaherpesvirus US3 kinase studies that guide the search for roles of ORF66

Several roles of ORF66 may be speculated from identified roles of the HSV and PRV US3 kinases, since there are clear structural similarities. In addition to the kinase catalytic domain, all have a high proportion of acid residues in the amino terminal region, although this region is functionally ill-defined. Here, we summarize the known features of the US3 kinases of other alphaherpesviruses.

1.4.6.1 US3 Kinases and Inhibition of Apoptosis

Viral perturbation of the host cell often triggers apoptosis, and herpesviruses have mechanisms to block programmed cell death and thus extend cell survival time to allow for viral replication (5). HSV-1 US3 kinase has been the most extensively examined in its role in blocking apoptosis, although the US3 kinases of others such as VZV, HSV-2, and PRV may have similar activities. US3 kinases block apoptosis by the virus as well as by a variety of ectopic treatments. HSV-1 US3 is one of four blockers of apoptosis (in addition to UL39, glycoproteins gD, gJ). Kinase activity is required in HSV and PRV suggesting that cellular components are phosphorylated. The possible targets include the pro-apoptotic protein Bad, whose phosphorylation (and

inactivation) was found to be US3-dependent (22). Recent studies indicate HSV-1 US3 kinase acts at a post-mitochondrial level, since US3, but not its inactive form US3 K220N, inhibited the cleavage and activation of procaspase 3, the zymogen form of caspase 3 - a major effector of the pro-apoptotic pathway. This was also phosphorylated *in vitro* by US3(10).

Two forms of HSV-1 US3 have been seen initiating at different ATGs and these appear to differ in their ability to block apoptosis. A US3 blocked apoptosis but US3.5 did not, even though both were able to localize in mitochondria (161). PRV also encodes two forms, a long (US3a) and short isoform (US3b) differing by an additional N terminal 54 residues from US3a that encodes a mitochondrial localization signal. However both block apoptosis, suggests that the mitochondrial signal and localization of the protein may only be partly responsible for the increase in its anti-apoptotic function (59). There is evidence for the block in apoptosis to be downstream of cell signaling pathways activated by US3. HSV-1 US3 activates PKA, and PKA activation by forskolin inhibits apoptosis (9). In sum, evidence points to the US3 kinases as one means to prevent programmed cell death, but several cellular targets may be involved.

1.4.6.2 US3 Modulation of HDAC

Inhibition of histone deacetylases is needed for efficient viral gene expression. Although ICPO is thought to be the key player in blocking genomic silencing, HSV-1 US3 may contribute by post translationally modifying HDAC1 and HDAC2 (163, 165). HSV-1 US3.5 shares this ability (161). US3 and 3.5 enable viral or host gene expression from restrictive cells and enhance expression from permissive cells transduced with baculovirus carrying CMV immediate early promoter-driven genes (162). While phosphorylation regulates HDAC 1 and 2 enzymatic

activity, it is not yet clear how US3 or ORF66 facilitates viral gene expression, but the suspicion is that HDAC1 and 2 are direct phosphorylation targets of US3 in infection .

1.4.6.3 Nucleocapsid Egress

Herpesvirus nucleocapsids assemble in the nucleus, and DNA packaged nucleocapsids pass through the inner (INM) and outer nuclear (ONM) membranes to the cytoplasm in an envelopment/de-envelopment fusion mechanism. Capsids then acquire most of the tegument and their final envelope as they bud through membranes of the *trans*-Golgi network (60). In both HSV and PRV infection, deletion of the US3 kinase only moderately affects growth rates and infectious virus production in culture. However, EM analyses reveal that such mutants accumulate capsids in extended folds in between the INM and ONM, or perinuclear space (103, 176). The US3 kinase thus facilitates egress of the capsid from the intranuclear space. US3 kinase mediated phosphorylation of several viral and cellular proteins have been implicated in this process, including UL34, a type 2 integral membrane protein that localizes to the INM, and UL31, both which are critical regulators of primary envelopment of nucleocapsids (88, 139, 169, 179). In HSV-1 infection, the UL34 forms a complex with UL31 and displays a smooth localization along the nuclear envelope, while in the absence of US3 kinase activity, the complex forms aberrant punctate accumulations at the nuclear membrane (175-176). UL34 was the first established target of the US3 kinase, but studies now indicate that UL34 phosphorylation at the C terminal end does not appear to be directly involved (89) in directing the normal localization of the UL34-UL31 complex. The US3 kinase does phosphorylate UL31 *in vitro* (88) and prevention of phosphorylation at the serine rich N terminus of UL31 leads to virions accumulating in the perinuclear space. Thus the US3 specific phosphorylation of UL31 may

facilitate virion nuclear egress (139). The VZV homolog of UL34 and UL31 do not have obvious corresponding regions.

Additional roles of the US3 kinase in nucleocapsid egress stem from recent studies indicating the kinase phosphorylates nuclear membrane forms of the major glycoprotein gB at the cytoplasmic tail. HSV with gB altered at the site of US3 mediated phosphorylation shows the same phenotype to the US3 kinase deletions, in that nucleocapsids accumulate in perinuclear invaginations that protrude into the nucleoplasm. The US3 kinase may modulate gB-mediated fusion events at the ONM to allow de-envelopment during nuclear egress (221). With regards to VZV ORF66, VZV gB does have predictable IE62-like potential motifs for phosphorylation in the cytoplasmic tail which bear similarities to that targeted by US3, but it is not yet known if ORF66 phosphorylates gB. Schaap-nutt indicated no obvious accumulation of VZV nucleocapsids at the nuclear rim in T cells, but rather showed vastly decreased nucleocapsid formation (186).

The US3 kinase also modulates host components of the nuclear envelope, including lamin A/C and emerin, an integral nuclear membrane protein which associates with lamin proteins (109, 138). The US3 kinase leads to the redistribution of these proteins in HSV-1 infection, which normally lie just inside the nuclear membrane and act as a barrier for virions budding into the INM. In the presence of US3 kinase, emerin becomes hyperphosphorylated, increasing its mobility during infection. It was postulated that this causes dissociation of emerin and lamin A/C to facilitate the nuclear egress of nucleocapsids. In the case of lamin A/C, it is theorized that US3 is involved in a careful balance in breaching the lamina network barrier to ease virion access to budding sites at the INM yet maintaining laminar structure (138).

1.4.6.4 Alteration of the host cytoskeleton

Many viruses restructure the host cell cytoskeleton to promote viral inter and intracellular spread. The HSV-1, PRV and MDV US3 kinases have joined the group of increasing viral effector proteins reported to manipulate the host cell cytoskeleton (197). PRV US3 has been shown to disassemble the actin cytoskeleton and induce novel formation of actin and microtubule-containing cell projections in both the context of viral infection and in US3-transfected cells (56, 208). Viral particles found within these dynamic projections were shown to move directionally towards the tip of projections as infection progressed (56) enabling more efficient spread to adjacent cells. This may allow more efficient infection in the presence of virus neutralizing antibodies. The US3-mediated actin disassembly also induced loss of cell-cell contacts and disassembly of focal adhesion which may be important to PRV spread (206). Interestingly, US3 was found to induce activation of group A p21-activated kinases through a threonine residue in the activation loop, and induce phosphorylation of PAK1 and PAK2 *in vitro*. These host proteins are players in Rho GTPase signaling pathways involved in actin disassembly and lamellipodia or filopodia formation. PAK1 and PAK2 were found to be required for infection-induced actin cell projections and disassembly, respectively (207).

In HSV-2, US3 kinase induced cell rounding and dissolution of actin stress fibers in transfected cells and US3 expressing cell lines. Dominant active forms of the RhoGTPases - Rac and Cdc42, co-transfected with US3 kinase reduced cell rounding, suggesting that US3 affects the Cdc42/Rac signaling pathway. Interestingly, the Rho family proteins regulate various aspects of actin dynamics and can activate PAKs (143). Transient disassembly of the actin cytoskeleton was also seen for MDV in infections and was dependent on expression of US3. Addition of cytochalasin D, which inhibits G actin repolymerization, blocked MDV plaque

formation. This taken together with the growth defects observed for US3-deficient MDV and the US3-dependent actin disassembly, support the idea that actin but not microtubule restructuring is important for virus intercellular spread (189). In contrast to PRV, MDV US3 kinase activity was not needed for actin remodeling in transfected cells (188), indicating US3-dependent actin disassembly may be dependent on its structure. With regard to VZV, my work found that cellular stress fibers are reduced in wild type VZV- infected cells and are more prominent and abundant in VZV-infected cells if the kinase is disrupted. Thus it seems likely that a common target for ORF66 and the US3 kinases is the modulation of the actin-based cytoskeleton. This is of interest for future studies.

1.4.6.5 Concluding Remarks

VZV ORF66 clearly has important multifunctional roles in the infectious process which are highly cell type dependent. Thus it is likely that the critical functions of the kinase are inducing the phosphorylation of cellular targets or the induction of cellular signaling pathways that drive the altered phosphorylation states of cellular proteins. It is clear that VZV has both novel functions as well as targets that are common to those targeted by other US3 kinases in other alphaherpesviruses. What those common pathways and cellular targets are remain to be resolved.

Table 3. *In vivo* and *in vitro* protein substrates of the ORF66/US3 kinases

Specific US3 kinase and its protein target are noted. Evidence of US3 induced phosphorylation *in vivo* or *in vitro* is denoted by a plus (+) sign or not done (ND). Functions associated with phosphorylation of each protein are also listed.

αherpesvirus	ORF66/US3 phosphorylated protein substrate	<i>In vivo</i> / <i>In vitro</i> target?	Function
VZV (52, 54, 99, 102)	IE62 (ICP4)	+/+	IE62 cytoplasmic accumulation / IE62 tegument inclusion
VZV, HSV, PRV	Matrin 3	+/ND	?
VZV(210), HSV-1(165)	HDAC 1 &2	+/ND	Block HDAC transcriptional repression
HSV-1 (86, 221)	gB	+/+	Downregulate gB surface expression, promote virion nuclear egress
HSV-1 (88, 139)	UL31	+/+	promote virion nuclear egress
HSV-1 (88, 169, 179)	UL34	+/+	?
HSV-1 (138)	Lamin A/C	+/+	Disrupt nuclear lamina, promote virion nuclear egress
HSV-1 (109)	Emerin	+/ND	Disrupt nuclear lamina, promote virion nuclear egress
HSV1,2 (41, 88)	US9	+?/+	?
HSV-1 (88, 168, 196)	ICP22	+?/+	?
HSV-2 (42)	UL12	ND/+	?
HSV-2 (144)	Cytokeratin 17	+?/+	Cell morphological changes
HSV-1 (22, 88)	Bad	+/+	Block apoptosis
HSV-1 (21, 88)	Bid	ND/ +/-	Block apoptosis, Mediates protection from granzyme B cleavage of Bid
HSV-1 (116)	IFN α	+/ND	Inhibit activation of IFN- γ genes
HSV-1 (9)	PKA	+/ND	PKA activation
PRV (207)	PAK1 and PAK2	+/+	Actin projection formation & stress fiber disassembly
HSV-1 (10)	Procaspace 3	ND/+	Block activation of procaspase 3 and apoptosis
HSV-1 (196)	cdc25C phosphatase	ND/+	Enhance interaction with ICP22, optimize viral gene expression

1.5 STATEMENT OF GOALS

VZV ORF66 kinase is responsible for the direct phosphorylation of IE62 and induced phosphorylation of cellular proteins HDAC 1 & 2. Additionally it is involved in the modulation of diverse cell signaling pathways such as causing surface MHC-I downregulation, inhibiting apoptosis and IFN- γ signaling pathways. Moreover, it is known that ORF66 is essential to viral growth in T cells. The US3 kinases have been implicated in the phosphorylation of multiple viral and cellular proteins in other α herpesviruses. In sum, the ORF66/US3 kinases are a group of multifunctional proteins important for establishing an optimal cellular environment for viral growth. The mechanisms of how ORF66 modulates cell signaling pathways are unknown since specific targets of this kinase and the US3 kinases as a group are mostly unidentified. The goals of this thesis work are to discover novel protein substrates for VZV ORF66 kinase to further define the specific roles of this kinase during the VZV life cycle. These findings may also further highlight the potential of ORF66 kinase as a target for VZV antiviral therapy.

Specific Aim 1: In chapter 2, we explore whether ORF66 expression is needed for VZV growth in primary stromal corneal fibroblasts. Thus far, ORF66 has been reported to be non-essential for VZV growth except in T cells. This study was based on our observations that VZV expressing ORF66kd did not replicate efficiently in corneal fibroblasts. We hypothesize that either loss of VZV growth in this PCF is due to ORF66 kinase inability to function in phosphorylation of IE62 at the S686 site, or the inability to impede VZV-induced apoptosis. For this purpose, we constructed a recombinant VZV with IE62 serine to alanine mutation at the 66 targeted phosphorylation residue and also characterized this virus for IE62 localization and virion incorporation.

Specific Aim 2: The basis for the studies in chapter 3, was the observation that the residue directly phosphorylated by ORF66 on IE62 is similar to that of PKA-substrate motif. We hypothesize that we can utilize an antibody that recognizes proteins phosphorylated at serines or threonines within PKA-substrate-like motifs to find novel ORF66 substrate proteins. Once a candidate protein was identified – matrin 3, we confirmed its phosphorylation induced by ORF66 and tested if it is a conserved target for the alphaherpesvirus US3 family, as well as characterized the 66-targeted phosphorylation site and determined changes in subcellular localization of matrin 3. In these studies, we utilize VZV or adenovirus recombinant proteins expressing functional ORF66 kinase or mutated ORF66 that is kinase-inactive, in addition to HSV and PRV US3-expressing or US3 null viruses.

2.0 VARICELLA-ZOSTER VIRUS ORF66 PROTEIN KINASE IS REQUIRED FOR EFFICIENT VIRAL GROWTH IN PRIMARY HUMAN CORNEAL FIBROBLASTS

Angela Erazo^{1,2†}, Michael B. Yee^{2†}, Nikolaus Osterrieder⁴ and Paul R. Kinchington^{2,3*}

Graduate Program in Molecular Virology and Microbiology¹, and Departments of Ophthalmology², Microbiology and Molecular Genetics³, School of Medicine, University of Pittsburgh, Pittsburgh, PA; and Department of Microbiology and Immunology⁴, Cornell University, Ithaca, NY.

Note: For this manuscript, I performed all immunofluorescence and image correction, as well as MRC-5 growth curves, NHS growth curve in Figure 2-6, growth curve enumeration by flow cytometry, and apoptosis experiments. I also did all statistical analyses, and wrote the manuscript. Recombinant VZV, virion purification and characterization, figure 2-3, 2-5, and PCF growth curve in figure 2-2 were done by M.B.Y..

2.1 ABSTRACT

Varicella-zoster virus (VZV) open reading frame (ORF) 66 encodes a serine/threonine protein kinase that is not required for VZV growth in most cell types, but is needed for efficient growth in T cells. The ORF66 kinase affects nuclear import and virion packaging of IE62, the major regulatory protein, and is known to regulate apoptosis in T cells. Here, we further examined the importance of ORF66 using VZV recombinants expressing green fluorescent protein (GFP)-tagged functional and kinase-negative ORF66 proteins. VZV with truncated or kinase-inactivated ORF66 protein were marginally reduced for growth and progeny yields in MRC-5 fibroblasts, but were severely growth and replication impaired in low passage primary human corneal stromal fibroblasts (PCF). To determine if the growth impairment was due to ORF66 kinase regulation of IE62 nuclear import, recombinant VZV were made that expressed IE62 with alanine residues at S686, the suspected target by which ORF66 kinase blocks IE62 nuclear import. IE62 S686A expressed by the VZV recombinant remained nuclear throughout infection and was not packaged into virions. However, the mutant virus still replicated efficiently in PCF cells. We also show that inactivation of the ORF66 kinase resulted in only marginally increased levels of apoptosis in PCF cells, which could not fully account for the cell-specific growth requirement of ORF66 kinase. Thus, the unique short region VZV kinase has important cell type-specific functions which are separate from those affecting IE62 and apoptosis.

2.2 INTRODUCTION

Varicella-zoster virus (VZV) is a highly communicable human alphaherpesvirus that causes chickenpox following a primary infection and herpes zoster (“shingles”) following reactivation from neuronal latency. Current models (106-108) predict that VZV infects many cell types in the course of primary pathogenesis, including epithelial cells, fibroblasts, keratinocytes, T lymphocytes, dendritic cells, monocytes and sensory neurons (33, 137). Furthermore, VZV reactivation from latency leads to viral replication in neuronal and non-neuronal cells in the sensory ganglion, and in skin tissues at multiple locations belonging to the affected dermatome. Reactivation may also lead to VZV replication in ocular tissues. Reactivation involving the ophthalmic division (division V1) of the trigeminal nerve occurs in approximately 10-25% of zoster cases, a condition second only in frequency to thoracic zoster (155). It causes herpes zoster ophthalmicus (HZO), a condition that leads to severe ocular diseases in both anterior and posterior compartments, which may ultimately threaten vision . Two-thirds of HZO patients report serious ocular complications, most commonly involving the cornea(155). VZV DNA, antigen and replication have been found in the corneal epithelium at the ocular cell surface, as well as in stromal keratocytes that sparsely populate the stroma to form an interconnected network in the clear extracellular matrix (141, 216). VZV has also been found in the vitreous fluids and the retinal layers (155, 216). As such, VZV genes affecting viral replication in ocular cell types have important implications for ocular disease.

VZV encodes two serine/threonine (S/T) specific protein kinases, from ORF66 and ORF47, which have been shown to be dispensable for replication in many cultured cells used for VZV growth (73-74). Both kinases, however, have important roles that are needed for viral growth in specific cell types (14, 80). Disruption or inactivation of the ORF66 protein kinase

leads to minimal impairment of VZV growth in MeWo cells, but significant growth defects in T cells, both in culture (199) and in human thymus/liver xenografts in severe combined immunodeficiency (SCID-hu) mice (133, 185-186). The functional roles directing the growth requirement of ORF66 in T cells are not yet clear. ORF66 affects several host cell processes, including pathways that lead to the downregulation of surface class I major histocompatibility complex (MHC-I)-associated antigen presentation (1, 53). In T cells, ORF66 modulates the interferon (IFN) γ -induced activation of the IFN signaling pathway (186), and inhibits virus-induced apoptosis (57, 58). Apoptosis is also inhibited by ORF66 orthologues (US3 kinases) in several alphaherpesviruses, including herpes simplex virus type 1 (HSV-1), HSV-2, and pseudorabiesvirus (PRV) (9-10, 48). Loss of ORF66 reduced VZV nucleocapsid production in T cells (186), but did not lead to the accumulation of virions in the nuclear membrane seen in HSV and PRV lacking US3. HSV US3 is thought to be involved in the breakdown of the nuclear lamina to facilitate primary envelopment and egress of the nucleocapsid across the nuclear membrane (109, 138). Several additional functions have been attributed to specific US3 kinases, but it is not known if ORF66 shares these functions. These include modulation of the cytoskeletal actin structure (56), and in HSV-1, modification of histone deacetylase function (162).

The only well-characterized target of the ORF66 protein kinase is the IE62 regulatory protein, orthologous to the well-studied HSV ICP4. IE62 is encoded by a diploid gene (ORF62 and ORF71) and is a 1310 residue phosphoprotein with strong transcriptional transactivator functions. It activates all VZV genes studied to date and can positively or negatively autoregulate its own promoter in transfection assays, depending on the cell type (157-158). Functions of IE62 are predicted to be similar to HSV-1 ICP4, because IE62 can

complement HSV-1 ICP4 deletion mutants and partly replace ICP4 in the context of the HSV-1 genome (51). ICP4 facilitates the recruitment of cellular activating and basal transcriptional factors to viral promoters to enhance RNA polymerase II-mediated transcription (228). In VZV infections, IE62 is at first nuclear, but transitions to the cytoplasm as infection progresses to a predominantly cytoplasmic distribution at late stage infection. Unlike HSV-1 ICP4, IE62 is an abundant tegument protein incorporated at levels approximately 50% of the major capsid protein (100). Virion packaging requires the ORF66 kinase, as kinase-negative mutant VZV fail to accumulate IE62 in virions (99-100). In co-expression studies, ORF66 kinase phosphorylates IE62 directly *in vitro* at two sites, mapped to serine residues 686 (S686) and S722. IE62 protein containing a S686A mutation does not accumulate in the cytoplasm in the presence of the ORF66 kinase, strongly suggesting that the ORF66 kinase phosphorylation of S686, immediately adjacent to the IE62 nuclear localization signal, drives IE62 exclusion from the nucleus (52, 99). Recent studies have suggested that the ORF66 kinase is not the only means by which IE62 can accumulate in the cytoplasm, since T cells infected with VZV lacking ORF66 kinase still show cytoplasmic forms of IE62 (185). This suggests that a host cell component may be involved in the cytoplasmic accumulation of IE62 in infection.

Recently, we detailed the development of recombinant VZV which express enhanced green fluorescent protein (GFP) tagged to the amino terminus of either functional or truncated ORF66 protein (53). Using these and a VZV expressing a kinase-inactivated ORF66 protein, we show that VZV lacking ORF66 kinase activity fail to grow in PCF cells. The ORF66 growth requirement is, however, separate from its role in regulating IE62 nuclear import to enable virion packaging. Furthermore, while cells infected with VZV expressing inactivated ORF66 show higher levels of apoptosis in PCF cells, this does not account for the failure of

ORF66 kinase- negative VZV to replicate in this cell type. PCF cells represent the first non-lymphocytic cell type in which the kinase has a critical role for VZV replication.

2.3 MATERIALS & METHODS

2.3.1 Cells.

MRC-5 (human lung fibroblasts) (ATCC, Manassas, VA) and MeWo cells (human melanoma cell line; kindly provided by C. Grose, University of Iowa, Iowa City) were maintained and used to grow VZV as described previously (52). Primary corneal stromal fibroblasts (PCF) were derived through the Tissue Culture and Morphology Core Module of the Department of Ophthalmology at the University of Pittsburgh. All primary cells were isolated under protocols approved by the University of Pittsburgh Committee for Oversight on Research Involving the Dead (CORID). Briefly, discarded donor rims of human corneas for transplantation were delivered under anonymous condition. The scleral, endothelial and epithelial tissues were removed by mechanical debridement using forceps. Washed corneal stroma was cut horizontally to expose internal stromal tissue to media. Sections were then treated with 1 mg/ml collagenase for 30 s and then washed with 10% fetal bovine serum (FBS) in Dulbecco's Modified Eagle Medium (DMEM) media before placement into plastic culture dishes overlaid with a glass coverslip. Following incubation at 37°C under media for 2-3 days, cells on the coverslip and plastic support were trypsinized and passaged twice before being mixed with other donor fibroblasts and frozen in aliquots under liquid nitrogen. PCF cells were used in experimental studies within 5-9 passages and were maintained in Dulbecco's Modified Eagle Medium

Nutrient Mixture F-12 (Ham) (1:1) containing sodium bicarbonate and sodium pyruvate (Invitrogen) supplemented with 10% FBS and antibiotic/antimycotic mixture (100 U/ml Penicillin G, 100 µg/ml Streptomycin , and 0.25 µg/ml Fungizone; Gemini Bio-Products).

2.3.2 VZV and derivation of rVZV

VZV used here is based on the parent of Oka vaccine (pOka). The construction and derivation of VZV.GFP-66 and VZV.GFP-66s from pOka-based cosmids have been detailed previously (53). These express amino-terminal GFP-tagged functional ORF66 protein or one that has been disrupted by insertion of stop codons at residue 84, respectively. The same cloning procedure detailed in that study was used to derive VZV.GFP-66kd, which contains GFP-tagged ORF66 protein with two highly conservative changes in the catalytic loop domain of the kinase (D206E, K208R) (98). The derivation of a rescuant VZV was carried out by subcloning a unique SgrAI - AvrII fragment from the pSpe23 cosmid that was used to derive VZV.GFP-66kd into a modified pUC19 derivative containing sites for SgrAI and AvrII (53). The AvrII-BamHI fragment within this construct that contains the ORF66 promoter and amino terminal portion of ORF66 with the inactivating mutations was replaced with the same corresponding DNA fragment containing functional GFP-tagged ORF66 (53). The SgrAI-AvrII fragment was then reengineered back into the pSpe23 cosmid to generate pSpe23GFP66rsc, which was then used in conjunction with pFsp73, pSpe14 and pPme2 to derive rVZV designated VZV.GFP-66Rsc.

Additional rVZV were derived from viral DNA cloned as a bacterial artificial chromosome (BAC) containing the entire pOka genome (204). To generate S686A changes in ORF62 and ORF71, we conducted mutagenesis using the markerless two-step recombination

system, detailed previously (205). All oligonucleotides were obtained from IDT, Inc. (Coralville, IA) and were SDS-PAGE purified by the manufacturer. PCR was performed with Expand proofreading polymerase (Roche Diagnostics, Indianapolis, IN). Two oligonucleotides used for mutagenesis were S686AF 5'-GTGTGTCCACCGGATGATCGTTTACGAACTCCGCGCAAGCGCAAGGCTCAACCGGTCGAGAGCAGAAGCCTCCTCGACAAAGGATGACGACGATAAGTAGGG-3' and S686AR 5'-CGACGGGTGTCTCCCTAATCTTGTCGAGGAGGCTTCTGCTCTCGACCGGTTGAGCCTTGCCTTGCGCGGAGTTCGTAAACAACCAATTAACCAATTCTGATTAG-3' (underlined residues mark the altered sequence discussed in the text). The two oligonucleotides were used to PCR amplify the kanamycin resistance cassette (kan^r) from the plasmid pEP-kanS2 (205) to add the IE62 flanking sequences required for homologous recombination and mutagenesis. The gel purified PCR product was then electroporated into *E. coli* SW105 (a kind gift of N. Copeland, NCI Frederick MD) containing the pOka VZV BAC. Recombination was induced by heating to 42°C for 15 min, and growth of recombinants were selected by plating at 32°C on LB agar plates containing 15 µg/ml kanamycin (kan) and 25 µg/ml chloramphenicol (chm). DNA of individual colonies was mapped for the correct insertion of the cassette (the first recombination occurred in ORF71) by restriction analyses using HindIII digestion. Resolution of the construct to remove the kan^r cassette was achieved by transformation of the plasmid pBAD-*I-SceI* into the SW105 cells containing the modified VZV BAC, which was then growth-selected on LB-agar plates additionally containing 50µg/ml ampicillin. *I-SceI* expression was induced by growth in liquid culture containing 1% arabinose, and a second round of recombination was induced by heating cultures to 42°C for 15 min. Colonies growing at 32°C on LB agar containing chm, amp and

arabinose were checked for loss of the kan^r cassette by replica plating individual colonies onto plates containing kanamycin. *E.coli* containing the altered BAC were then subjected to a second round of mutagenesis with the same PCR fragment, selecting for homologous recombination into ORF62. The BAC DNAs were transfected into MeWo cells using Lipofectamine 2000 (Invitrogen Corp, Carlsbad, CA) and derived VZV plaques were visible after 3-5 days of incubation at 35°C. VZV containing a single change in ORF71 was termed VZV.71.S686A, whereas rVZV with mutations in both IE62 genes was termed VZV.IE62(S686A)². The insertion of AgeI sites into both genes was confirmed by restriction analyses. The presence of the changes in VZV was carried out through Southern blotting of AgeI digested infected cell genomic DNA (gDNA), purified from VZV-infected MeWo cells using Qiagen's Blood and Cell Culture DNA Midi Kit (Valencia, CA) onto a positively charged nylon membrane (Nytran SuPerCharge, Schleicher & Schuell, Keene, NH). The 1018 bp fragment isolated from an AgeI digest of pKCMV62 DNA was used as a probe following radiolabeling with dCTP- $[\alpha\text{-}^{32}\text{P}]$ (Perkin Elmer, Waltham, MA) and random prime labeling kit (Roche Diagnostics Corp., Indianapolis, IN).

2.3.3 Antibodies & Immunological Procedures

Rabbit polyclonal antibodies to IE62 (99) and to VZV proteins ORF 4, 61, and 63 were detailed previously (97). Previously detailed anti-peptide antibodies to ORFs 10 (97) and 29 (101) were also used in this work. Antibodies to ORF 9 (26) were a kind gift of W.T. Ruyechan, SUNY at Buffalo NY and antibodies to ORF 47 were a kind gift of C. Grose (University of Iowa, Iowa City, IA). Mouse antibodies to β -actin (Sigma, St. Louis, MO) and to ORF40 major capsid protein (MCP) (Virusys Corp., Sykesville, MD) were purchased commercially. All

immunofluorescent staining procedures were carried out as described previously (53), and antibodies were detected using goat anti-rabbit immunoglobulin G-antibody conjugated to Alexa Fluor 546 or goat anti-mouse immunoglobulin G-antibody conjugated to Alexa Fluor 488. Immunofluorescence was visualized using a Nikon Eclipse TE2000-E epifluorescence microscope equipped with a xenon lamp.

2.3.4 Analysis of viral growth

VZV for growth rate studies was prepared from aliquoted and titrated stocks of virus in MeWo cells stored in liquid nitrogen. Stocks were 80-95% infected at the time of preparation, to minimize addition of uninfected cells. Viral growth rates were determined using similar procedures detailed elsewhere (53). Briefly, confluent monolayers of cells were established, and infected with cell-associated VZV at an estimated 300 infectious centers (IC) per well. Serial dilutions of the infecting virus were immediately titrated on MeWo cell monolayers to determine the exact titer of the inoculum. At specific times, cells were trypsinized, diluted in fresh media and added to fresh MeWo monolayers. At 4-5 days post-infection (p.i.) plaques were quantified using either autofluorescence of GFP, or were immunofluorescently stained for IE62. Statistical analysis to compare overall growth curves was done using Dunnett's multiple comparison test using GraphPad Prism software v. 4.0. For growth curve enumeration by flow cytometry, a similar setup was established, except that trypsinized cells were immediately fixed in 1% paraformaldehyde, washed in 1X PBS and counted using a FACSaria cytometer/cell sorter (Becton-Dickinson). GFP gates were set using mock infected cell controls.

2.3.5 Virion purification and characterization

Virion purification was performed as described previously (21). Briefly, monolayers of MeWo cells infected with VZV were grown at 35°C until showing ~80% cytopathic effect. Harvested cells were washed with ice-cold PBS containing a protease inhibitor cocktail (Complete EDTA-free; Roche Diagnostics, Indianapolis, IN), and subjected to dounce homogenization to obtain cytoplasmic extract. Virion particles were also collected from the cell-free media by high speed centrifugation and combined with cytoplasmic fractions. Virions were purified by velocity gradient ultracentrifugation for 2 hours (hrs) at 17,000xg on 5-15% Ficoll gradients made in PBS. The diffuse virion band migrating approximately 2/3rd down the tube was harvested, concentrated by centrifugation, and resuspended overnight at 4°C in PBS containing protease inhibitors. Virions were then subjected to 10-50% sucrose gradients made in PBS, which were then fractionated using a piston gradient fractionator. For protein analyses, proteins were precipitated from the fractions with 10% trichloroacetic acid, washed with ice-cold acetone and resuspended in 100 µl protein gel loading buffer for SDS-PAGE. For immunoblotting, proteins were separated by SDS-PAGE, transferred to Immobilon-P membrane (Millipore, Billerica, MA) and probed with rabbit polyclonal antibodies to ORF10 to identify the peak virus fractions. These were pooled for further studies for VZV proteins. Virion samples for protein stain were run on 4-15% Tris-HCl linear gradient polyacrylamide SDS gels (Bio-Rad Laboratories, Hercules, CA), and stained with SYPRO Ruby Protein Gel Stain (Invitrogen, Carlsbad, CA). Proteins were visualized using a Bio-Rad Fluor-S MultiImager.

2.3.6 Apoptosis Assay

Confluent cells were seeded onto 6 well plates, and infected with VZV at a multiplicity of infection (MOI) of approximately 0.02 or mock infected. At times indicated, cells were harvested and stained according to manufacturers' instructions for APC Annexin V (BD Pharmingen). Briefly, cells were washed twice in cold PBS, resuspended in the supplied binding buffer, and counted. Approximately 1×10^5 cells were then stained with APC Annexin V and 7-Amino-Actinomycin D (7-AAD). Stained cells were analyzed by flow cytometry and GFP gates were set using mock infected cell controls. Cells were characterized and analyzed using BD FACSDiva v4.1 software. Experimental values are the fraction of GFP positive cells showing APC Annexin V positive stain as a percentage of the total GFP positive cells. Values represent the mean of three identical experiments. Statistical analysis was done by Student's *t*-test using GraphPad Prism software v4.0.

2.4 RESULTS

2.4.1 ORF66 is required for efficient growth in PCF cells

The VZV ORF66 protein kinase is categorized as a non-essential gene in culture, yet recent studies indicate it is needed for VZV growth in T cells . To explore the growth properties of VZV with or without ORF66 kinase in other cell types, we employed two fluorescent VZV recombinants, which express a GFP-tagged and functional ORF66 protein or one that is disrupted at residue 84. GFP has no apparent effect on VZV growth when compared to parent

pOka virus (53). We also generated VZV which expressed the full length ORF66 protein in which the kinase was inactivated by two point mutations in the catalytic loop (VZV.GFP-66kd), as well as a rescuant of this change (VZV.GFP-66Rsc) in which the two point mutations were reversed. These mutations abrogated the ability of ORF66 to induce accumulation of cytoplasmic IE62 or phosphorylate IE62 peptides in co-expression assays (99). The rescuant was phenotypically indistinguishable from VZV.GFP-66 and parental Oka in all assays examined.

IE62 produced by viruses expressing functional ORF66 protein in both MRC-5 cells (Fig. 2-1A) and PCF cells (Fig. 2-1B) showed predominantly cytoplasmic forms in most GFP-positive cells (Fig. 2-1A. a,c,j,l & Fig. 2-1B. a,c,j,l). In contrast, IE62 expressed by VZV.GFP-66kd and VZV.GFP-66s displayed a predominantly nuclear localization in both cell lines in GFP positive cells (Fig. 2-1A. d,f,g,i & Fig. 2-1B. d,f,g,i). GFP-66s showed a diffuse cellular localization (Fig. 2-1A. h,i & Fig. 2-1B. h,i), but GFP-66kd protein exhibited a distinct predominantly nuclear localization in both cell lines (Fig. 2-1A. e,f & Fig. 2-1B. e,f) that was clearly different from functional kinase produced by VZV.GFP-66, suggesting that the kinase activity of ORF66 affected its cellular localization. Some cells displayed marked nuclear rim accumulations of GFP-66kd.

In addition to differences in cellular distribution patterns, it was obvious that ORF66-negative VZV formed tiny plaques on PCFs that involved far fewer cells. In MRC-5 cells, plaque size of all four viruses increased in size during the duration of the study (up to 7 days post-infection), although plaques of VZV not expressing kinase were slightly smaller (data not shown). In PCF cells, plaques of the VZV lacking the kinase formed very small centers of infection at day 1-2 that involved 10-20 cells, but these failed to increase further in size,

suggesting that infections were initially established but failed to progress. We also found severe growth impairment of a previously described ORF66 kinase-deficient VZV made in the Vaccine Oka background. To quantify this more accurately, we determined yields of progeny virus on both cell types for all four viruses. In MRC-5 cells, VZV without the kinase were marginally impaired for virus growth as compared to VZV.GFP-66, yielding 0.4 to 0.7 log reduction at 96 hours (hrs) post-infection (p.i.) (Fig 2-2A). Maximal titers of VZV.GFP-66s and VZV.GFP-66kd were lower (7.5×10^3 and 4.8×10^3 IC, respectively) than that of VZV.GFP-66 (2.0×10^4 IC) and VZV.GFP-66Rsc (2.2×10^4 IC), at 96 hrs p.i. However, the overall growth curve differences compared to VZV.GFP-66 were not statistically significant ($p > .05$). In contrast, a much greater impairment for growth of ORF66-negative viruses was observed in PCF cells. While VZV.GFP-66 and VZV.GFP-66Rsc reached maximum titers of 3.2×10^4 and 4.0×10^4 IC respectively at 96 hrs p.i., VZV.GFP-66s and VZV.GFP-66kd maximal titers peaked at 48 hrs (1.1×10^3 and 4.3×10^2 IC, respectively) and declined thereafter (Fig. 2-2A). Extension of the growth curves to seven days did not lead to any increases in viral titer (data not shown). These results indicate that PCF cells do not permit efficient growth of VZV if the ORF66 kinase is not functional.

The growth impairment in PCF cells was also detected when flow cytometry was used to quantify GFP-positive cells as an indicator of infection. In MRC-5 cells infected with VZV.GFP-66, greater than 40% of cells showed GFP positive signals by day 9 p.i. (Fig.2-2B). ORF66 kinase-negative viruses showed a reduced rate of increase in the number of GFP-positive cells, with VZV.GFP-66kd showing marginally greater impairment. However, in PCF cells, VZV with non-functional kinase showed only a very small increase in the number of GFP positive cells at day 1, which then subsequently diminished. VZV.GFP-66 infection resulted in a

reduced rate of increase of GFP positive cells as compared to that seen in MRC-5 cells, but this reflects a slightly reduced growth rate in PCF cells (see Figure 2-2a) rather than a loss of GFP positive cells in flow cytometry. We did not find there was untoward significant loss of cell structure due to mechanical damage in these studies. Thus, these results reflect growth curve studies and further establish that PCF cells are unable to support VZV replication in the absence of functional ORF66 protein kinase.

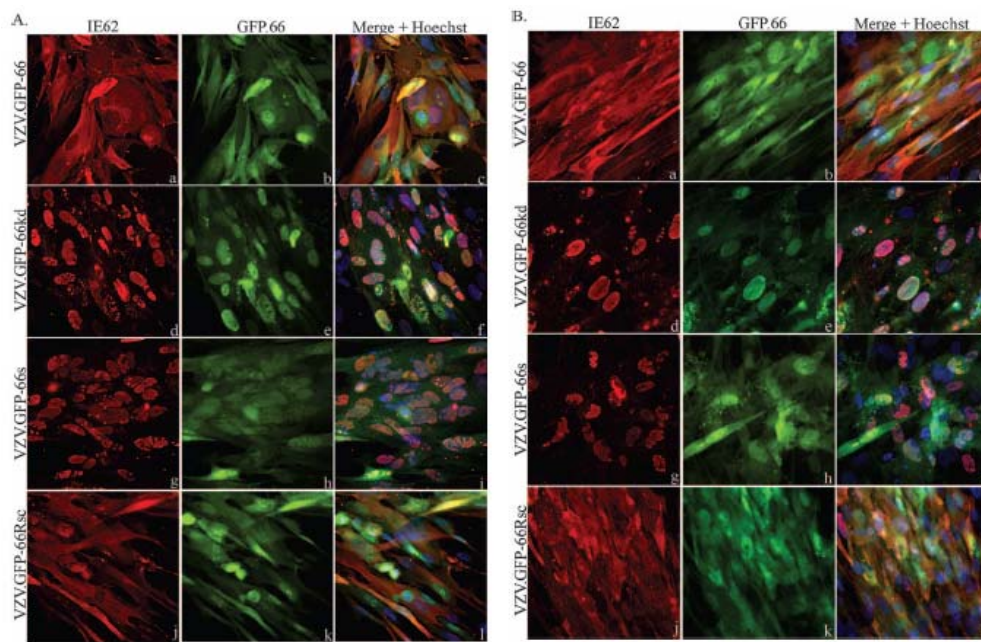


Figure 2-1. IE62 cellular distribution and GFP expression in VZV-infected cells

IE62 cellular distribution and GFP expression in VZV-infected cells. MRC-5 cells (A) or PCF cells (B) were infected at an MOI of 0.0005 with MeWo cell-grown VZV.GFP-66 (panels a-c); VZV.GFP-66kd, expressing complete GFP-tagged kinase-inactivated ORF66 protein (panels d-f); VZV.GFP-66s, expressing GFP tagged to residues 1- 84 of ORF66 (panels g-i); or VZV.GFP-66Rsc (panels j-l). Cells were fixed with 4% paraformaldehyde at 3 days p.i. and immunostained with rabbit anti-IE62, which was then detected with anti-rabbit Alexa Fluor 546 (panels a,d,g,j). ORF66 expression was determined using GFP autofluorescence (panels b,e,h,k). The merge panels (panels c,f,i,l) are overlays of GFP (green), IE62 (red) and nuclei stained with Hoescht dye (blue). Fluorescence images were taken using a 40X objective.

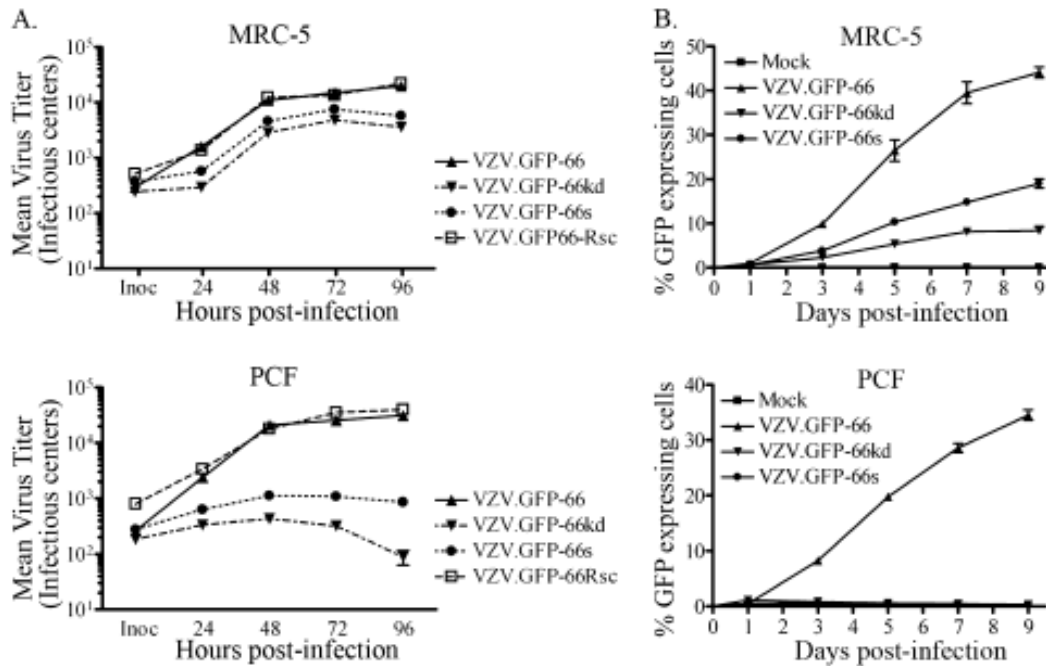


Figure 2-2. Progeny virus growth curves reveal a requirement for ORF66 for VZV growth in PCFs

Progeny virus growth curves reveal a requirement for ORF66 for VZV growth in PCF cells. (A) Growth curves were performed as detailed in Methods, and the titers of the progeny VZV in MRC-5 cells (top) and PCF cells (bottom) are shown. Confluent monolayers were infected at an MOI of 0.001 with VZV.GFP-66 (▲), VZV.GFP-66kd (▼), VZV.GFP-66s (●), or VZV.GFP-66Rsc (□). The inoculum (Inoc) of each virus was immediately determined upon the setup of the studies at time 0 h. At 24, 48, 72 and 96 h post-infection, infected cells were trypsinized and titrated onto subconfluent monolayers of MeWo cells. Plaque formation and enumeration were assessed by fluorescent microscopy at 4-5 days post-infection. X-axis values represent hours post-infection when cells were harvested and Y-axis values represent average total number of infectious centers at each time point. Each data point was determined in quadruplicate, and results represent the mean \pm SE of these values. (B) GFP-positive infected cell numbers fail to increase in PCF cells if the ORF66 protein is disrupted. MRC-5 cells (top) or PCF cells (bottom) in confluent monolayers in 35 mm dishes were infected with VZV.GFP-66 (▲), VZV.GFP-66kd (▼), VZV.GFP-66s (●) at an MOI of 0.001, or mock infected (■). At the day after infection indicated (X-axis), cells were harvested and counted by flow cytometry, gating for GFP-positive cells. The ratio of GFP-positive cells to the total number of cells in the harvested monolayers is expressed as a percentage (Y-Axis). Values represent the mean \pm SE of three parallel but independent values.

2.4.2 Derivation of VZV expressing IE62 protein mutated at the critical ORF66 phosphorylation site.

The most well characterized target of the ORF66 kinase is IE62, the VZV major regulatory protein. In transfection studies, IE62 expressed alone is largely nuclear, but when it is coexpressed with the ORF66 kinase, IE62 accumulates predominantly in the cytoplasm. We have previously shown that the accumulation of cytoplasmic IE62 requires the ORF66 kinase activity, and that the kinase phosphorylates IE62 both *in vivo* and *in vitro* at two residues, S686 and S722. However, IE62 containing S686A changes (but not IE62 containing S722A mutation), were resistant to ORF66 induced cytoplasmic accumulation, and remained predominantly nuclear in cells expressing the ORF66 protein kinase. While it was concluded that ORF66 kinase phosphorylated IE62 at residue S686 to induce its cytoplasmic accumulation, the interaction has not been addressed in the context of VZV infection. It is clear that VZV-infected cells not expressing the ORF66 kinase show only nuclear IE62 (Fig. 2-1A, B) and loss of the kinase abrogates virion packaging of the IE62 protein (52). Thus it was possible that the requirement of the kinase in PCF cells reflected a loss of the cytoplasmic accumulation and virion packaging of IE62.

To test this possibility, we developed recombinant VZV in which the IE62 residue targeted by the kinase, S686, was altered to alanine (VZV.IE62(S686A)²). Our previous studies predict that IE62 with this change would not be regulated by the ORF66 kinase during VZV infection. The mutations were generated in a VZV pOka BAC, and were designed to simultaneously introduce a marker AgeI site with the S686A mutation (Fig. 2-3A). In the parental BAC, AgeI digestion produced a 2-molar 1018 bp fragment, representing an internal fragment of ORF62 and ORF71 (Fig. 2-3B). DNA of BACs engineered to contain the S686A

mutation in only the ORF71 gene showed a loss of one copy of the 1018 bp fragment, while DNA from BACs containing S686A mutations in both the ORF62 and ORF71 genes showed loss of both 1018 bp fragments (Fig. 2-3B). The introduction of the mutation resulted in the generation of two smaller AgeI DNA fragments of 605 and 413 bp. While these could not be easily identified in ethidium bromide stained gels (Fig. 2-3B) due to small size and comigration with other DNA fragments, we confirmed their presence by Southern blot analyses. Viruses derived from each BAC were used to generate infected cell DNA, and AgeI digests were examined by Southern blotting and probing with a radiolabeled 1018 bp AgeI DNA fragment (Fig. 2-3C). As expected, a prominent 1018 bp fragment was detected in pOka, one copy was reduced to 605 and 413 bp fragments in VZV with the ORF71 mutation, and both copies were converted to the smaller fragments in DNA of VZV.IE62(S686A)². VZV with single and double copies of the S686A mutations grew and formed plaques that were similar in size and appearance to that formed by BAC-derived pOka VZV in MeWo cells. We then confirmed the presence of the S686A mutations by DNA sequencing.

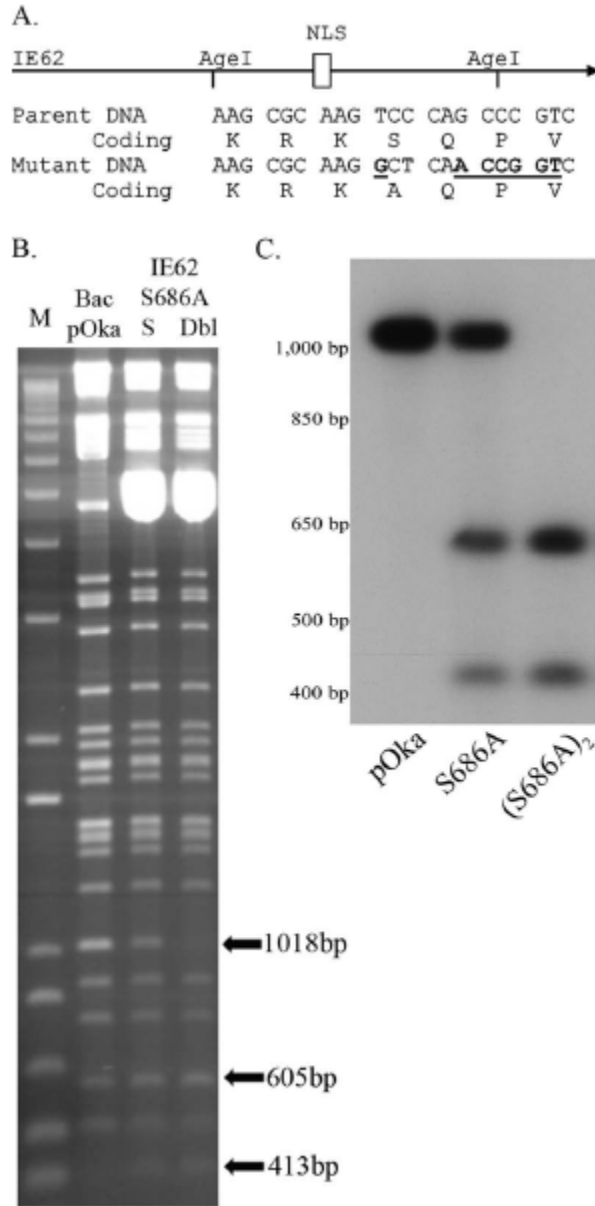


Figure 2-3. DNA characterization of BAC DNA and of VZV-infected cell of the recombinants VZV.71.S686A and VZV.IE62(S686A)²

DNA characterization of BAC DNA and of VZV-infected cell DNA of the recombinants rVZV.71.S686A and VZV.IE62(S686A)². (A) Schematic representation of the mutagenesis of IE62 residue S686. The top portion represents IE62 and its nuclear localization signal (NLS), with the presence of the existing AgeI sites. Part of the DNA sequence and encoded amino acids of the target region in the parental DNA and in mutant DNA are shown underneath. The DNA sequence of the alterations induced by mutagenesis that introduce the novel AgeI site is underlined. (B) 1.2% agarose gel showing DNA fragments generated by AgeI digestion of the VZV BAC DNAs derived from pOka and BACs containing the mutation in ORF71(S) or in both ORF62 and ORF71 (DbI). M is the DNA size marker (1Kb plus, Invitrogen). The abundant 5 Kbp DNA seen in the mutant BACs represents the pBAD-*I-SceI* plasmid used to select for loss of the kan^r cassette. The positions of the 1018 bp fragment in the pOka BAC and

the resultant smaller digestion fragments in the mutants are arrowed. (C) Southern blot of rVZV-infected MeWo cell genomic DNA, digested with AgeI and probed with a dCTP- $[\alpha\text{-}^{32}\text{P}]$ -labeled 1018 bp fragment obtained from an AgeI digest of pKCMV62. The autoradiograph shows DNA of VZV pOka, the VZV.71.S686A and VZV.IE62(S686A)². The approximate sizes of DNA markers are indicated to the left.

2.4.3 VZV.IE62(S686A)² IE62 remains nuclear in the presence of functional ORF66.

The prediction was that IE62 expressed from VZV.IE62(S686A)² would remain nuclear throughout viral infection, because IE62 could not be phosphorylated by the ORF66 protein kinase at the site affecting its cellular distribution (52). While VZV.GFP-66 formed abundant cytoplasmic forms of IE62 in MeWo cells, VZV.IE62(S686A)² expressed IE62 that remained exclusively nuclear at all stages of infection, even in cells expressing the late ORF40 major capsid protein (Fig. 2-4A). VZV.71.S686A produced IE62 that showed an intermediate phenotype (data not shown). Extension of these studies to MRC-5 and PCF cells revealed that IE62 remained exclusively nuclear in both cell types, fully overlapping the Hoescht nuclear stain (Fig. 2-4B). Thus, it is clear that residue S686 of IE62 is critical for ORF66 to regulate IE62 nuclear import in the context of viral infection of several cell types.

The predominantly nuclear localization of IE62 in VZV.IE62(S686A)²-infected cells is similar to that seen for ORF66 kinase-negative VZV. To confirm the integrity of the ORF66 protein kinase, we sequenced the ORF and its promoter and also evaluated the ORF66 gene in VZV.IE62(S686A)² by PCR amplifying it, placing it into an expression vector and then examining it for the ability to induce cytoplasmic forms of IE62 in co-expression studies. As the kinase retained the ability to regulate the cellular localization of IE62 (data not shown), we conclude that the exclusively nuclear phenotype of IE62 was due to a loss of the IE62 S686 site rather than a spurious kinase-inactivating mutation in the ORF66 protein.

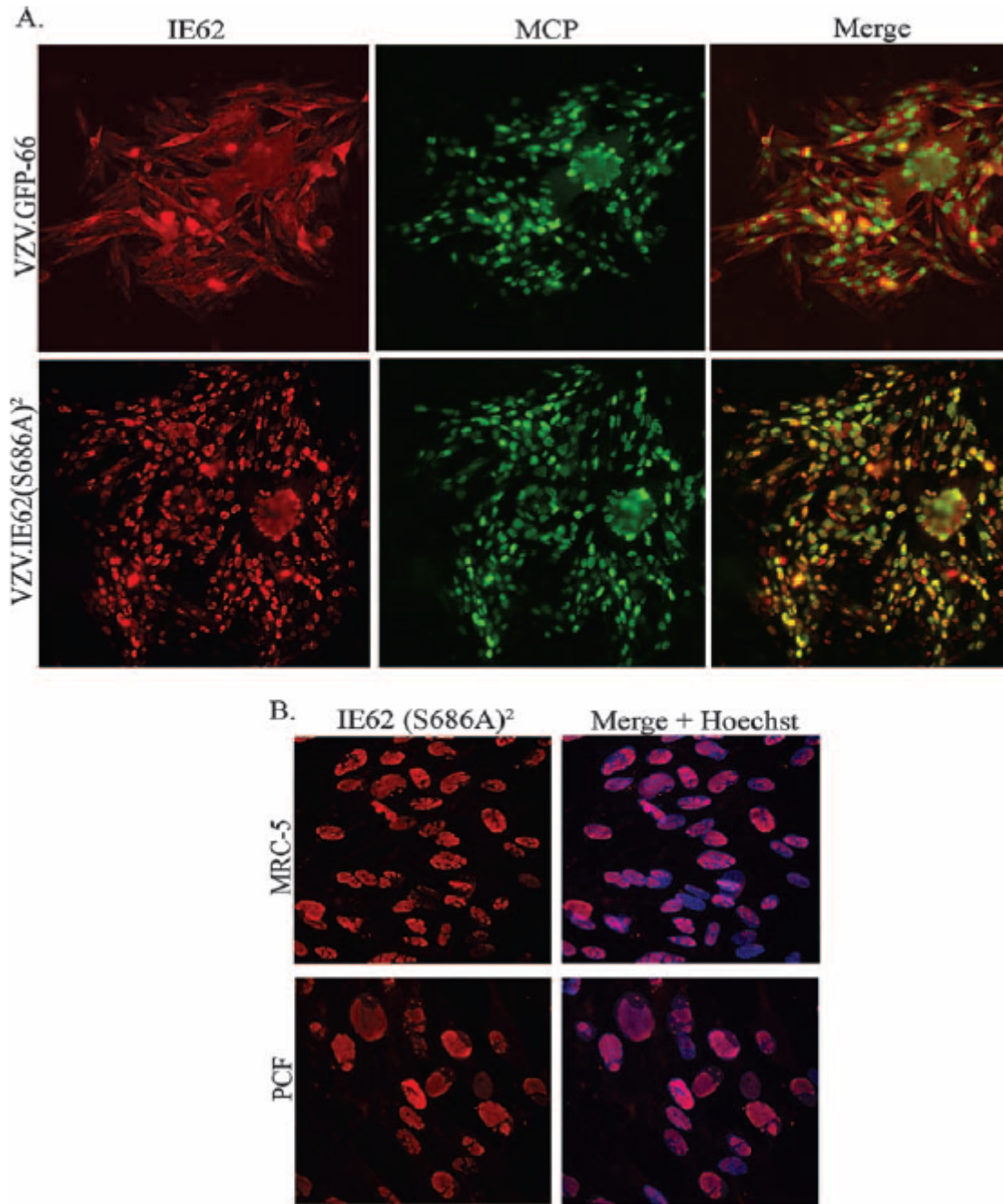


Figure 2-4. IE62 localizes to the nucleus in VZV.IE62(S686A)² - infected cells

(A) Scanned images of VZV.GFP-66 and VZV.IE62(S686A)²-infected MeWo cell plaques, immunostained with rabbit anti-IE62 and mouse anti-major capsid protein (MCP), which was then detected with anti-rabbit Alexa Fluor 546 or anti-mouse Alexa Fluor 488, respectively. The merge panels are overlays of IE62 (red) and MCP(green). (B) Immunofluorescence images of VZV.IE62(S686A)²-infected MRC-5 (top row) or PCF cells (bottom row) immunostained for IE62 (red). Nuclei detected using Hoescht stain (blue) are displayed in the merge images. All cells were fixed at 3 days p.i. with 4% paraformaldehyde and images were taken using a 40X objective.

2.4.4 Tegument proteins of VZV.IE62(S686A)²

Previous studies demonstrated that genetic disruption of the ORF66 kinase in VZV resulted in the IE62 protein remaining completely nuclear throughout infection, and simultaneously abrogated the packaging of IE62 into virions, leading us to conclude that the cytoplasmic distribution of IE62 during infection was required for its virion packaging (98). The predominantly nuclear IE62 seen in VZV.IE62(S686A)²-infected cells would also be predicted to abrogate IE62 packaging into VZV.IE62(S686A)² virions. To examine this possibility, we infected MeWo cells with VZV.IE62(S686A)² or VZV.GFP-66 and used methods established previously to obtain purified virions from the cytoplasmic extracts (98). We consistently obtained lower levels (approximately 1/3rd to 1/5th) of VZV.IE62(S686A)² virions compared to virions obtained from VZV.GFP-66 infected cells, based on total protein content of the Ficoll gradient-purified virion fraction, although virion bands migrated to the same relative position in the gradients. Comparison of Ficoll gradient-purified virions to cell extracts of VZV.GFP-66 (Fig. 2-5A), showed that virions contained a prominent polypeptide of 155 kDa, the major capsid protein, and had a virion protein profile that was similar to that previously reported. We noted that two polypeptides of 175 kDa and 180 kDa seen only in infected cell extracts (arrowed in Fig. 2-5A) were likely the predominant forms of IE62 seen in infected cells in a past study. Comparison of 15% of the total Ficoll gradient virion preparations from VZV.GFP-66 with 30% of the total virion preparation from VZV.IE62(S686A)²-infected cells revealed that both virions had similar protein profiles, with the exception that the 175 kDa polypeptide was not seen in VZV.IE62(S686A)² virions. This is the size of virion-packaged IE62 reported previously (98).

To further assess virion protein content, virions were then purified on sucrose gradients, which were subsequently fractionated. Fractions containing virions (identified by probing SDS-

PAGE separated proteins in each fraction for ORF10 protein) were restricted to three fractions from the central region of each gradient. The total protein stain for VZV.GFP-66 virions was highly similar to that seen from the Ficoll gradient, although the low levels of virions obtained for VZV.IE62(S686A)² virions did not permit a total protein comparison. It is possible that virions produced by VZV.IE62(S686A)² may have reduced stability, although this has not been investigated further. Based on the levels of the ORF10 major tegument protein, proteins of the sucrose gradient-purified virions were normalized, and probed for additional VZV proteins. The absence of non-structural proteins encoded by ORF29 (the homologue of HSV ICP8, which is also non-structural) and ORF61 established that the preparations were not contaminated with infected cell material (Fig. 2-5B). Virions of VZV.IE62(S686A)² showed no reactivity to IE62 specific antibodies, although IE62 was present in VZV.GFP-66-infected whole cell extracts and virions. This supports the conclusion that the major immediate early regulatory protein is not packaged into VZV.IE62(S686A)² virions, and that virion packaging of IE62 required IE62 localization to the cytoplasm.

The VZV tegument contains additional VZV regulatory proteins encoded by ORFs 4, 10, 47, 62, and 63. The ORF9 protein, which has recently been shown to interact with IE62, is also a suspected structural protein, based on its orthologue, the major tegument protein VP22 in HSV-1. We conjectured that the abrogation of cytoplasmic IE62 accumulation may also impair the tegument incorporation of some of these proteins, particularly the proteins encoded by ORFs 4, 9, 47 and 63, which are known to physically interact with IE62. Probing of blots of ORF10-normalized virion proteins of VZV.GFP-66 and VZV.IE62(S686A)² revealed that ORF4 and ORF47 proteins were present at similar levels for each virus (Fig. 2-5B). The ORF9 protein was incorporated into virions as predicted, and multiple forms of the protein were seen in both

infected cell extracts and in virions. Interestingly, we consistently observed from two studies that VZV.IE62(S686A)² virions exhibited increased levels of ORF9 and ORF63 proteins. Interestingly, we did not detect actin as a component of VZV virions from either virus. From this work, we conclude that the mutation of S686A in both copies of IE62 abrogated the incorporation of IE62 into virions. While virion packaging of other tegument-associated regulatory proteins did not require virion IE62, some appeared to compensate for the absence of tegument IE62.

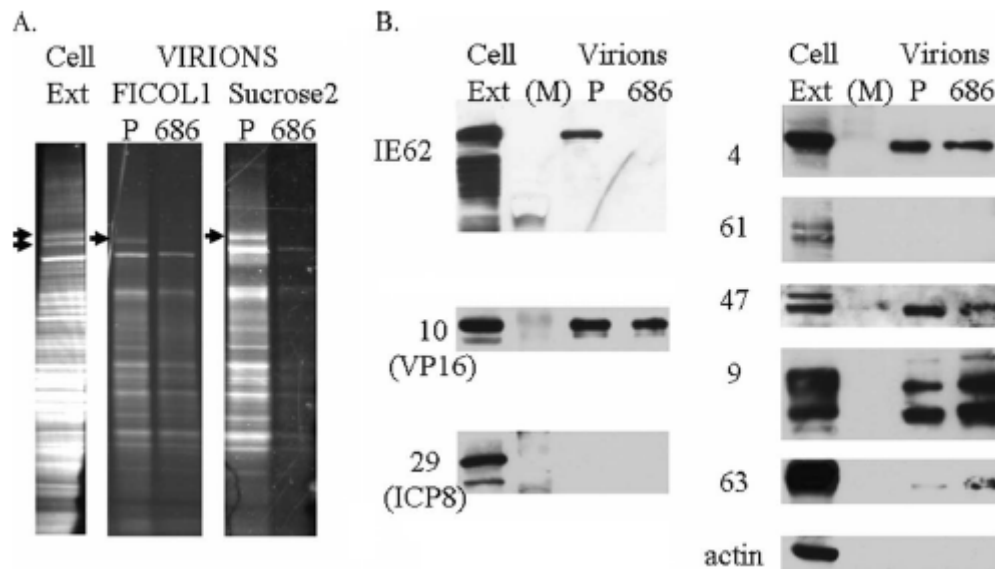


Figure 2-5. VZV.IE62(S686A)² does not incorporate IE62 into the virion tegument

(A) Sypro Ruby staining of purified VZV virion particles harvested from infected MeWo cells following separation on a 4-15% Tris-HCl linear gradient SDS gel. A MeWo-infected cell extract is also shown (cell ext), with arrows indicating two suspected forms of IE62. Virion particles were obtained from cells infected with VZV.GFP-66 (P) or VZV.IE62(S686A)² (686). Virions are shown following purification after the 5-15% Ficol gradient step (Ficol 1), and after the second fractionation on 10-50% sucrose gradients (Sucrose 2). Arrows depict the 175 kDa protein in the VZV.GFP-66 virion fractions. (B) Immunoblot analysis of cell extracts and sucrose gradient purified virions that were equalized based on the abundance of ORF10 protein, and then probed with rabbit antibodies to VZV proteins derived from ORFs 4, 9, 10, 29, 47, 61, 62, 63 and β -actin. The HSV homologs of some VZV proteins are indicated in brackets. M indicates the marker lane.

2.4.5 Growth comparisons of VZV.IE62(S686A)² and rVZV lacking functional ORF66 in PCF cells

The previous data established that VZV.IE62(S686A)² showed a similar phenotype to VZV deficient in functional ORF66. However, comparative reassessment of growth curves of VZV.IE62(S686A)² revealed differences to VZV.GFP-66kd, and VZV.GFP-66s in PCF cells (Fig. 2-6). Specifically, by 96 hrs p.i., VZV.IE62(S686A)² grew to titers in PCF cells (2.2×10^3 IC) that were only marginally lower than those of VZV.GFP-66 (5.2×10^3 IC). In contrast, VZV.GFP-66s and VZV.GFP-66kd showed little increase in progeny virus titers subsequent to 24 hrs p.i., and at 96 hrs p.i, titers were 3.4×10^1 and 7.3×10^1 IC, respectively. The difference between titers of ORF66-negative viruses and VZV.GFP-66 were statistically significant ($p < .01$), mirroring the results shown in Fig.2-2A. As VZV.IE62(S686A)² clearly replicated in PCF cells, we conclude that the critical ORF66 function required for productive VZV growth in PCF cells is independent of its functions in regulating IE62 nuclear import through phosphorylation of the IE62 S686 site. We presume that virions produced in PCF cells by VZV.IE62(S686A)² and by ORF66 kinase-negative VZV do not incorporate IE62 in VZV virions, as IE62 would not localize to the site of tegumentation in the cytoplasm of these cells.

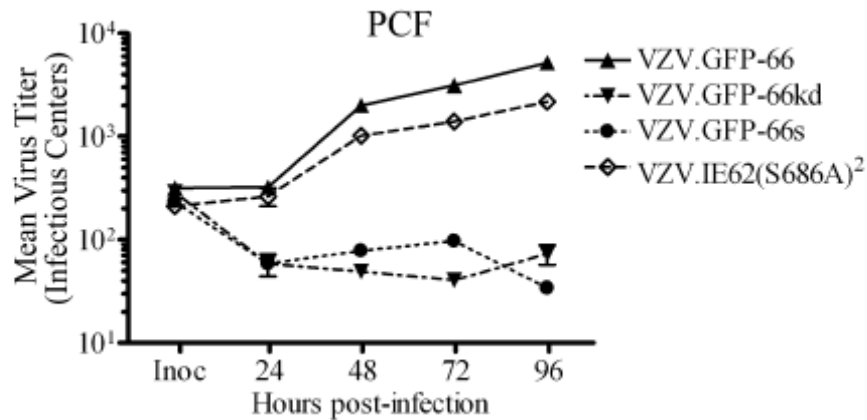


Figure 2-6. Progeny growth curves of VZV.IE62(S686A)², VZV-66, and ORF66 mutants in PCFs

Growth curves were performed as detailed in Fig. 2, using confluent PCF cell monolayers infected with VZV.GFP-66 (▲), VZV.GFP-66kd (▼), VZV.GFP-66s (●), or VZV.IE62(S686A)² (◇) after infection at an MOI of 0.001. To quantify plaques of VZV.IE62(S686A)², cells were fixed in 4% paraformaldehyde at 4-5 days p.i., permeabilized and immunostained with primary rabbit anti-62 antibodies so that plaques could be enumerated using fluorescent microscopy. Inoculant data values represent direct seeding onto MeWo cells on the same day PCF cells were infected. X-axis values represent hrs p.i. when cells were harvested and Y-axis values represent infectious centers. Each data point was done in quadruplicate and represent the mean +/- SE of these values. Growth curves are representative of two independent experiments.

2.4.6 Detection of apoptosis levels in recombinant VZV-infected corneal fibroblasts

Several alphaherpesvirus US3 kinases orthologous to ORF66 have been shown to block apoptosis in response to both the stress of viral infection and to exogenous agents or treatments. Recent studies have indicated that ORF66 inhibits apoptosis in VZV-infected T cells (186), as a fraction of cells infected with VZV lacking ORF66 show higher levels of caspase-3 activation (185). In the context of the corneal stroma, keratocytes are highly sensitive to apoptosis following injury (130, 217, 220). To test the role of apoptosis in the PCF cell-specific growth requirement for ORF66, we assessed MRC-5 or PCF infected cells for the early apoptosis marker Annexin V and the viability stain 7-AAD. Gating for GFP fluorescence enabled assessment of

VZV-infected cells in which the ORF66 promoter was active (Fig.2-7). In MRC-5 cells infected with VZV.GFP-66, indicators of apoptosis were seen in mean levels of 6.5, 10.5, and 18.9 % of GFP-expressing cells at 24, 48, and 72 hrs p.i., respectively. Cells infected with VZV.GFP66-kd displayed almost equivalent levels (9.2, 9.5 and 18.7%) and VZV.GFP-66s levels were slightly lower (6.4, 4.8, and 13.5 %, respectively). Statistical evaluation revealed no significant difference in numbers of cells showing APC Annexin V signal between VZV.GFP-66 and the 66 kinase mutants at any time. In contrast, PCF cells infected with VZV.GFP-66kd showed significantly higher levels of apoptosis (17.5, 13.6, and 19.7 %) as compared to VZV.GFP-66 (8.2, 8.5 and 11.1%) at the 24 and 48 hr time points, although the levels of apoptosis of cells infected with VZV.GFP-66s were not statistically significant at any time point (11.3, 10.5, and 14.0% at 24, 48 and 72 hr p.i.). Longer times of incubation (96 hrs) did not result in any further increase in levels of apoptosis. Of importance, the total levels of cells undergoing apoptosis under all conditions were in the minority, as seen previously in VZV-infected T cells (185). GFP negative cells present in VZV-infected cultures did not show variations in levels of Annexin V staining (data not shown). These results indicate that corneal fibroblasts infected with VZV lacking ORF66 kinase activity do not have dramatically increased levels of apoptosis, although the slightly increased levels of apoptosis in VZV.GFP-66kd may be a contributing factor to its growth phenotype. We conclude that apoptosis cannot fully account for the almost complete loss of viral growth in this cell type.

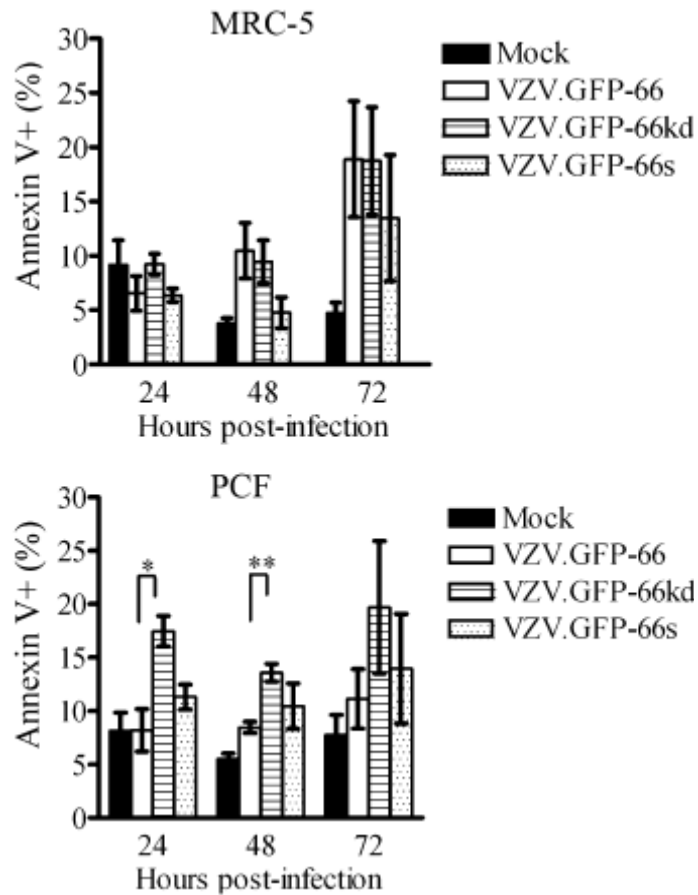


Figure 2-7. Apoptosis in PCF and MRC-5 cells infected with VZV and kinase negative mutants

MRC-5 (top) and PCF cells (bottom) were infected at a MOI of 0.02 with VZV.GFP-66, VZV.GFP-66kd, VZV.GFP-66s, or mock infected. At 24, 48, and 72 hrs p.i., cells were carefully harvested and stained with APC Annexin V, and the viability stain, 7-Amino-Actinomycin D (7-AAD). Cells for analysis were gated on GFP-positive cells for infection. The X-axis shows the fraction of GFP-positive cells that stained APC Annexin V-positive as a percentage of total GFP-positive cells. Results represent a mean +/- SE of values from three separate but identical experiments. Statistical analysis was done by Student's *t*-test. Asterisks represent the level of statistical significance: $p < .05$ (*), or $p < .001$ (**) compared to VZV.GFP-66 values.

2.5 DISCUSSION

In this work, we report the first non-lymphocytic cell line in which the ORF66 protein kinase is required for efficient VZV replication. We also show that ORF66 kinase-mediated phosphorylation of IE62 residue S686 is necessary and sufficient for IE62 cytoplasmic accumulation and virion packaging in the context of VZV infection. However, this activity is not the PCF cell-specific requirement for the kinase. Our data also indicate that the loss of the protein kinase does not result in a marked increase in VZV-induced apoptosis in the cell types studied, although it might contribute to growth impairment of VZV.GFP-66kd in PCF cells. Therefore, the ORF66 protein kinase has at least one additional critical role in VZV infection of this cell type.

This work contributes to the changing concept that ORF66 is required for VZV growth in certain cell types. It can thus be grouped with additional VZV genes that, when deleted, result in VZV with cell type-specific or conditional growth patterns, including glycoprotein I (gI) (31), ORF17 (183), ORF49 (180) and ORF63 (30). In addition, it has become clear that many VZV genes deemed not essential for VZV growth in cultured cells are, nevertheless, required for VZV growth in human tissue in SCID-hu mice models of pathogenesis. An example is gI, which is not required for VZV growth in MeWo cells, but is needed for growth in Vero cells and for efficient VZV replication in skin and T cells in the SCID-hu mouse model (131). A second example is the non-essential ORF10 gene, orthologous to the VP16 of HSV-1 which is required for growth in human skin implants (24). Third, deletion of the ORF47 kinase does not affect growth in culture, even though abnormal virions are formed. Such viruses show severe impairment of VZV growth in both T cells (132-133) and skin (15) implants in SCID-hu mice. Regarding ORF66, while its disruption was initially reported to have

no influence on growth of the VZV vaccine strain in cultured MeWo cells (74), its disruption in the pOka background marginally reduced replication in this cell type (185). As such, it was not unexpected to find that our mutants disrupted for ORF66 kinase expression exhibited reduced cell-to-cell spread and infectious virus yields in MRC-5 cells (53). The additional VZV detailed here expressing complete but kinase-inactive ORF66 protein also has some growth impairment in MRC-5 cells. However, the lack of growth in human corneal fibroblasts of both ORF66 kinase-negative VZV was not expected and highlights important cell type-specific functions for the kinase. Our data suggest that ORF66 kinase-negative mutants are able to enter PCF cells, as we detected small foci of infection in which both IE62 and the ORF66 kinase were expressed. This suggests the block is at a later stage of the infectious cycle after early gene expression. Previously, it was shown that viruses disrupted for ORF66 expression or kinase activity by mutation of the ATP binding region (G102A) abrogated virus replication in T cells in the SCID-hu thy/liv mouse model (185), and in cultured T cells. It was further demonstrated that functional ORF66 was needed to modulate host cell signaling pathways *in vitro* in human tonsillar CD4⁺ T cells, which have been proposed to be involved in the transfer of infectious virus from circulation to sites on the skin in this mouse model of VZV pathogenesis (108). We conclude that the important ORF66-encoded function involves the unique short kinase phosphorylating host or viral proteins in PCF cells. Identification of an easily cultured non-lymphocytic cell type in which the kinase is required opens up avenues to investigate these targets.

Since the PCF specific function of ORF66 likely involves phosphorylation of a target, it was logical to investigate the only well-defined target, IE62. Our work confirmed that S686 was the critical residue by which the kinase induces cytoplasmic IE62 in the context of VZV

infections and established its importance in the assembly and packaging of IE62 into virions. We also established that virion incorporation of proteins encoded by ORFs 4, 9, 10, 47, and 63 do not require IE62 in the tegument for packaging. The proteins from ORFs 4, 9, 47, and 63 have been suggested to physically interact with IE62, but it seems unlikely that these interactions with IE62 are required for their virion incorporation. The increased levels of ORF9 and ORF63 in the virion in the absence of structural IE62 is reminiscent of several reports in which absence of one tegument protein is compensated by an increase in the incorporation of other tegument components (128) or even host proteins such as actin (129). McKnight et al., in their investigation of the essential α -TIF tegument protein speculated that protein-protein interactions in the tegument allows a certain level of flexibility of packaging, and noted that larger virion-fusion protein mutants were still packaged into virions (128).

Our work has separated ORF66 phosphorylation of IE62 S686 from the PCF cell-specific function of the kinase. VZV.IE62(S686A)² expresses a functional kinase but showed the IE62 phenotypes of ORF66-negative VZV, yet displayed only slightly diminished growth by 96 hrs. This also suggests that IE62 tegument inclusion is not required for viral growth in PCF cells. A similar conclusion was proposed from studies in tonsillar T cells, such that the ORF66 function critical for VZV growth is independent of its effects on IE62. It was reported that in T cells, IE62 locates to the cytoplasm in a VZV ORF66 stop mutant or ORF66 kinase-inactive mutants (185). This suggests that IE62 sub-cellular localization is controlled by an ORF66-independent mechanism in tonsillar T cells, possibly a cellular kinase that regulates IE62 nuclear import. It is not known if IE62 incorporates into virions from T cells infected with ORF66-deficient VZV.

We also show that the disruption of the kinase does not result in greatly increased levels of apoptosis in PCF cells that would account for the loss of VZV replication. Modulation of

apoptotic pathways seems to be conserved for many alphaherpesvirus US3 kinases, although the mechanisms have not been fully elucidated. It has been suggested that the kinase enables maintenance of survival of the infected cell long enough to allow virion production and spread (5). Keratocytes are known to be highly susceptible to apoptosis in the corneal stroma, particularly following a corneal wound or infection (220). Our data show that stromal fibroblasts derived from corneas show only significantly more apoptosis at 24 and 48 hr following infection with VZV expressing the kinase-dead protein. The fraction of cells showing apoptosis are similar to that seen in T cells (185). However, unlike that study, we found that the levels of apoptosis in VZV expressing ORF66 stop mutants were not significantly different from those in cells infected by VZV with functional kinase. The significantly higher apoptosis in VZV.GFP-66kd-infected PCF cells may reflect binding of the kinase-dead protein to a pro-survival factor that is normally phosphorylated, leading to dominant negative effects. Interestingly, in HSV-1, anti-apoptotic activity stems from the amino terminus of US3 in transfected cells induced for programmed cell death (161, 165). Thus, while ORF66 kinase activity may have a role in inhibition of apoptosis in PCF, it is unlikely to be the ORF66 function responsible for the severe growth deficiency of VZV lacking functional ORF66 in PCF cells.

The critical target(s) of the kinase in this cell type remain to be defined, and our current studies are aimed at determining if the VZV kinase shares the same functions attributed to other alphaherpesvirus US3 kinases. The US3 kinases of HSV-1, Marek's disease virus (MDV), and PRV have been implied to modulate the nuclear membrane to facilitate de-envelopment of nucleocapsids into the cytoplasm, since absence of US3 kinases causes irregular nucleocapsid accumulations in the perinuclear space. It has been suggested that phosphorylation of lamin A/C and emerin hyperphosphorylation aid in nuclear lamina breakdown that is required for proper

virion nuclear egress. Our recent studies (Eisfeld and Kinchington, unpublished studies) indicate that nuclear rim concentrates of GFP-66kd co-localize with nucleocapsid proteins. Work by Schaap-Nutt et al. suggests that complete virion formation is not affected in T cells infected with VZV encoding ORF66 stop mutants, and there is no similar nucleocapsid accumulation in the perinuclear regions (186). Rather, they reported lower levels of nucleocapsids in infected cells. It is possible that in PCF cells the kinase may have a more important role in virion egress than in T cells, and studies are ongoing using the GFP tag to cell sort and concentrate the initially infected PCF cells for electron microscopy studies of nucleocapsid maturation at the nuclear membrane.

It is possible that the ORF66 kinase augments activity of a cellular protein kinase which has different levels of activation or expression in different cell types. The US3 kinase of HSV-1 overlaps the targets of protein kinase A, which may be reduced in PCF cells (9). ORF66 also modulates the induction of the IFN pathway, as the level of Stat1 phosphorylation in a small fraction of tonsillar T cells is higher in response to IFN- γ when the kinase is not expressed (186). In SCID-hu mouse skin xenografts, VZV lesions are surrounded by a defined region of uninfected epidermal cells positive for Stat1 phosphorylation (triggered in the IFN signaling pathway), yet actual VZV-containing lesions downregulate IFN- α . Although ORF66 only has a modest effect on VZV titers in skin xenografts infected with pOka VZV66 stop mutants (186), it is thought that inhibition of IFN signal transduction may promote the survival of infected tonsillar T cells. Thus, it is possible that PCF cells express higher levels of IFN and that this may exert an antiviral effect. Human corneal epithelial cells have been found to increase transcriptional expression of various cytokines including IFN- β in response to HSV-1 infection in vitro (113). Interestingly, addition of recombinant human IFN- α 2a can inhibit VZV

replication in human corneal stromal fibroblasts cultures (166). Investigation of the role of interferon pathway modulation by ORF66 in PCF is an area under study.

In conclusion, VZV deficient in functional ORF66 protein kinase expression is severely growth-impaired in human corneal stromal fibroblasts, but this is not due to the kinase mediated phosphorylation of IE62 residue S686, that drives cytoplasmic accumulation and virion packaging of IE62. While our data suggests that there is a role for ORF66 in inhibition of viral induced apoptosis in PCF cells, this effect seems unlikely to be solely responsible for the complete growth deficiency. This work establishes that ORF66 may be critical for productive VZV growth in some non-lymphocytic cell types and additional primary cell cultures are now being explored.

3.0 THE ALPHAHERPESVIRUS ORF66/US3 KINASES DIRECT SPECIFIC PHOSPHORYLATION OF THE NUCLEAR MATRIX PROTEIN, MATRIN 3

Angela Erazo^{1,2}, Michael B. Yee², and Paul R. Kinchington^{2,3*}

Graduate Program in Molecular Virology and Microbiology¹, and Departments of Ophthalmology², Microbiology and Molecular Genetics³, School of Medicine, University of Pittsburgh, Pittsburgh, PA.

Note: For this manuscript I performed all experiments, plasmid construction, and immunofluorescence image correction, and created adenovirus & baculovirus recombinants. I also made all figures and wrote the manuscript. VZV recombinants and HSV US3 mutants were created by MBY. PRV recombinants were a gift from Dr. B. Banfield.

3.1 ABSTRACT

Alphaherpesviruses express a protein kinase termed US3 in herpes simplex virus type 1 (HSV-1) and ORF66 in varicella zoster virus (VZV), that affects multiple viral and host cell processes, although targets of the kinases remain poorly studied. The HSV-1 US3 substrate motif overlap to that of cellular protein kinase A (PKA) prompted use of an antibody specific for phosphorylated PKA substrates to address possible US3/ORF66 targets. While HSV-1, VZV and pseudorabiesvirus induced very different profiles of substrates, most species were US3/ORF66 kinase dependent. The predominant VZV 125KDa species was identified was Matrin 3, one of the major nuclear matrix proteins. Matrin 3 was phosphorylated by coexpression with the VZV ORF66 kinase alone but not by point mutant inactivated kinase. It was also phosphorylated by HSV-1 and PRV in a US3 dependent manner. The phosphorylation occurred primarily at residue T150, which was not a major residue targeted by PKA, and as T150 phosphorylation was not blocked by inhibitors of PKA nor induced by forskolin activation of PKA, we conclude that herpesvirus-induced matrin 3 phosphorylation at this site is PKA-independent. However, purified VZV ORF66 kinase did not phosphorylate matrin 3 *in vitro*, suggesting additional intermediate cellular kinase(s) were involved. In VZV-infected cells matrin 3 showed subtle nuclear differences in localization in the absence of the ORF66 kinase, while a pronounced

cytoplasmic location in late stage cells infected with US3 negative HSV-1 and PRV suggests matrix 3 phosphorylation is required for its nuclear localization late in infection. This work thus defines a new conserved substrate protein of this kinase group.

3.2 INTRODUCTION

All mammalian and avian herpesviruses studied to date include one to several proteins that are predicted to be protein kinases, based on the presence of conserved signature domains found in all cellular kinases. Two such protein kinases are found in the genomes of the alphaherpesviruses- that termed UL13 in herpes simplex virus types 1 and 2 (HSV-1, HSV-2) has recognizable homologs in all known mammalian herpesviruses, while the second, termed US3 in HSV and ORF66 in VZV and its close relative Simian Varicella Virus, are only in members of the alphaherpesvirus subfamily. Studies of the VZV ORF66 and US3 kinases of HSV-1 and pseudorabies virus (PRV) have revealed them as all basophilic serine/threonine (S/T) kinases, in which the preceding residues of the target serine or threonine are composed of multiple arginine and/or lysine residues.

Multiple functions have been associated with various members of the alphaherpesvirus US3 kinases. In VZV, PRV, HSV-1 and HSV-2, the kinase appears to be not essential for viral growth in most cell types. However kinase deficient viruses are unable to replicate in certain cell types and invariably show significant attenuation in animal models of disease. Functions attributed include establishing an environment conducive to viral replication by modulation of the nuclear membrane facilitating virion nuclear egress (86, 109, 138-139, 221), inhibition of apoptosis (10, 21-22, 88), restructuring cytoskeletal networks to aid in intercellular spread (56, 143, 165, 189, 207), chromatin regulation through modification of histone deacetylases 1 and 2 (HDAC 1 and 2) (165), and downregulation of interferon gamma (IFN- γ) signaling (116). The HSV-1 and PRV US3 kinase show multiple forms: US3 in HSV-1 includes a predominant 481 a.a. full length US3 kinase and a second form that can initiate at an alternate ATG to encode for the US3.5 kinase lacking the amino-terminal 76 a.a. of US3. PRV US3 also encodes for two forms of its US3 kinase, differing by an additional amino-terminal 54a.a. in its long form. For HSV and PRV, these forms have demonstrated to have different kinase function capabilities (20, 161). The 393 residue VZV ORF66 kinase is only seen as one form in VZV infected cells.

VZV lacking ORF66 or its kinase activity shows modest growth impairment in several tissue culture cell types, and severe impairment of VZV growth in T cells (133, 185-186, 199) and in primary corneal stromal fibroblasts (54), leading it to become increasingly recognized for its importance for viral replication. ORF66 is also expressed during the VZV neuronal latent state in human sensory ganglia that is established after the primary infection, varicella, or chickenpox (35). ORF66 kinase has one known direct phosphorylated viral target, which is the VZV major regulatory transcriptional activator and immediate early 62 (IE62) protein (52). IE62 phosphorylation by ORF66 leads to nuclear exclusion of IE62 and its redirection to the trans-

Golgi network for incorporation into the assembling VZV tegument (52, 54, 98-99). Its detection in neurons may explain the apparent cytoplasmic location of neuronal IE62 seen during latency (35). More recently, VZV has been shown to have a role in transcriptional regulation through an ability to induce the hyperphosphorylation of HDAC1 & 2 (210). This feature, initially recognized for HSV-1 US3, is theorized to be viral attempts to resist transcriptional silencing of viral DNA by the infected host, since chemical inhibition of HDAC activity relieves the growth defects seen for ORF66 deficient VZV. VZV ORF66 contributes to immune evasion tactics by modulating apoptosis and IFN- γ pathways in infected human tonsil T cells (186), and displays a mechanism to inhibit viral antigen presentation by reducing class I major histocompatibility complex surface expression (1, 53) in VZV-infected cells.

Collectively, the US3 kinases and ORF66 kinase are basophilic S/T kinases. The HSV and PRV US3 kinase motif, determined by optimal peptide substrates, is characterized by $(R)_nX-(S/T)-Y-Y$ where $n > 2$, Ser/Thr is the phosphorylated site, and X can be absent or preferably Arg, Ala, Val, Pro, or Ser and Y cannot be an absent amino acid, Pro, or an acidic residue (167) (110-111). The known ORF66 kinase sites on IE62 suggest it also target serines or threonines carboxy-terminal to multiple basic residues (RKRKS₆₈₆QPV and KRRVS₇₂₂EPV). Furthermore, such motifs are similar to the target motifs of cAMP-dependent protein kinase (PKA), defined by RRX(S/T). Bennetti et al. used this overlap to show that multiple proteins were similarly targeted by US3 and PKA, and that US3 may induce PKA activity in HSV-1 infected cells (9). PKA is found ubiquitously in eukaryotic organisms and has pleiotropic effects and many substrates, directing phosphorylation of metabolic enzymes, ion channels, regulatory & structural proteins, and transcription factors (193). In its inactive form, PKA is a tetrameric holoenzyme composed of catalytic subunits (C) bound to a regulatory subunit dimer.

Cooperative binding of cAMP to the regulatory subunits releases the active C subunits that in turn can phosphorylate specific S/T residues on substrate proteins (195). Benneti et al. suggests that US3 activates PKA and can parallel its anti-apoptotic function through phosphorylation of common protein substrates. One study in VZV reports evidence for increased expression of the catalytic subunit of PKA early in VZV infection, as well as phosphorylation of some PKA substrates (49).

Despite accumulating evidence that ORF66 kinase is critical for growth in a certain cell types and has a role in mitigating host cell defense mechanisms, much is unknown about further viral and host cell targets. Here, we described a novel host cell phosphorylation target for this kinase family, the nuclear matrix protein matrin 3 (MATR3). The nuclear matrix is a fibrogranular network within the nuclear interior characterized as a proteinaceous subnuclear non-histone fraction resistant to high salt, detergent and nuclease treatment of the interphase cell (147). Proteins forming the nuclear matrix are participant in many nuclear functions, including DNA replication & transcription, since they serve as a structural framework for these activities & their binding to key protein factors (3, 11, 83). Approximately 12 major proteins make up this internal matrix, composed of Lamins A, B, and C, the nucleolar protein B-23, residual components of nuclear ribonuclear proteins, and 8 nuclear matrins (Matrin 3, 4, D, E, F, G, 12, & 13) (147). Here we report the nuclear matrix protein, matrin 3 as an unprecedented protein target of the alphaherpesvirus US3 kinase family.

3.3 MATERIALS & METHODS

3.3.1 Cell culture

MRC-5 (human diploid lung fibroblasts), human embryonic kidney (Hek) 293 , Hek 293T (ATCC, Manassas, VA) and MeWo cells (human melanoma cell line; a gift from C. Grose, University of Iowa, Iowa City) were maintained as described previously (52). SF9 cells (Invitrogen Corp.) were grown at 28°C in Grace's Insect Medium (Gibco) supplemented with 10% fetal bovine serum (FBS) & gentamicin (50µg/ml) (Gibco) & antibiotics as detailed by the supplier.

3.3.2 Viruses

(i) VZV. VZV used here are based on the parent of the Oka vaccine strain and were amplified in MeWo cells as detailed previously (98). Recombinant VZV.GFP-66, VZV.GFP-66kd (kinase dead), VZV.GFP-66s (truncated ORF66 protein), and rescuant VZV were constructed from pOka-based cosmids as described previously (53-54). VZV.GFP-66kd contains two conservative mutations (D206E, K208R) within the catalytic loop domain to inactivate kinase activity (99). VZV.GFP-66s was constructed with a stop codon at 84 a.a. of the 393 a.a. ORF66 kinase, to form a truncated protein that is also kinase inactive.

(ii) HSV-1. The HSV-1 RE strain has been detailed by us previously. Recombinant wild-type (containing US3 or 3.5 with an N-terminal GFP tag) and *US3* deleted HSV-1 were generated as follows. Plasmids were developed following PCR amplifying the HSV-1 RE genomic template using the GC-RICH PCR Proofreading System (Roche, Indianapolis, IN) under hot start

conditions and primers US3F 5' - GGAATTCATGGCCTGTCGTAAGTTTTGTCGCGTTTAC - 3' or US3.5F 5' - GGAATTCATGTACGGAAACCAGGACTAC - 3', each in conjunction with US3R 5' - GGAAGATCTTCATTTCTGTTGAAACAGCGGCAA - 3'. The PCR products for US3 and US3.5 were digested with BglIII and EcoRI and ligated to BamHI/EcoRI digested pEGFP-C so as to be downstream and in frame of EGFP. These plasmids express the EGFP tagged versions of each kinase from the human cytomegalovirus immediate early (hCMV IE) promoter (pEGFP-US3 and pEGFP-US3.5, respectively). To derive HSV-1 US3null, the *US3.5* construct was collapsed with Xho I, which removed the N terminal part of the *US3* coding sequence encoding residues 1 to 169 and placed the remaining sequence out of frame with respect to EGFP and without an initiating ATG. Any aberrant protein that might be unpredictably expressed would not retain sufficient domain to be kinase functional. For derivation of recombinant viruses, all three plasmids were treated to replace the CMV IE promoter with DNA containing the *US3* promoter immediately upstream of the US3 ATG, which was PCR amplified using primers US3PF 5' - GCGCCCTAGGGCTAGCTCGCCGCACCGTGAGTGCCA - 3' and US3PR 5' - GCCATTAATATTAATGCCGCGAACGGCGATCAGAGGGTCAGT - 3'. The PCR product was digested with Ase I and Nhe I and ligated to constructs which had been digested with Ase I and Nhe I to remove the CMV IE promoter. Viruses were derived by cotransfecting ssI-linearized constructs with RE DNA and were identified and plaque purified based on gain of EGFP fluorescence as detailed previously (172). Insertion of GFP and the integrity or deletion of US3 coding sequences were confirmed by Southern blot analysis of viral DNA.

(iii) PRV. Wild-type PRV (Becker strain) was described previously. PRV-US3 null virus (PRV645) was constructed by co-transfecting purified PRV DNA (Kaplan strain, kindly

provided by Dr. T. C. Mettenleiter, Federal Centre for Virus Diseases of Animals, Insel Riems, Germany) and SpeI linearized plasmid, pML7 into PK15 cells. Virus produced after co-transfection was plated on PK15 cells, and plaques expressing EGFP were identified. Virus was isolated from EGFP-expressing plaques and subjected to three rounds of purification. Southern blot analysis was performed on PRV645 genomic DNAs to verify that the appropriate recombination events had occurred. US3 protein expression was examined in PRV645 and wild-type PRV Kaplan strain (PRV-WT) infected cell lysates by western blot to confirm the absence or presence of US3 expression, respectively. Virus titer was determined on vero cells as detailed previously.

(iv) Baculoviruses. Baculoviruses expressing glutathione S-transferase (GST) tagged ORF66 (GST.66) or GST.66kd were derived using the BaculoGold system (BD pharmingen, San Diego, Calif.) Full length HA tagged ORF66 or ORF66kd were excised using BstZ 17I and PstI sites from pGK2-HA66 or pGK2-HA66kd which contain an HCMV IE promoter and IE1 polyadenylation site, as well as encode a HA epitope (YPYDVPDYA) (52). HA66kd is a kinase inactive mutant containing two highly conservative changes in the catalytic loop domain of the kinase (D206E, K208R) (99). These were inserted into pAcGHLT-A using SmaI and PstI sites. This vector contains a 6xHis tag and a glutathione S-transferase (GST) tag upstream of the multiple cloning site. Resulting positive clone plasmid DNA were cotransfected with baculogold DNA in Cellfectin reagent (Invitrogen) and Grace's insect media (serum/antibiotic free) (Invitrogen) into SF9 cells. After 5 days, primary supernatant was collected (1^o virus). GST66 or GST66kd expressing viruses were then amplified in SF9 cells. A control baculovirus expressing GST was also utilized. Cells infected with later stocks of these viruses were checked for proper protein expression by immunoblot analysis using HA or GST-specific antibodies.

(v) Adenoviruses. Replication-incompetent adenoviruses expressing GFP-HA-66 (Ad.GFP-66) or GFP-HA-66kd (Ad.GFP-66kd) containing tetracycline or doxycycline – responsive cassettes were constructed using the Adeno X Tet-Off system (Clontech) described previously (53). These were used in conjunction with an Adeno.Tet-off (Ad.Toff) regulatory virus expressing a tetracycline-controlled transactivator as previously detailed (53) .

3.3.3 Protein identification by MALDI TOF

Confluent Hek293 cells were infected with Ad.GFP-66 at an MOI of 0.05, and then amplified by transferring infected cells to two 50% confluent 175-cm² flasks. Cells were harvested when showing signs of cytopathic effect at 50%. Cells were lysed for at least 30 min' with three 10 second sonication pulses on ice using a solubilization buffer (20mM Tris-HCl pH 7.0, 0.5M KCl, 1mM EDTA, 1% NP40 with protease inhibitor cocktail (Complete, Roche Diagnostics) and phosphatase inhibitors (20mM NaF, 1mM Na₄P₂O₇ · 10 H₂O, 1mM Na₃VO₄). Soluble fractions were collected and added at 4°C to Protein G agarose beads (Sigma, Saint Louis, MO) bound to rabbit α -phospho-PKA substrate antibody (1:10 for IP) for immunoprecipitation. The beads were then washed with a modified RIPA buffer (20mM TrisHCl pH 7.4, 1% NP40, 150mM NaCl, 1mM EDTA) with a final wash in low salt buffer (20mM TrisHCL pH7.4 100mM KCl) and lastly resuspended in SDS-sample buffer and boiled. Samples were then seperated by 6% sodium-dodecyl sulfate-polyacrylamide gel electrophoresis (SDS-PAGE). The gel was then stained with Bio-Safe Coomassie G-250 stain (BioRad, CA). The region approximately between the 100 and 150kDA marker was cut out of the gel and sent for LC tandem MS/MS at the

University of Pittsburgh Proteomics Core Facility. Returned candidate proteins were subsequently identified through the use of specific antibodies.

3.3.4 Plasmid construction

Plasmids expressing maltose binding protein (MBP) and the MBP-IE62 peptide fusion of IE62 residues 571 to 733 were described previously (52). To generate an MBP fused to the full length matrin 3, a commercial plasmid of the matrin 3 gene was purchased from InVitrogen. The gene was placed in frame with MBP protein using the vector pMalC2 and a PCR amplifications of 2 PCR products forming full length Matrin 3 using the proofreading polymerase combination sold as Expand (Roche). MBP-Matrin 3 protein was purified using amylose affinity chromatography, as recommended by the manufacturer.

An HA tagged version of Matrin 3 with or without single residue point mutations was prepared using Splicing by overlap (SOE) PCR with the proofreading polymerase Expand. All Matrin 3 constructs were developed using the terminal PCR oligonucleotides Matrin3Start (5'-**gcgcaattgtcgaccacc atgtccaagtcattccagc**-3') and Matrin 3 end (5'- **gcgggatccttaactagt ttccttcttctgtctgcgttcttctgccaat**-3') so that the resulting constructs were cut with MfeI and BamHI (sites shown in bold) and then cloned into the EcoRI and BamHI sites in the vector PGK2-HA detailed previously (53) so as to be in frame with an N terminal HA tag. Candidate residues were mutated using SOE of left and right sides of Matrin 3 gene with the terminal primers and the following pairs, followed by reamplification of the entire matrin 3 gene with the terminal primers and a 1:1 mix of left and right ends as substrates. Primers to mutate T150A and insert a novel silent AscI site for identification were T150Fasc (5'-

cttaaaaggaggcgcgcggaagaaggccctacc-3') and T150Rasc (5'-ggtagggccttcttccgcgcgcctcctttaag-3'): those to mutate S188A also inserted a novel silent NsiI site S188Fnsi (5'-cactttagaagagatgcatttgatgatcgtggt-3') and S188Rnsi (5'-accacgatcatcaaatgcatctcttctaaagt-3'): mutation of S592A, S596A and S598A simultaneously and insert a silent BsiWI site were nucS123fbsiw (5'-ctgaaaaagataaagcccgaaaaagagcgtac gctccagatggcaaagaa and nucS1Rbsiw (5'-ttctttgccatctggagcgtacgctcttttcgggctttatctttttcag-3'): and primers to mutate S596A and S598A and insert a novel BsiW I site were nucS23Fbsiw (5'-gataaatcccga aaaagagcgtacgctccagatggcaaagaa -3') and nucS23Rbsiw 5'-ttctttgccatctggagcgtacgctcttttcgggattatc-3'). Primers to mutate S596A and insert a BsiWI site were nucS2FbsiW (5'-gataaatcccgaaaaagacgctactctccagatggcaaagaa-3') and nucS2RbsiW (5'-ttctttgccatctggagagtagcgtcttttcgggattatc-3'). All constructs were identified for expression in transfected cells followed by immunoblotting with HA specific antibodies.

3.3.5 Drug treatments

Forskolin (Fisher BioReagents, Fair Lawn, New Jersey) and the PKA inhibitor (PKI) 14-22 amide (EMD Biosciences, San Diego, CA) were purchased commercially. Forskolin and PKI 1422 amide were reconstituted in DMSO and minimum essential media (MEM), respectively. PKI 1422 amide treatment was started 2 hours prior to infection & continued until time of cell harvest. Forskolin treatment was started at the time of infection & continued until the time of cell harvest as indicated in the figure and text.

3.3.6 Transfections & Infections

For transfections for optimal expression, Hek 293T were seeded onto poly-lysine-coated 6-well culture dishes. Cells were transfected with DNA using Fugene HD (Roche, Indianapolis, IN) and as recommended by the manufacturer. For transfection – infection experiments, MeWo cells were transfected with DNA using Fugene HD, and then infected the following day with either HSV-1 using MOI of 5, or overlaid with VZV infected cells at a 10:1 ratio uninfected to infected. Adenovirus infections were performed in MRC-5 cells that were incubated under low serum conditions (Minimum Essential Media, 1% FBS, plus antibiotics) for 1 day prior to infection. Infections were done at an MOI of 5 for Ad.GFP66, Ad.GFP66kd, or Ad.Vector and Ad.Toff at an MOI of 2.5 under low serum conditions. Infections for immunoblot analysis were performed by binding of virus at room temperature, change of media, and subsequent transfer to 37°C, for the times indicated in the figures. For HSV and PRV immunofluorescence (IF) analyses, the binding step was done at 4°C using chilled cells and 4°C media, with subsequent wash, addition of warm media and transfer to 37°C, then fixed with 4% paraformaldehyde at 18 hrs p.i. (HSV) or 11 hrs p.i. (PRV). For VZV IF analyses, cells were infected with VZV at an approximate ratio of 1 infected to 25 uninfected cells, and then immediately transferred to 37°C. Cells were fixed with 4% paraformaldehyde at 36hrs p.i.. All VZV infections were performed using titrated stocks of virus in MeWo cells stored in liquid nitrogen.

3.3.7 Antibodies & Immunological Procedures

Rabbit polyclonal antibodies to VZV proteins IE62 and ORF4 were detailed previously (97, 99). Antibodies to VZV ORF 9 (26) were a kind gift of W.T. Ruyechan, SUNY at buffalo, NY. The

mouse monoclonal antibody that recognizes the 9 amino acid epitope (YPYDVPDYA) from the influenza protein hemagglutinin (HA) has been described previously (52) and used at 1:600 for immunoblot analyses or approximately 4 μ l per immunoprecipitation. Mouse monoclonal antibodies to α -tubulin (Sigma-Aldrich, St. Louis, MO) and α -Ku-86 (Santa Cruz Biotechnology, Inc, Santa Cruz, CA), were purchased commercially & used at 1:8000 and 1:500, respectively for immunoblot analysis. Monoclonal antibody pools that recognize HSV-1gB were a kind gift from William F. Goins, University of Pittsburgh) and was used at 1:6000 for immunoblot. Mouse α -ICP4 (Virusys, Taneytown, MD) was used at 1:1000 for IF. PRV goat α -UL34 (a kind gift from Dr. Bruce Banfield) was used at 1:1000 for immunoblot and 1:500 for IF. Rabbit monoclonal α -phospho-PKA-substrate antibody was purchased commercially (Cell Signaling Technology, Danvers, MA). This p-PKA-sub antibody was used at a dilution of 1:800 for immunoblot analysis and 1:50 for IP. Rabbit α -matrin 3 antibody (Bethyl Laboratories, Inc, Montgomery, TX) was purchased commercially and used at 1:3000 for IF and 1:8000 for immunoblot. Goat α -glutathione S-transferase (GST) (GE Healthcare, Piscataway, NJ) was purchased commercially, and used at 1:20,000 for immunoblot analysis. Rabbit α -MBP (New England Biolabs, Inc, Beverly, MA) was purchased commercially, & used at 1:15000 dilution for immunoblots. Secondary antibodies used in immunoblot analysis used were goat α -mouse, goat α -rabbit, and donkey α -goat conjugated to horseradish peroxidase (ICN-Cappel, Aurora, OH) were purchased commercially and used between 1: 20,000 -1:40,000.

All immunofluorescent staining procedures were carried out as described previously (53). Briefly, MRC-5 cells were grown on glass coverslips or on 2-well slides. At the indicated time point, cells were fixed with 4% paraformaldehyde, permeabilized with 0.2% Triton-X, and antibody incubations done in heat-inactivated goat serum or donkey serum. For VZV and HSV

IF staining, antibodies were detected using goat α -rabbit immunoglobulin G antibody conjugated to Alexa Fluor 546 or goat α -mouse immunoglobulin G antibody conjugated to Alexa Fluor 647. For PRV IF staining, donkey α -rabbit immunoglobulin G antibody conjugated to Alexa Fluor 555 or donkey α -goat conjugated to Alexa Fluor 647 (Invitrogen Corp). Immunofluorescence was visualized using an Olympus Fluoview FV1000 confocal microscope equipped with a 60X oil objective. Images are of one slice of Z-stacks acquired in 0.48 μ m steps.

3.3.8 Immunoblot analysis & Immunoprecipitation

For analysis of protein expression, infected or transfected cells, whole cell lysates, soluble fractions or protein bound to IgG beads were treated with SDS- sample buffer and separated by sodium dodecyl sulfate – polyacrylamide gel electrophoresis (SDS-PAGE) and transferred to PVDF membranes (Immobilon- P membrane , Millipore, Billerica, MA) as previously described (52). When soluble fractions were needed, lysates were treated with protease inhibitors (Complete protease inhibitor cocktail (Complete EDTA-free; Roche Diagnostics, Indianapolis, IN) and phosphatase inhibitors (20mM NaF, 1mM Na₄P₂O₇ ·10 H₂O, 1mM Na₃VO₄). Where indicated Immobilon-P membranes were stripped by using 0.2 M NaOH for 5 minutes and rinsed with distilled H₂O, then reblotted. Following exposure to film, digital images were acquired using an Epson Perfection 4990 photo scanner with Silver Fast Ai and Adobe Photoshop CS imaging software.

For immunoprecipitations, equivalent numbers of cells per condition were washed with ice-cold 1X phosphate-buffered saline (PBS) and lysed using a solubilization buffer (20mM Tris-HCl pH 7.0, 0.5M KCl, 1mM EDTA, 1% NP40) plus protease and phosphatase inhibitors for 30 minutes on ice. During the lysing period, cells were sonicated on ice 3 times in 30 second

pulses. Soluble fraction was collected by centrifugation at 16.1 RCF for 35 min, then incubated with antibody-bound protein G beads for 3-4 hours. Protein G agarose beads bound to antibodies were prepared by washing with 1XPBS and incubated with mouse or rabbit antibodies for 3 hrs. Following incubation of Protein G beads to soluble fractions, beads bound to antigen were now extensively washed in solubilization buffer with a final wash in 1X PBS, and lastly resuspended in SDS-sample buffer and boiled. When specified in figure legend, blocking peptide (Bethyl Laboratories, Inc, Montgomery, TX) against matrin 3 antibody was used. Here, antibody bound beads were prepared, washed, then were incubated with excess blocking peptide (5-fold more peptide than antibody) for 45 min'. This preparation was then incubated with soluble fractions, with subsequent steps as described above.

3.3.9 GST fusion protein purification & *In vitro* kinase assay

GST proteins were purified from SF9 infected cells by first solubilizing infected SF9 cells in radioimmunoprecipitation (RIPA) buffer (20mM Tris-HCL pH8.5, 50mM KCl, 1mM EDTA, 1mM DTT, 1% NP-40, and 0.5% deoxycholate). These were sonicated on ice in the presence of protease and phosphatase inhibitors. Soluble fractions were then collected and combined with glutathione beads (Glutathione Uniflow Resin) (BD Biosciences) for 3 hrs or overnight. GST beads were then collected and washed extensively in 2M KCl (pH7.5), followed by RIPA buffer, and finally kinase buffer (pH7.5) for a total wash time of 1hr. GST fusion proteins were then eluted overnight at 4°C with glutathione elution buffer containing 0.1% Triton X-100 and protein levels were measured by Bradford assays. MBP proteins were constructed and purified as detailed previously (52) except inductions were carried out in *E. coli* BL21 cells at 30C for 3 hrs.

In vitro kinase assay. Approximately 2 µg of GST or GST fusion protein were incubated with 2µg of MBP or MBP fusion proteins in 70ul kinase assay buffer (20mM Hepes-KOH (ph7.5), 50mM KCl, 10mM MgCl₂, and 5ug/ml Heparin) and 5µCi of [γ -³²P] ATP (6000 Ci/mmol) for 25 min' at 35°C. Kinase assays were normalized so that they were performed in equal reaction volumes. Reactions were stopped by addition of SDS-PAGE sample buffer. Proteins were then separated on 7% SDS-PAGE gel and then transferred to an Immobilon-P membrane. Phosphorylated bands were then detected by autoradiography directly from Immobilon-P membranes. Following exposure, membranes were then subject to immunoblot using Rabbit α -MBP or Goat α -GST antibodies to ensure equivalent protein levels. For PKA kinase assays, PKA catalytic subunit (New England Biolabs, Inc, Beverly, MA) was purchased commercially and *in vitro* kinase assays were performed as recommended by manufacturer. Briefly, approximately 2 µg of PKA and MBP fusion proteins were incubated using PKA reaction buffer or ORF66 kinase assay buffer for 30 min' at 30°C. Reactions were then stopped with SDS-sample buffer. Where indicated, protein G beads bound to HA-tagged matrix 3 proteins were subject to a PKA *in vitro* kinase assays.

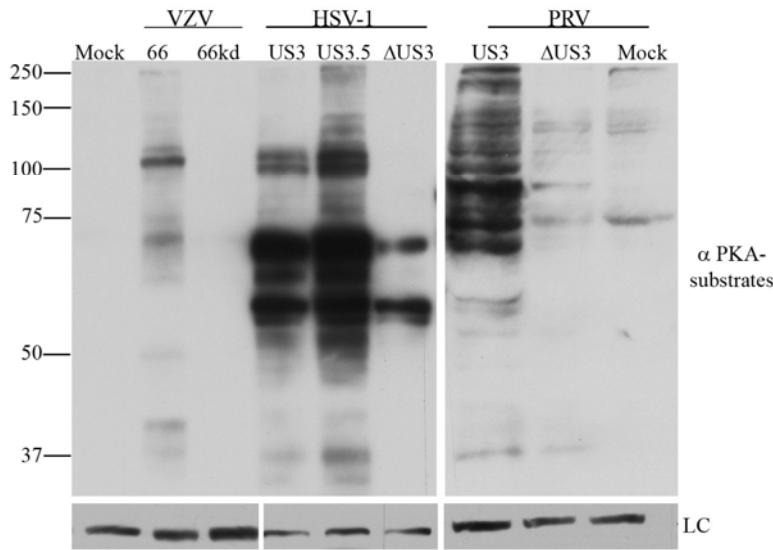
3.4 RESULTS

3.4.1 PKA-substrate profiles show drastic differences between VZV, HSV, &PRV

The ORF66 phosphorylation motifs found in IE62 are similar to the consensus motifs for HSV US3 and, by extrapolation from the work of Benetti and Roizman, were suspected to also overlap the substrates of PKA. We thus speculated that a phosphospecific (p) PKA-substrate antibody

would identify candidate protein substrates of ORF66 kinase. The p-PKA-substrate profile of whole cell extracts (WCE) of MeWo cells infected with VZV expressing functional ORF66 (VZV.GFP-66) or a point mutated kinase-dead (kd) ORF66 (VZV.GFP-66kd) revealed a modest number of protein species (approximately 9) in ORF 66-expressing VZV infected cells that were absent in VZV ORF66kd-expressing cells. Intriguingly, the predominant species was a 125 kDa species (Fig. 3-1a). The predominant 125 kDa species was also observed in several cell types infected with VZV, including MRC-5s, human foreskin fibroblasts and primary human corneal fibroblasts, and was also seen in cells infected with VZV lacking the expression of the ORF47 protein kinase (data not shown). Comparison to wild type HSV-1 and HSV-1 expressing only the the US3.5 form in the same cell type revealed many more species that were absent from HSV not expressing either form of the US3 kinase (Δ US3), and several species that were present in HSV infected cells that were kinase independent. It has been reported that US3 and US3.5 drive PKA activation (9). Furthermore, the same cell type infected with PRV and PRV not expressing its US3 kinase (Δ US3) revealed a very different profile of species that was US3 dependent. Species in the 125kDa region were less obvious yet distinguishable over other areas (Fig 3-1a.). To demonstrate equal infections, WCE were also probed for VZV ORF9 (a tegument protein), HSV-1 gB (an envelope glycoprotein) and PRV UL34 (membrane associated phosphoprotein) (Fig 3-1b.). We conclude that the p-PKA-substrate profiles differed extensively for these three alphaherpesviruses and may indicate that each kinase has very different influences on the host cell targets.

A.



B.

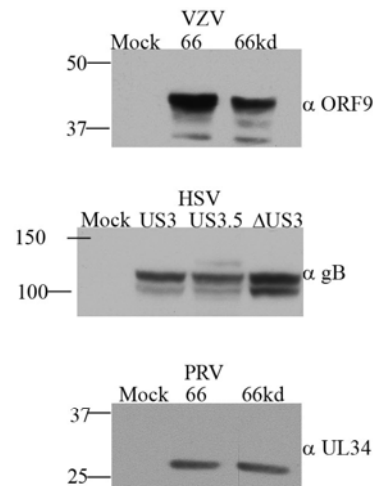


Figure 3-1. Conserved ORF66/US3-dependent phosphorylation of a 125kDa protein by alphaherpesviruses displaying different PKA-substrate profiles

MeWo cells were infected at an MOI of 0.1 with VZV.GFP-66 (66), or VZV.GFP-66kd expressing kinase-inactivated ORF66 protein (66kd) or mock infected. Cells were infected at an MOI of 1 with HSV-1 (US3), HSV-EGFP-U_S3.5 expressing truncated US3 which lacks the N terminal 76 a.a. of the kinase (US3.5), HSV-EGFP-XhoΔUS3 that does not express US3 (ΔUS3), PRV (US3), or PRV.ΔUS3 that does not express US3 (ΔUS3). WCE were harvested 20hrs p.i. and separated by 7% SDS-PAGE gel and immunoblot analysis of proteins is shown. Membranes were probed with (A) rabbit α-p-PKA-substrate antibody, then stripped and reprobed for loading controls (LC) mouse α-tubulin (VZV & PRV) and α-Ku-86 (HSV-1) antibody. (B) Immunoblot analysis of viral proteins to show equal infections (rabbit α-VZV ORF9, mouse α-HSV gB, or goat α-PRV UL34 antibodies). Protein size markers in kDa are specified to the left.

3.4.2 The 125 kDa protein represents a host cell target

We have previously detailed the use of replication defective adenoviruses expressing EGFP and HA tagged forms of the ORF66 protein kinase (53). To determine if the 125 kDa species seen in VZV-infected cells was a cellular protein, Hek293 cells were infected with replication-deficient adenoviruses expressing ORF66 (Ad.66) or ORF66kd (Ad.66kd), together with a regulatory virus, Ad.Toff, and in the absence or presence of doxycycline to turn off expression of ORF66 and 66kd. WCE extracts analyzed by western blot & probed with a p-PKA substrate antibody show the appearance of a 125 kDa species when ORF66 was expressed. Its absence in all controls, including when ORF66 gene expression was turned off with doxycycline, or in conditions of kinase inactive forms (Fig 3-2.) establishes the 125 kDa species as a host cell protein. In this study, Hek293 cells show a constitutively expressed 135 kDa species that was not ORF66 dependent. Antibody to HA showed expression of the HA tagged 66 and 66kd proteins.

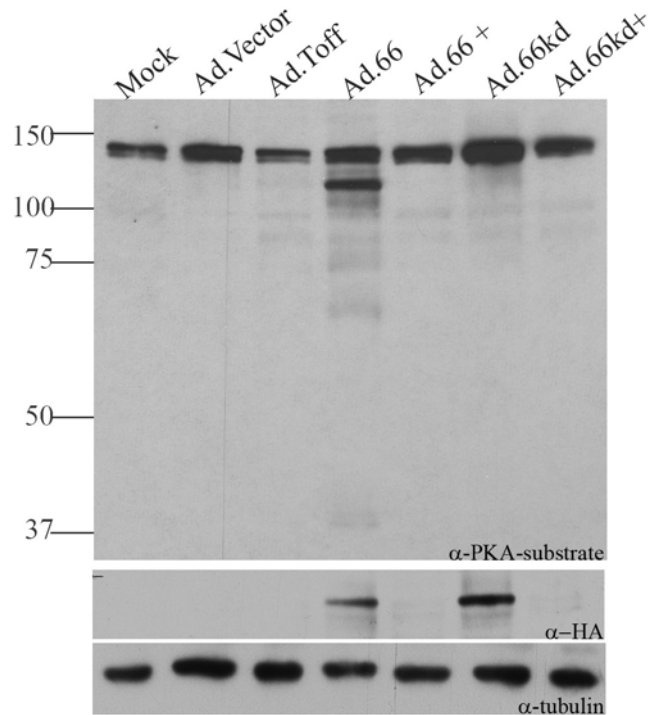


Figure 3-2. The 125 kDa 66-specific PKA-substrate is a host cell protein

MRC-5 were coinfecting with replication-deficient adenoviruses Ad.Toff which expresses a tetracycline-controlled transactivator at an MOI of 2.5 and one of the following : Ad.GFP-66 expressing functional ORF66 (Ad.66), Ad.GFP-66kd expressing kinase-inactive ORF66 (Ad.66kd), or Ad.Vector at an MOI of 5 or mock infected. Doxycycline was added (+) to turn off ORF66/66kd gene expression. Cells were harvested 1 day p.i. and immunoblot analysis was done of WCE. Membranes were probed with rabbit α -p-PKA-substrates, then stripped and reprobed with mouse α -HA to analyze for ORF66/66kd expression. Mouse α -tubulin was used to evaluate equal amount of total protein levels. Protein size markers in kDa are specified to the left.

3.4.3 Matrin 3 is a conserved phosphorylation target for the alphaherpesvirus

ORF66/US3 kinases.

To identify the 66-induced p-PKA-substrate 125 kDa protein(s), the 125 kDa species in adenovirus infected ORF66 expressing HeK293 cells was scaled up and immunoprecipitated

with p-PKA substrate antibody. SDS-PAGE gel fragments stained with colloidal coomassie blue without fixation for the 100kDa to 140kDa species were sent for LC MS/MS analysis. A returned target candidate was the nuclear matrix protein, matrin 3.

The identification of matrin 3 as the 125 kDa species differentially phosphorylated by VZV ORF66 was then confirmed using commercial matrin 3 specific antibodies. Anti-Matrin 3 immunoprecipitated extracts of Hek 293 cells transduced with Ad.66 or Ad.66kd at an MOI of 0.3, followed by western blot using the p-PKA-sub specific antibody (Fig 3-3a) revealed that immunoprecipitated matrin 3 was differentially recognized by p-PKA-substrate proteins in an ORF66 kinase-dependent manner. In a similar experiment in which anti PKA-sub reactive proteins were immunoprecipitated & probed for matrin 3, results were similar in that the ORF66-induced 125 kDa p-PKA-sub protein was recognized by the matrin 3 specific antibodies. We then confirmed that matrin 3 was differentially phosphorylated in a 66-dependent manner in VZV infection. MeWo cells infected with VZV.GFP-66 or kinase-inactive mutants (VZV.GFP-66kd and VZV.GFP-66s) were analyzed in a similar manner, in which extracts were immunoprecipitated for either matrin 3 (Fig. 3-3B, top panel) or PKA-sub proteins (Fig. 3-3B middle panel) and probed for PKA-sub reactive proteins or matrin 3, respectively. These approaches revealed that functional ORF66 expression in the context of VZV infection induced phosphorylation of multiple forms of matrin 3 during VZV infection, although matrin 3 was present in the IP fraction for all VZV infections (Fig. 3-3B lower panel). These studies also indicated that VZV infection did not radically alter global levels of matrin 3 as a result of infection, since similar amounts of matrin 3 were seen by western blot and from immunoprecipitates.

A final approach to establish matrin 3 was the detected 125kDa protein and not a similarly sized protein contaminating the IP fraction used a matrin 3 blocking peptide. The blocking peptide contains the epitope that is recognized by the matrin 3 antibody, thus blocks the antibody-antigen interaction. An IP was done on VZV-infected cells using matrin 3 or p-PKA substrate antibody in the presence or absence of a blocking peptide added to the soluble fractions containing functional ORF66 kinase. The peptide efficiently blocked α -matrin 3 from binding matrin 3 (Fig. 3-3c left) and this prevented immunoblot detection of a 125kDa PKA-sub antibody in the presence of ORF66 kinase (Fig. 3-3c right); hence, matrin 3 is the ORF66-dependent 125kDa p-PKA substrate protein and not a contaminating phosphorylated protein.

These approaches were then extended to examine US3 kinase-dependent matrin 3 phosphorylation in cells infected with HSV-1 and PRV. Immunoprecipitates of matrin 3 that were subsequently probed for p-PKA- sub antibody revealed that matrin 3 was phosphorylated in cells infected with HSV expressing US3 or US3.5, and in PRV infected cells expressing US3, but were not phosphorylated or only marginally phosphorylated in cells infected with each virus lacking its respective US3 kinase (Δ US3). Fig 3-4a (left top panel) cells probed with PKA-substrate showed that the 125 kDa protein was strongly detected when functional HSV US3 or US3.5 was present, but diminished in Δ US3 virus infected cells. Global matrin 3 levels did not change during HSV or PRV infection (Fig. 3-4a left middle panel). Similar findings resulted in PRV- infected cells, where phosphorylation in the 125 kDa region occurred in cells infected with PRV expressing functional US3 (Fig. 3-4b left panels). PRV Δ US3 reproducibly showed a small level of matrin 3 phosphorylation (Fig. 3-4b right top panel). We conclude from these data that matrin 3 is a conserved phosphorylation target for the VZV, HSV and PRV US3 kinases.

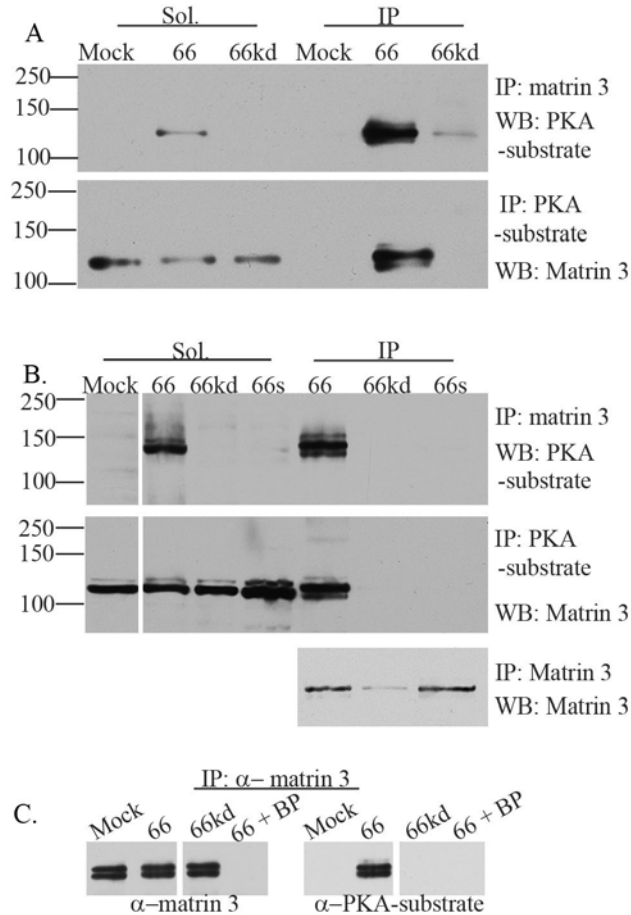


Figure 3-3. VZV ORF66 kinase activity induces specific matrin 3 phosphorylation

(A) Hek 293 cells were infected with Ad.GFP-66 or Ad.GFP-66kd at an MOI of 0.3 or mock infected. Soluble fractions (sol) & immunoprecipitation (IP) products were separated on a 7% gel and analyzed by immunoblot (WB). IPs were performed using rabbit α -matrin, followed by probing of membranes with rabbit α -PKA-substrate antibody (*top panel*), or IPs were performed using rabbit α -PKA-substrate followed by probing of membranes with rabbit α -matrin 3 antibody (*bottom panel*). (B) MRC-5 cells were infected with VZV.GFP-66 (66), VZV.GFP-66kd (66kd), or VZV.GFP-66s expressing a.a. 1 to 84a of ORF66 (66s) at an MOI of 0.01 or mock infected, then harvested 2 days p.i. & separated on a 7% SDS-PAGE gel, then transferred to a PVDF membrane. Immunoprecipitations followed by immunoblot analysis (*top & middle panel*) were performed as described above. The top membrane was then stripped and reprobed for Matrin 3 to analyze levels of matrin 3 in IP fractions (*bottom panel*). Protein size markers in kDa are specified to the left. (C) MRC-5 were infected with VZV expressing 66 or 66kd at an MOI of 0.01 or mock infected and harvested at 2 days p.i.. Cleared lysates were then immunoprecipitated using rabbit α -matrin 3 antibody in addition to matrin 3 blocking peptide (BP) where indicated. Proteins were separated on a 6% SDS-PAGE gel and membranes were then probed with rabbit α -matrin 3 antibody (*left panel*) to test for efficiency of IPs and the blocking peptide, or to analyze for phosphorylation of matrin 3 with rabbit α -PKA-substrate antibody (*right panel*).

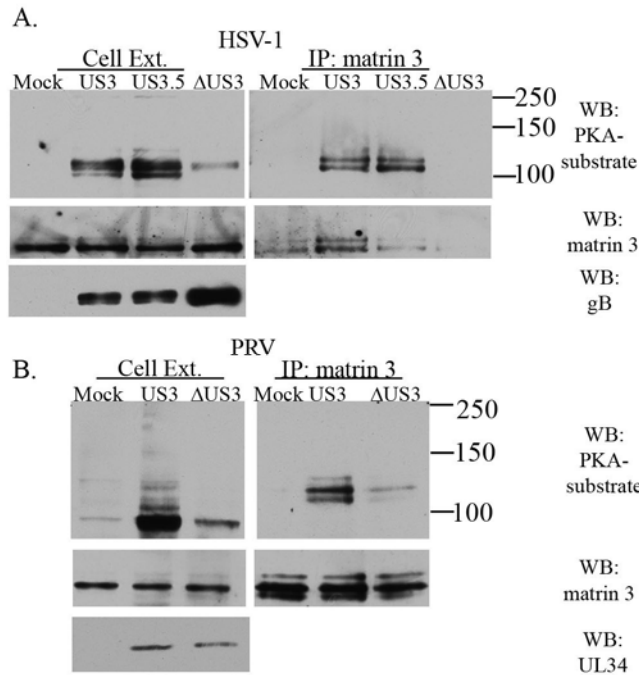


Figure 3-4. Matrin 3 is a conserved phosphorylation target for the US3 kinases during infection

MRC-5 cells were infected with (A) HSV-1 (US3), HSV-EGFP-U_S3.5 (US3.5) or HSV-EGFP-XhoΔUS3 (ΔUS3) at an MOI of 0.1 or (B) PRV (US3) or PRV.ΔUS3 (ΔUS3) at an MOI of 1 or mock infected, then harvested 1 day p.i.. Cleared lysates were immunoprecipitated using rabbit α-matrin 3 antibody. Whole cell extracts (Cell Ext.) or immunoprecipitation (IP) products were separated by 7% (HSV) or 6% (PRV) SDS-PAGE gel and analyzed by immunoblot. Membranes were probed with rabbit α-PKA-substrate antibody, and then stripped and reprobbed using rabbit α-matrin 3 antibody as indicated on the autoradiograph above. Cell extracts were also analyzed for viral protein expression using mouse α-HSV gB (A) or goat α-PRV UL34 antibodies (B). Protein size markers in kDa are specified to the right.

3.4.4 Identification of matrin 3 target residues for the ORF66/US3 kinases

Screening of matrin 3 for the phosphorylation target residue(s) of matrin 3 was based on the manual identification of serine and threonine residues immediately preceded by multiple basic residues. To identify the key residues targeted by ORF66 for phosphorylation, a series of HA

tagged matrin 3 mutants was generated in which the full length matrin 3 was expressed from the CMV IE promoter (HA-Matr3) with key S/T residues changed to alanine. S/T residues chosen reflected sites that fit the PKA-substrate motif or those that showed similarity to the US3 phosphorylation motif or IE62-target-like motifs. 293T cells were transfected with each HA tagged construct either alone or cotransfected with CMV IE driven EGFP-66, harvested the next day, followed by immunoprecipitation of soluble fractions using HA monoclonal antibodies. Immunoprecipitates were then analyzed by western blot and probed with p-PKA-sub or HA antibody. All constructs expressed in cells without the ORF66 kinase showed no detectable phosphorylation, as detected using the p-PKA sub antibody (Fig 3-5a), but when coexpressed with functional ORF66 kinase, all showed strong phosphorylation of matrin 3 with the exception of the HA-Matr3 - T150A mutant (T150A). This construct was expressed at the same levels, but showed only trace levels of phosphorylation (Fig. 3-5a). These results strongly indicate that the T150 residue is the major ORF66 dependent phosphorylation site on matrin 3. Matrin 3 with the T150A mutation showed identical cellular localization to wild type and all other mutants, with a strong nuclear localization, suggesting the differences in phosphorylation were not due to aberrant cellular localization due to misfolding or aggregation (data not shown). As such we conclude that T150A changes remove the predominant residue targeted for phosphorylation.

The T150 mutation was subsequently examined for phosphorylation in the context of wild type VZV and HSV infections. MeWo cells were transfected with HA vector, HA-Matr3-T150A, or HA-Matr3, and the next day infected with VZV or HSV-1. 24 h post infection, the HA tagged Matrin 3 protein was assessed for specific ORF66 directed phosphorylation as just detailed. The T150A mutant was found to display greatly diminished levels of phosphorylation compared to HA-Matr3 in both VZV and HSV-1 infections (Fig. 3-5b). Thus these results are

consistent with an ORF66/US3 directed phosphorylation of matrin 3 at residue T150 by both VZV and HSV-1.

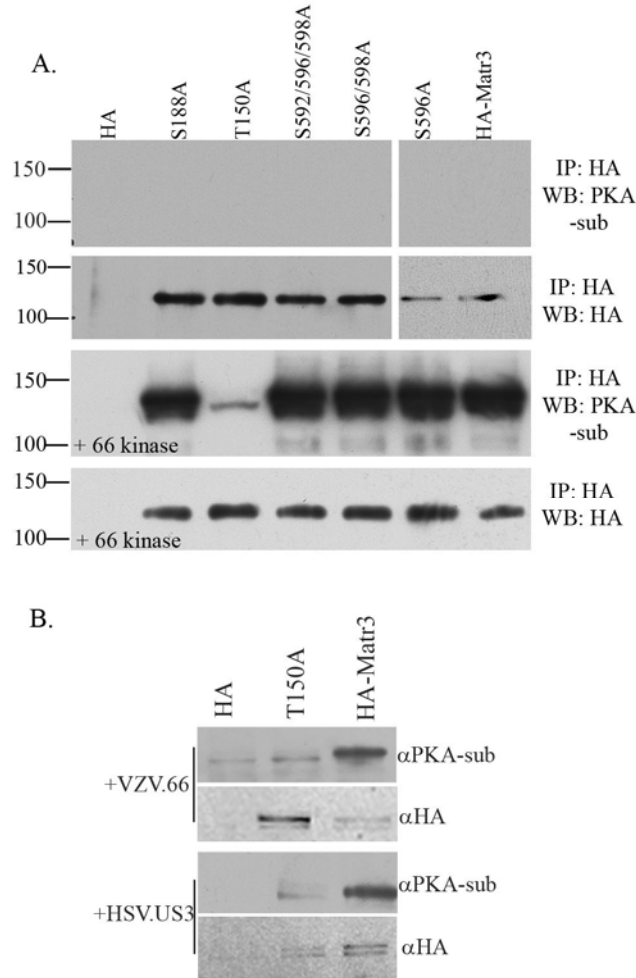


Figure 3-5. Matrin 3 a.a. T150 is the major phosphorylation site for VZV ORF66 and HSV-1 US3 kinase

(A) Immunoblot analysis of Hek 293T cells transfected with plasmids expressing HA alone, HA tagged to full length matrin 3 (HA-Matr3), or one of the following five HA tagged matrin 3 serine/threonine to alanine mutants: S188A, T150A, S592/596/598A, S596/598A or S596A (*top panels*). Alternatively, cells were cotransfected with one of the HA tagged proteins and EGFP.66 (*bottom panels*). The next day cells were harvested and cleared lysates were immunoprecipitated using mouse α -HA antibody, followed by separation of IP products on a 6% SDS-PAGE gel and transfer to PVDF membranes. Membranes were probed with rabbit α -PKA-substrate antibody to analyze matrin 3 phosphorylation or with mouse HA antibody to analyze equivalent HA immunoprecipitation. Protein size markers in kDa are specified to the left. (B) Immunoblot analysis of a MeWo cell transfection-infection. Cells were transfected with plasmids expressing HA alone, or HA matrin 3 containing a T150A mutation (T150A), or HA tagged to

full length matrin 3 (HA-Matr3), and the following day infected with VZV (*top panels*) at an MOI of 0.3 or HSV-1 (*bottom panels*) at an MOI of 5. Cells were harvested 1 day p.i. and clear lysates were then immunoprecipitated using mouse α -HA antibody. IP products were separated by 6% SDS-PAGE gel and analyzed by immunoblot using rabbit α -PKA-substrate or mouse α -HA antibodies.

3.4.5 ORF66-induced matrin 3 phosphorylation is through a non-PKA dependent pathway

As outlined in the introduction, the HSV-1 US3 kinase has been shown to induce the activation of PKA (9). The possibility existed that matrin 3 phosphorylation was the result of a similar ORF66 mediated activation of PKA. To address this question, cells were infected with Ad.GFP-66 or Ad.GFP-66kd in the absence or presence of increasing doses of a PKA-inhibitor (PKI), 14-22 amide. Cells were pretreated with PKI 2 hours prior to infection, and treatment continued till the time of harvest. An immunoblot of cell extracts probed for p-PKA-substrates showed that most detectable PKA substrate bands were essentially unchanged with the presence of 30-50uM of PKI, but at 60uM PKI, the p-PKA-sub antibody still detected the 125kDa species and a 47KDa species without recognition of most other PKA-substrate bands species (Fig. 3-6a). Probing for HA shows that ORF66 or ORF66kd were similarly expressed in infected cells. These results indicate the inhibition of PKA signaling did not prevent phosphorylation of the 125 kDa PKA-substrate band/matrin 3.

Further studies utilized the well established PKA activator forskolin, which acts by activating adenylate cyclase, leading to increases in intracellular cAMP and activation of PKA. Assessment of extracts of cells infected with VZV.GFP-66 or VZV.GFP-66kd in the presence of forskolin or DMSO control added at the time of infection show that the p-PKA-sub antibody recognized several novel protein species following forskolin treatment, with 37 and 60

kDa proteins being the most apparent. However the 66 kinase – dependent 125 kDa species identified as matrin 3 was virtually unchanged in the absence or presence of forskolin (Fig.3-6b). To ensure that matrin 3 phosphorylation was unaffected by forskolin treatment as detected by the p-PKA-substrate antibody, matrin 3 immunoprecipitates were analyzed and found to show no increase in detection of phosphorylated matrin 3 with forskolin treatment (Fig. 3-6b lower panels). Taken together with the inhibitor studies, these results suggest PKA did not play a significant role in the 66-directed matrin 3 phosphorylation.

It is known that matrin 3 can be targeted by PKA in neurons (64). We subsequently addressed whether the matrin 3 T150 residue affected PKA directed phosphorylation of matrin 3. The premise was that if PKA was not involved in the 66-dependent PKA phosphorylation, then a mutation at T150 should not affect PKA direct phosphorylation of matrin 3. To investigate this, an *in vitro* kinase assay was performed using purified PKA protein kinase and immunoprecipitated HA tagged matrin 3 proteins obtained from transfected cells. Mutants chosen for this assay were those that fit the PKA-substrate target motif RRXS/T. Tagged matrin 3 proteins were precipitated using HA-antibodies and these showed extensive phosphorylation *in vitro* when incubated with approximately 2 µg of PKA catalytic subunit alpha (Fig. 3-6c). HA-Matr3, S596A, and T150A mutants all demonstrate similar levels of phosphorylation by PKA. Interestingly, matrin 3 with S188A mutations showed diminished phosphorylation compared to HA-Matr3. This data supports the conclusion that ORF66 dependent phosphorylation of matrin 3 is not mediated through PKA, and suggests that the S188 site on matrin 3 accounts for a significant amount of the PKA-specific phosphorylation of matrin 3 *in vitro*.

To test if ORF66 kinase could directly phosphorylate matrin 3, we employed an *in vitro* kinase assay. Here, ORF66 or ORF66kd are fused to GST and matrin 3 is fused to MBP. GST

proteins were produced in SF9 using recombinant baculoviruses and MBP proteins expressed in *E. coli* BL21, and proteins were subsequently affinity purified. Equal amounts of GST, GST.66 or GST.66kd were incubated alone or with either MBP, MBPmatr3, or a positive control-MBP62p under optimal kinase assay conditions. After 25 minutes, reaction mixtures stopped using SDS sample buffer and were separated by SDS-PAGE gel, then transferred to an Immobilon-P membrane. These were then exposed to film and subsequently probed for GST or MBP proteins. The autoradiograph shows a band at 75kDa for GST.66 (Fig. 3-7, lane 2, 6, 10, 14), that was much diminished in GST.66kd (Fig 3-7lane 3, 7, 11, 15). This was expected as ORF66 has previously been reported to autophosphorylate (52). As shown previously (52), MBP62p is extensively phosphorylated by GST66 (Fig. 3-7, lane 10) and this phosphorylation is much diminished when the protein was combined with GST66kd (Fig. 3-7, lane 11). No phosphorylation is detected for GST or MBP proteins alone (Fig. 3-7, lane 1, 4, 5, 8, 9, 12, 13). MBPmatr3 migrated as two bands, one at approximately 170 kDa & 125kDa, neither of which were appreciably phosphorylated by any of the GST fusion proteins (Fig. 3-7, lanes 12-15). These results indicate that matrin 3 is not an *in vitro* ORF66 target under the conditions optimal for MBP62p phosphorylation. Because MBPmatr3 is bacterially expressed, we wanted to ensure that the protein was in a folded form that allowed phosphorylation. Thus, MBPmatr 3 was incubated with PKA which is known to phosphorylate matrin 3 (64). Results showed that both MBPmatr3 bands were phosphorylated by PKA, hence indicating that MBPmatr3 was in a properly folded form to serve as target of PKA in both PKA reaction buffer (Fig. 3-7, lane 17) as well as optimal 66 kinase buffer (Fig. 3-7, lane 18). Together, this data suggests that 66-dependent phosphorylation of matrin 3 is not a direct ORF66 target and phosphorylation occurs through a non-PKA signaling pathway.

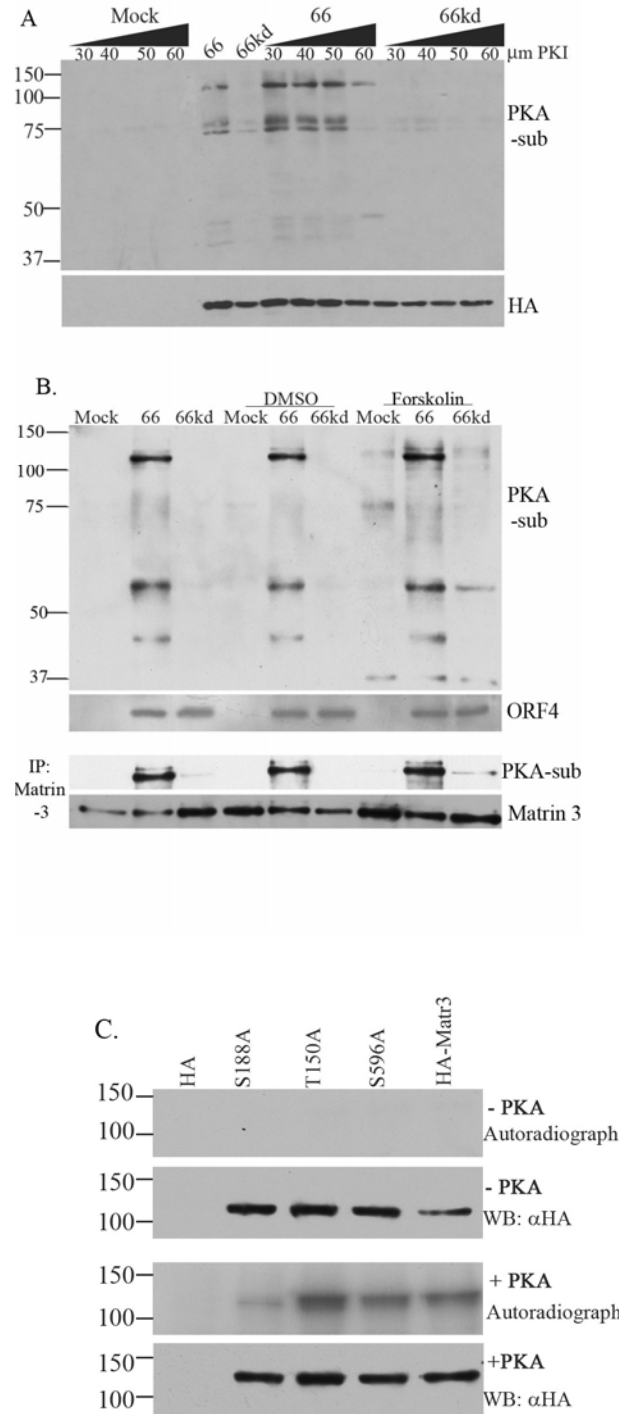


Figure 3-6. The 125kDa PKA-substrate protein is phosphorylated through a non-PKA pathway

(A) MRC-5 cells were pre-treated with a PKA-substrate inhibitor, 14-22 amide (PKI), 2 hours prior to infection. Cells were then infected with Ad.Toff at an MOI of 2.5 and Ad.GFP-66 (66) or Ad.GFP-66kd (66kd) at an MOI of 5 with or without PKI, or mock infected. Dose of PKI at increasing μM levels are indicated at the top of the figure. An immunoblot was done of whole cell extracts. The membrane was first probed with mouse α -HA antibody, stripped, then reprobed with rabbit α -PKA-substrate antibody.

The arrow denotes the 125kDa PKA-sub/matrinx 3 protein. The star denotes an undefined protein whose phosphorylation is PKI resistant. (B) MRC-5 cells were infected with VZV.GFP-66 (66) or VZV.GFP-66kd (66kd) at an MOI of 0.1 or mock infected. When indicated, cells were treated with 10 μ M forskolin or DMSO at the time of infection. Cells were harvested 1 day p.i., analyzed by immunoblot, and probed with rabbit α -PKA-sub antibody. Viral protein expression was analyzed using rabbit VZV ORF4 antibody. Cleared lysates were immunoprecipitated for matrinx 3 and subsequently analyzed by immunoblot using rabbit PKA-substrate, stripped, and reprobbed with rabbit matrinx 3 antibody. (C) In vitro kinase assay of immunoprecipitated HA alone or HA tagged matrinx 3 (HA-Matr3) or HA tagged matrinx 3 mutants S188A, T150A, and S596A incubated with PKA where specified (*lower panels*). HA proteins were derived from transfected Hek293T cells, that were purified from immunoprecipitations using mouse α -HA antibody. Following the kinase assay, proteins were separated on a SDS-PAGE gel, and transferred to a PVDF membrane, exposed to film as shown in the above autoradiograph. These membranes were then analyzed for HA fusion protein expression by probing with mouse α -HA antibody. Protein size markers in kDa are specified to the left.

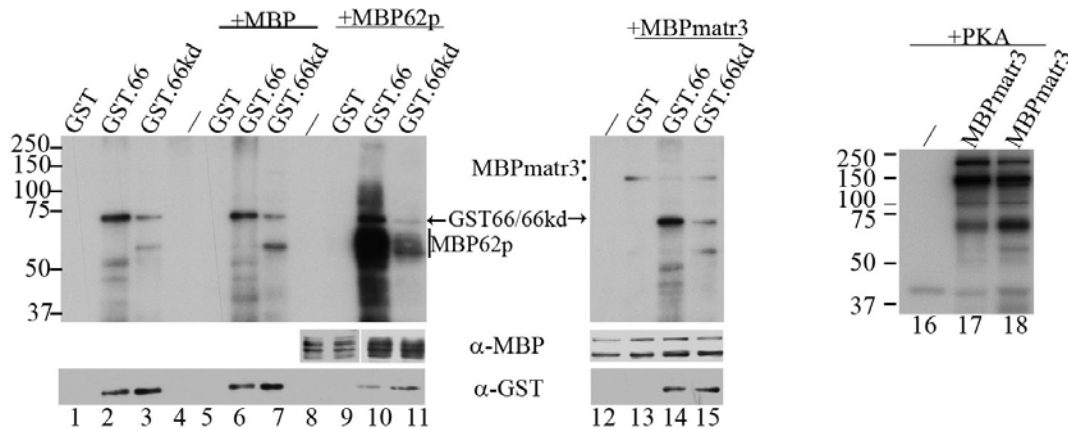


Figure 3-7. ORF66 does not target matrinx 3 under the conditions required for IE62

Purified MBP proteins and GST kinase were incubated in optimal kinase buffer, separated by 7% SDS-PAGE gel, transferred to PVDF membranes and exposed to film for autoradiography. Lanes 1-4 contain GST, GST.66, or GST66kd, or MBP incubated alone respectively. Lanes 5-7 contain MBP incubated with GST, GST.66, or GST.66kd respectively. Lane 8 contains MBP62p alone, and lanes 9-11 contain MBP62p incubated with GST, GST.66, or GST.66kd, respectively. Lane 12 contains MBPmatr3 alone, and lanes 13-15 contain MBPmatr3 incubated with GST, GST.66, GST.66kd, respectively. Lane 16 also contains MBPmatr3 alone, and lanes 17-18 contain equivalent levels of PKA incubated with MBPmatr3 in PKA reaction buffer (lane 17) or optimal 66 kinase buffer (lane 18). Protein levels were then analyzed by immunoblot using rabbit MBP and goat GST antibodies (lanes 1-15). Protein size markers in kDa are specified to the left of autoradiographs.

3.4.6 Matrin 3 localization in VZV-infected cells

Protein kinases often induce subcellular localization changes following phosphorylation of their target substrates in order to modulate function. This is certainly exemplified by ORF66 kinase phosphorylation of IE62, where phosphorylation induces radical changes in subcellular localization. In this case, IE62 is excluded from the nucleus and localized in the cytoplasm which is a requirement for IE62 tegument incorporation (52, 54, 98). We then asked whether ORF66-specific phosphorylation of matrin 3 lead to changes in the protein's intracellular localization. MRC-5 cells were infected with VZV.GFP-66Rsc, VZV.GFP-66kd, or mock infected. In mock-infected cells matrin 3 exhibited dominantly nuclear localization, with exclusion from what appeared to be nucleoli (Fig. 3-8a (panels *i* and *iv*) and 3-8d (panel *i*)). This is in accordance with previously described subcellular localizations for matrin 3 in other cell types. In infected cells expressing ORF66, matrin 3 was largely retained in the nucleus with a slightly more diffuse intranuclear localization (Fig. 3-8d (panel *ii*)), even late in infection as depicted in the shown syncytia (Fig. 3-8 b (panels *i* and *iv*)). In cells expressing the kinase-inactive ORF66kd, matrin 3 was still retained in the nucleus but many cells displayed multiple areas within the nucleus that were devoid of matrin 3 (Fig. 3-8c (panels *i* and *iv*) and Fig. 3-8d panel *iii*), yet were filled with IE62 and followed early replication compartment patterns. Additionally, few cells also exhibited matrin localizing in 2-10 nuclear punctae. As reported previously, IE62 was cytoplasmic - nuclear excluded in ORF66-expressing cells (Fig. 3-8b panel *iii* & *iv*) and exclusively nuclear in ORF66kd-expressing cells (Fig. 3-8c panel *iii* & *iv*). Furthermore, GFP.66 showed both cytoplasmic and nuclear localization (Fig. 3-8b panel *ii* and *iv*), compared to the more predominant nuclear localization of GFP.66kd (Fig. 3-8c panel *ii* and *iv*). Overall, our immunofluorescence analysis indicates that matrin 3 localizes to the nucleus

late into VZV infection, and presents subtle differences in its intranuclear localization when kinase activity is abrogated.

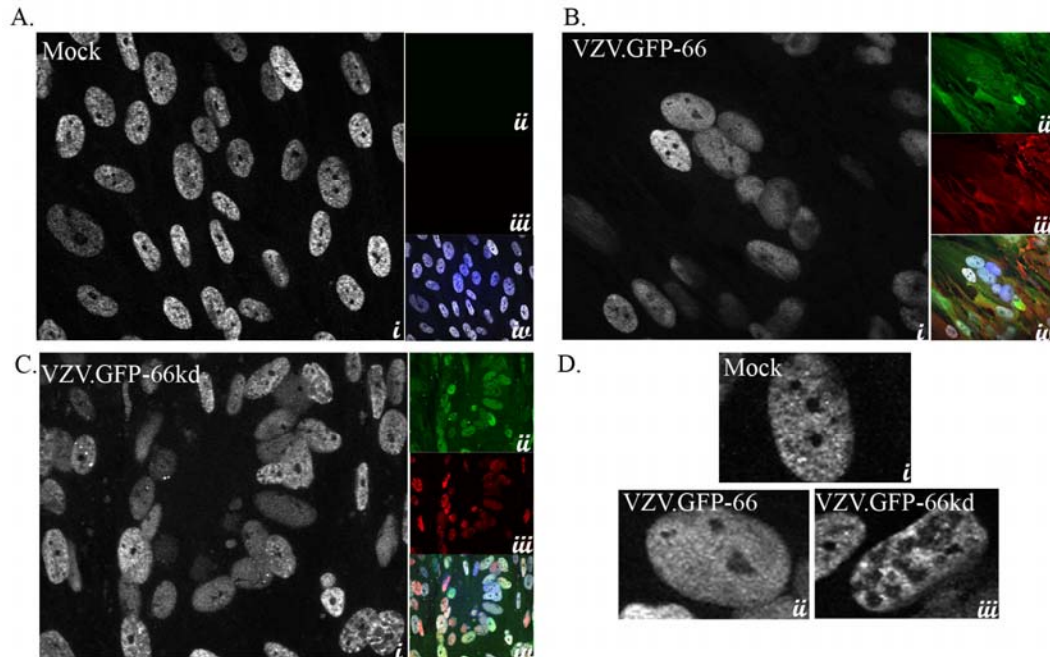


Figure 3-8. VZV infection leads to subtle differences in matrix 3 cellular localization

Immunofluorescence analysis of MRC-5 cells (A) mock infected or infected with (B) VZV.GFP-66Rsc or (C) VZV.GFP-66kd at an MOI of 0.003. Cells were fixed with 4% paraformaldehyde 3 days p.i. and immunostained with rabbit anti-matrix 3 antibody (A-C (*panel i*) detected with α -rabbit Alexa Fluor 546, D) or mouse anti-IE62 (A-C (*panel iii*) detected with α -mouse Alexa Fluor 647. ORF66 expression was determined by GFP autofluorescence (A-C (*panel ii*)). The merge image (A-C (*panel iv*)) are overlays of matrix 3 (gray), GFP (green), IE62 (red), and nuclei stained with Hoechst dye (blue). (D) Single cell representative images depicting matrix 3 localization. Infection conditions are indicated in the image. Fluorescence images were taken using a 60X objective.

3.4.7 Matrin 3 efficient nuclear retention is dependent on US3 kinase expression

Our previous data had indicated that ORF66/US3 – dependent matrin 3 phosphorylation was conserved for the alphaherpesvirus, and shared a common phosphorylation site. We extended our immunofluorescence analysis to HSV-1 and PRV, to investigate whether US3 kinase activity had any influence on matrin 3 cellular localization. MRC-5 cells were synchronously infected with HSV-1, HSV-1 expressing GFP.US3.5 (HSV.US3.5), HSV that did not express US3 (HSV.ΔUS3), PRV, PRV that did not express US3 (PRV.ΔUS3) or mock infected. At 18hrs p.i., cells expressing HSV US3 (Fig. 3-9 B) or US3.5 (Fig. 3-9C) displayed matrin 3 predominantly in the nucleus (Fig. 3-9B,C panels *i* & *iv*), although many instances of nuclear condensation were visible for US3.5-expressing cells. Localization did not differ substantially from mock-infected cells (Fig. 3-9A) except matrin 3 exhibited a more diffuse nuclear localization, in addition to what appears to be loss of most detectable nucleoli. Redistribution of nucleolar proteins have been reported previously in HSV infected cells (19). However, when HSV US3 was not expressed, cytoplasmic accumulation of matrin 3 were consistently observed in addition to nuclear localization (Fig. 3-9D panel *i* & *iv*). To visualize HSV infection, an ICP4 IF stain was included in our analysis. HSV-1 ICP4 was observed in all cells, and exhibited a mainly nuclear localization in all infected cells (Fig. 3-9B-Dpanel *iii*), with some cytoplasmic accumulations in HSV.ΔUS3 infected cells (Yee, MB unpublished results). GFP.US3.5 located in the cytoplasm and nucleus of infected cells (Fig. 3-9B panel *ii*), and GFP alone was expressed from the US3 native promoters in HSV.ΔUS3 (Fig. 3-9C panel *ii*). In PRV infected cells 11 hrs p.i., matrin 3 again displayed a mostly nuclear localization late in infection (Fig. 3-9E panel *i* & *iv*) although some cytoplasmic forms were noted. Interestingly, in the absence of PRV US3 expression, matrin 3 exhibited nuclear exclusion in multiple cells, with accumulation now in the

cytoplasm of infected cells (Fig. 3-9F panel *i* & *iv*). All cells were infected as displayed by UL34 stain (Fig.3-9 E &F panel *iii*), and GFP expression was evident from the PRV US3 native promoter in PRV. Δ US3- infected cells (Fig. 3-9F panel *ii*). Our results reveal that both HSV and PRV US3 modulate matrin 3 cellular localization, and US3 expression is necessary for efficient matrin 3 nuclear localization.

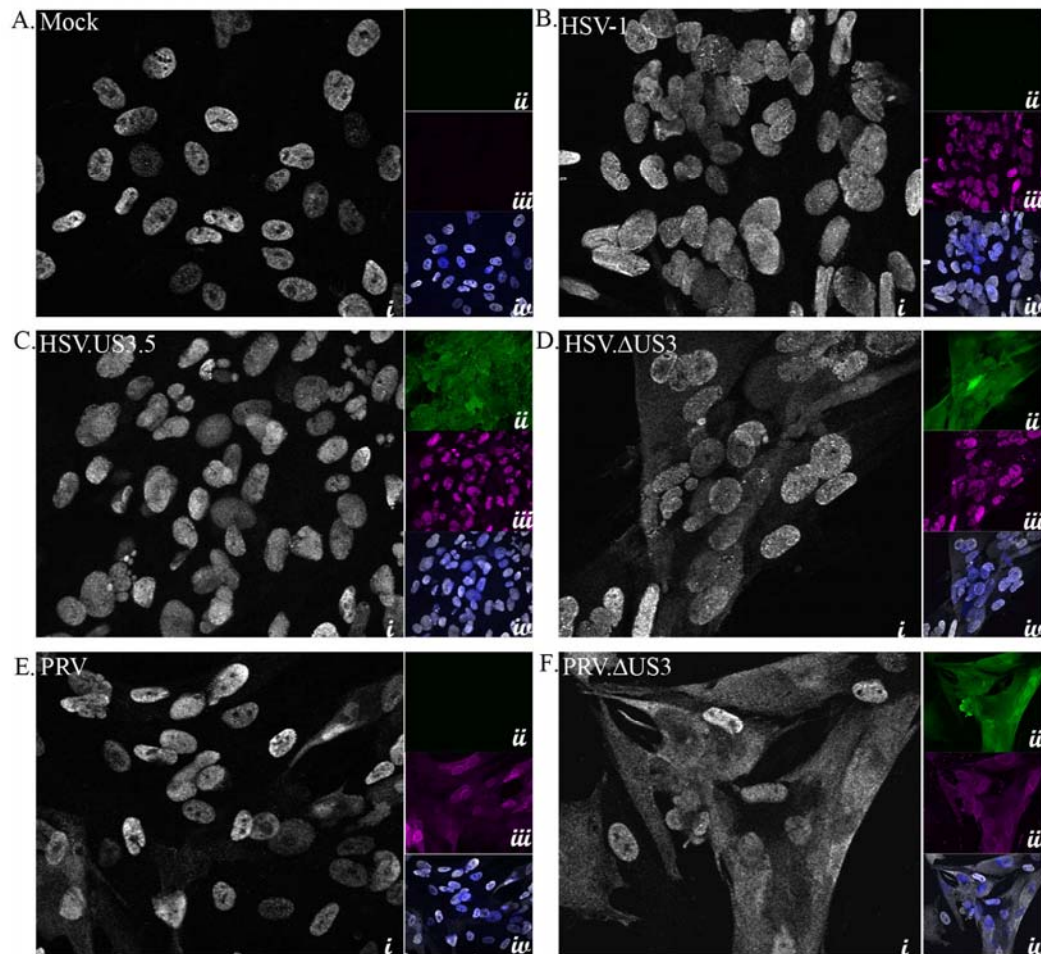


Figure 3-9. HSV-1 and PRV US3 kinase expression leads to matrin 3 nuclear retention or shuttling to the nucleus during infection

Immunofluorescence analysis of MRC-5 cells (A) mock infected or infected with (B) HSV-1, (C) HSV.US3.5, (D) HSV. Δ US3 (E) PRV, or (F) PRV. Δ US3 at an MOI of 5. Cells were fixed with 4% paraformaldehyde 18hrs p.i.(HSV) or 11hrs p.i (PRV), then immunostained with rabbit α -matrin 3 antibody (A-F (*panel i*)) detected with α -rabbit Alexa Fluor 546 (HSV) or α -rabbit Alexa Fluor 555 (PRV), mouse α -HSV ICP4 (A-D (*panel iii*)) detected with α -mouse Alexa Fluor 647, or goat anti-PRV UL34 (E & F (*panel iii*)) detected with α -goat Alexa Fluor 647. GFP-US3.5 expression or US3 promoter activity in HSV. Δ US3 and PRV. Δ US3-infected cells was determined using GFP autofluorescence (A-F (*panel ii*)). The merge image (A-F (*panel iv*)) are overlays of matrin 3 (gray), GFP (green), ICP4 (magenta) or PRV UL34 (magenta), and nuclei stained with Hoechst dye (blue). Fluorescence images were taken using a 60X objective.

3.5 DISCUSSION

Increasingly, the multifunctional roles for ORF66 kinase are realized, as well as the kinases' cell-type dependent importance for proper VZV growth and replication in the hosts. This is in alignment with the multifunctional nature of the alphaherpesvirus US3 kinases. ORF66 kinase activity is key in regulating IE62 cellular localization & tegument inclusion, and modulates multiple cellular activities involved in immune evasion strategies, as well as induces phosphorylation of proteins involved in silencing viral gene expression. Additionally, ORF66 is critical for VZV growth in specific cell types. Nevertheless, many specific protein targets are yet to be determined. In this work, we reveal that matrin 3 is an indirect phosphorylation target of ORF66, and is a conserved target of the ORF66 orthologues, HSV-1 and PRV US3 kinases. Our data also suggests that a function of this phosphorylation is to maintain matrin 3 nuclear localization. This is the first report, to our knowledge, of matrin 3 protein modification by any virus.

Matrin 3 is a 847 a.a. 125 kDa slightly acidic protein with a predicted weight of 95kDa (7). The N-terminus contains a large number of free hydroxyl groups (26 of the first 100

residues) as characteristic of lamin proteins, in addition to an acidic C-terminus found in many nuclear proteins, and two tandem RNA recognition motifs (7). Specific functions for matrin proteins are mostly unknown, yet there are reports proposing intriguing roles for matrin 3 in host cell processes. Recent studies have implicated it as a component of functional nuclear microenvironments of chromatin replication & transcription (123). Moreover, matrin 3 has been found to interact with hnRNP-L, an RNA splicing regulator, & SAFB, involved in RNA processing & chromatin organization (229). Matrin 3 can bind DNA at scaffold/matrix attachment regions (S/MAR) sites which influence chromatin structure by associating with matrix-binding proteins that anchor chromatin into loop domains. Interestingly, matrin 3 is also part of a three protein complex including p54nrb and PSF that prevent the nuclear export of nuclear dsRNAs that are hyperedited by members of the ADAR (adenosine deaminase that act on RNA) enzyme family (45, 231). In rat neurons, activation of the glutamate receptor, NMDA by PKA induces matrin 3 phosphorylation. This phosphorylation in turn leads to matrin 3 degradation and subsequent neuronal death (64). Lastly, matrin 3 has been linked to the genetic disorders such as one type of autosomal-dominant distal myopathy, VCPDM, and found in decreased levels in fetal Down's syndrome brains (13, 192).

The goal of our analysis was to uncover novel phosphorylation targets of ORF66 kinase and get a clearer understanding of the roles of ORF66 in VZV infection. The phosphorylation motif for ORF66 is unknown, yet the target sites in IE62 are well-described. Based on the similarity between these sites and that of the cellular kinase PKA phosphorylation motif, we took advantage of a phosphospecific PKA-substrate antibody to find novel ORF66 protein targets. Interestingly, we found that these alphaherpesviruses varied widely in number and molecular weights sizes of bands that were induced with infection (Figure 3-1). These

proteins may be direct ORF66 or US3 targets, direct PKA targets, or downstream phosphorylation targets of activated PKA signaling pathways. HSV-1 displayed the strongest induction of phosphorylation of PKA-substrate proteins, agreeing with previous findings that US3 induced the phosphorylation of proteins fitting PKA substrate specificity, in addition to their model which predicts that HSV-1 infection activates PKA and may share protein substrates (9). VZV is reported to increase expression of the PKA catalytic subunit as well as induce detection of PKA-substrate bands. Although, some of the phosphorylated sizes were of similar molecular weight, it is unknown whether the same proteins are detected as these proteins have not been identified (49). Notably, in our study a novel ORF66-dependent 125 kDa PKA-substrate was the dominant protein present. Importantly, although profiles between the alphaherpesviruses differed, there was conservation of ORF66/US3-dependent phosphorylation of the 125 kDa protein/matrix 3 (Figure 3-1, 3-3, & 3-4). This leads to the prediction that because phosphorylation of this specific protein is conserved, it may be important for alphaherpesvirus replication. Also in figure 3-1, HSV. Δ US3-infected cells, a faster migrating band for gB protein was observed and likely represents an unphosphorylated gB fraction (86, 221). gB migrates at a similar molecular weight as matrix 3, and this may account for some phosphorylation seen in HSV-1. Δ US3 in the 125kDa region of cell extracts on longer exposures of autoradiographs (Figure 3-4a). Some gB phosphorylation in cells infected with HSV-1 expressing inactive US3 has been reported previously using PKA-substrate antibody (86).

We also observed that expression of ORF66 using adenovirus vectors, strongly induced phosphorylation of the 125 kDa protein, indicating that this band represented a cellular protein (Figure 3-2). Other host proteins bands were detected with expression of ORF66, albeit less strongly than the 125kDa protein but are of interest for future identification. Our mass

spectrometry analysis identified the protein as matrix 3. Interestingly, the results for this region of the gel did not identify additional proteins in this region except for keratin contaminants which are common for LC/MS/MS methods. Identification of matrix 3 and the observation that for all 3 viruses this nuclear matrix protein is phosphorylated in an ORF66/US3 – dependent fashion provides much evidence that matrix 3 is the 125kDa-PKA-substrate protein. While matrix 3 has not been linked as a modified protein of any virus, interaction of virus with matrix proteins have been described for HIV, SV40, PRV, HCMV and HPV (8, 66, 142, 182, 187, 201), and notably for HSV-1 (16-17, 23, 138, 223, 226). For most of our analysis at least two forms were detected in whole cell extracts and 2 or more in IP fractions. Importantly, both matrix 3 and p-PKA substrate antibodies detect a stronger faster migrating band, and a slower migrating 125kDa band in cell extracts. Because IP forms are detected by the p-PKA substrate antibody, we believe that these likely represent different phosphorylated forms. The fact that IP fractions are enriched for matrix 3, combined with the use of specific PKA-substrate antibody, we predict leads to additional forms of this protein revealed in this fraction. Differentially phosphorylated matrix 3 isoforms have been documented in rat cells, with a 130kDa and 123kDa matrix 3 localizing to the nucleus and extracellular compartments, respectively (75). Differing matrix 3 forms with slightly different isoelectric points have been isolated from neurons (64). Whether a specific function is attributed to these forms or whether they represent phosphorylation status in the process of turnover or degradation fragments is unclear. Two transcripts have been recorded for matrix 3, differing at the 5'UTR but encoded the same protein (NCBI). Nevertheless, alternate protein modifications should still be considered.

One of the objectives for analyzing 66-dependent phosphorylation of matrix 3 serine/threonine to alanine mutants was to explore potential functions of this specific matrix 3

targeting. MatrIn 3 contains two recognition RNA recognition motifs, matrin-type zinc fingers, and potential nuclear localization signal (a.a. 710-718). We chose candidate ORF66 sites with 2 or more basic residues adjacent and N-terminal to a serine or threonine. Interestingly, S592, 596 and 598 were within the human homologue region of the identified chicken matrin 3 bipartite nuclear localization signal (77). Our data shows that the T150 mutation to alanine drastically diminished phosphorylation detected for the HA-tagged matrin 3 mutant (Figure 3-5.). However, there was still some phosphorylation detected for this mutant indicating the possibility for additional matrin 3 residues that are phosphorylated in a 66-dependent manner. It is intriguing that different alphaherpesviruses would share a common target and phosphorylation site on that target protein; this may be due to the nature of similar phosphorylation target motifs for the US3 kinase. This would predict that this phosphorylation would have similar outcomes on matrin 3 function.

Activation of PKA-substrates during viral infection has been reported for HCV (55), and activated PKA pathways have been exploited by many viruses including adenoviruses, HIV (114, 203), HCMV (90), and HSV (222) to enhance infection. However our data suggest that PKA does not directly phosphorylate matrin 3 at the T150 major phosphorylation site (Figure 3-6), although matrin has been shown here and in previous studies to be a PKA target. Inhibition of PKA with a highly specific inhibitor, 14-22 amide, did not prevent detection of the phosphorylated 125kDa protein, although other PKA-substrates proteins were no longer detected. Activation of PKA using forskolin also did not increase matrin 3 phosphorylation and minimally increased its phosphorylation in ORF66kd-expressing infected cells (Figure 3-6.). Moreover, *in vitro* phosphorylation of HA-Matr-T150A mutant by PKA did not differ from the non-mutated form of matrin 3, yet there was reduced phosphorylation for HA-Matr-S188A.

These results indicate that PKA does phosphorylate matrin 3 at the S188 site *in vitro* and potentially other sites, but does not target the T150 site which is the 66-dependent matrin 3 phosphorylation site. Thus these data suggests that PKA or PKA signaling pathways have a minor role in the 66-dependent phosphorylation of matrin 3. We did note a prospective 60kDa likely viral protein that was phosphorylated in response to forskolin treatment in ORF66kd expressing cells. This indicates that there is a protein which is phosphorylated in response to activation of PKA pathways that is dependent on VZV infection. We then explored whether matrin 3 was directly phosphorylated by ORF66 *in vitro*. Surprisingly, ORF66 did not phosphorylate MBPmatr3 under the same *in vitro* kinase assay conditions for which ORF66 phosphorylates MPP62p (Figure 3-7), while PKA did phosphorylate matrin 3 under these same conditions. PKA phosphorylation of matrin 3 may reflect targeting of other S/T sites other than those sites phosphorylated (T150) in response to ORF66 expression. This data does suggest that ORF66 does not directly phosphorylate matrin 3. However, this does not exclude the possibility that matrin 3 may be phosphorylated by ORF66 under different kinase assay conditions, or require an additional nuclear protein; this will be the subject of further investigation.

ORF66 kinase has demonstrated the ability to regulate VZV IE62 localization and this determines IE62 inclusion in the virion tegument. HSV US3 kinase activity is known to cause the redistribution of a nuclear matrix protein, lamin A/C, involved in breaching the laminar network needed for proper nucleocapsid envelopment yet still maintaining laminar structure (138). In our immunofluorescence study, matrin 3 remained nuclear in VZV infection with a more diffuse localization of the protein compared to the mock-infected cells. In contrast, many cells in VZV.GFP-66kd expressing cells displayed regions devoid of matrin 3 of which were filled with IE62 protein (Figure 3-8). This is reminiscent of the findings for lamin A/C that

normally forms a reticular pattern in infected cells, yet in the absence of US3 kinase activity leads to larger intranuclear regions devoid of lamin A/C (138). Thus, similarly to what happens to lamin A/C distribution, ORF66 may also be responsible for maintaining a balance between disruption of a major component of the nuclear matrix yet retaining matrin 3 at replication compartments, where viral replication and transcription occurs. This implies that ORF66 kinase activity may be necessary for matrin 3 interaction with components of early replication compartments, such as IE62. HSV infection also causes reorganization of another nuclear matrix protein, nuclear mitotic apparatus (NuMA) protein and is excluded from replication compartments, with redistribution dependent on viral DNA synthesis (226). In HSV-1 and PRV immunofluorescence analysis, matrin 3 showed a diffusely nuclear localization in infected cells, as well as in HSV.EGFP-US3.5 expressing cells. In contrast, subtle yet reproducible cytoplasmic accumulation of matrin 3 was visible in cells that did not express US3 kinase in HSV-1. These differences were likely not due to apoptotic cells, as HSV-1 US3.5 like US3-null viruses do not possess the US3 function in inhibiting apoptosis (162), yet matrin 3 was still predominantly nuclear. Cytoplasmic accumulation were even greater in PRV-infected cells that lacked US3 with some cells displaying nuclear exclusion of matrin 3 (Figure 3-9), and for both viruses the difference between US3 and US3-non-expressing infected cells was most distinguishable late in infection. Together these findings point to a role for the US3s in the active retention of matrin 3 in the nucleus or increased shuttling of matrin 3 to the nucleus. Regulation of matrin 3 cellular localization by phosphorylation has been reported previously where the use of a general kinase inhibitor staurosporine leads to matrin 3 accumulation in the cytoplasm (77). It is possible that phosphorylation by US3 may be key for matrin 3 interaction with cellular proteins that are retained in the cytoplasm. In the absence of US3, matrin 3 may be

lost to the cytoplasm due to the nuclear component reorganization that occurs in HSV infection . Secondly, matrin 3 may be interacting with a viral protein that is also a US3 target which localizes to the cytoplasm late in infection in the absence of US3 expression. The nuclear exclusion seen in PRV.ΔUS3 may be explained by this latter scenario or an active export of matrin 3 to the cytoplasm. We also observed that in infection with VZV, HSV-1 & PRV, global matrin 3 levels remained unchanged as visualized by western blot. This suggests that matrin 3 is a very stable protein and supports the idea that matrin 3 is a necessary protein for alphaherpesvirus infection. This will be an interesting question to be addressed for future siRNA studies.

Our studies thus far have indicated that matrin 3 is specifically phosphorylated in an ORF66/US3 kinase-dependent manner, and the kinases' function in either modulating intranuclear localization or nuclear-cytoplasmic shuttling. This leads us to question the potential functions of matrin 3 in alphaherpesviral infection, and how the ORF66/US3 specific matrin 3 phosphorylation contributes to this function. However, matrin 3 cellular functions are not clearly defined but recent evidence points to a multifunctional nature for this protein. Nuclear matrix has long been reported to be the site of organization for numerous nuclear processes such as DNA replication, DNA loop attachment, transcription and RNA processing (3, 11-12, 83). Matrin 3 specifically locates in close proximity to nascent DNA replication and transcription zones within the nucleus. Thus, as matrin 3 is a major nuclear matrix protein, it may serve as a platform for these essential genomic functions. Furthermore, we can conceive that matrin 3 is also needed to be present at sites of viral replication and transcription. Recently, a comparable role has been proposed for lamin a/c as serving as a scaffold for HSV genomes and nuclear factors that reduce heterochromatin assembly on viral promoters (194). Matrin may also serve

as part the nuclear matrix that is involved as part of the site of capsid assembly due to findings that capsid proteins localized to nuclear matrix fractions (16, 23). If ORF66 is involved in capsid assembly, then this may explain the reduced intranuclear assembly of nucleocapsids in T cells from SCID-hu T cell xenografts infected with VZV lacking ORF66. MatrIn 3 is also involved as part of a complex that retains hyperedited nuclear dsRNAs in the nucleus and to prevent their export to the cytoplasm for translation. dsRNAs have been identified for HSV (84). The ORF66/US3 kinases may potentially be involved in regulating interaction of matrIn 3 with the p54nrb-PSF complex and modulate the balance between nuclear accumulation and release of viral dsRNA to the cytoplasm. Lastly, matrIn 3 degradation in neurons leading to neuron death may be in response to the hyperphosphorylation of matrIn 3 detected using PKA-substrate antibody. This leads to the speculation of whether ORF66 phosphorylates matrIn 3 leading to its degradation during VZV reactivation in neurons, and in turn causing the neuronal death or damage that is sometimes associated with herpes zoster (153).

In summary, this study describes a novel cellular target for ORF66 kinase, the essential nuclear matrix protein –matrIn 3, that is specifically phosphorylated in a 66-dependent manner through a non-PKA pathway. This is a conserved target for two other alphaherpesvirus US3 kinases from HSV-1 and PRV. This phosphorylation functions in modulation of matrIn 3 intranuclear localization, or in the case of HSV and PRV, in efficiently maintaining matrIn 3 nuclear localization. This is the first report of a viral manipulation of this nuclear matrix protein.

4.0 FUTURE DIRECTIONS & GENERAL SUMMARY

Overall, the results presented here offer new insights for roles in ORF66 in VZV biology as well as revealing a novel host protein target with potentially important implications for ORF66 manipulation of cellular biology. Previously, ORF66 was regarded as a non-essential protein for VZV replication, yet it was obvious that this kinase must be important for VZV pathogenesis as it specifically targeted the VZV major transcriptional activator, IE62, and its direct phosphorylation determined IE62 virion incorporation. In recent years, VZV ORF66 has demonstrated that it is indeed a multifunctional protein in that its kinase activities are aimed at both viral and cellular proteins. These diverse roles include downregulation of surface MHC-1 in fibroblasts, modulation of interferon and apoptosis pathways, and targeting of HDAC 1 and 2. Furthermore ORF66 is important for growth in human T cells, which are believed to be key for VZV pathogenesis as they can transfer virions to sites in the skin in SCID-hu mouse models.

Corneal Fibroblasts

The work presented here describes the first non-lymphocytic cell line, primary corneal fibroblasts (54), for which ORF66 kinase activity is important for VZV growth. Although our studies found that the basis for impaired growth was not an inability to phosphorylate IE62 at the major S686 site nor increased apoptosis, this study establish a new cell culture model for exploration of cell-type dependent functions of ORF66. For future studies, the IFN- α/β pathways have yet to be explored. It is thought that inhibition of IFN signal transduction may

promote the survival of infected tonsillar T cells. Thus, it is possible that PCF cells express higher levels of IFN, exerting an antiviral effect when ORF66 is inactive or not expressed. Human corneal epithelial cells have been found to increase transcriptional expression of various cytokines including IFN- β in response to HSV-1 infection *in vitro*. Interestingly, addition of recombinant human IFN- α 2a can inhibit VZV replication in human corneal stromal fibroblasts cultures. Thus, investigating whether there are differences in cytokine transcription induction in PCF cells compared to another VZV permissive cell line could point out possible ORF66 substrates.

In infected PCF cells, small VZV foci were produced when ORF66 was not expressed or inactivated. This suggests that there may be a block in late gene expression, therefore analyzing at what point the delay is occurring may highlight potential viral proteins that are important VZV targets for efficient PCF infection. Moreover, PCF expressing 66kd may have deficiencies in proper virion maturation or trafficking during nuclear egress. gB is a leaky late protein that is involved in nuclear egress of virion in HSV-infected cells and is phosphorylated by US3 kinase in addition to likely cellular kinases at the same site. Interestingly VZV gB contains a potential candidate ORF66 phosphorylation motif at RSRRS₄₉₅VP and potentially another at the C terminus.

Ultimately, the lack of growth for 66-inactive VZV in PCF is cell-type dependent and the likelihood is that there is a cellular protein that aids in ORF66 kinase functions that is absent or altered in PCF cells, or alternatively an efficient VZV antagonist that is present or altered in this cell type. Hence, a focus should be placed in outlining what signaling pathways and specific cellular proteins are targeted in VZV- infected versus VZV expressing 66kd in PCFs as compared to more permissive cell lines.

Viral cell Targets

While ORF66 has been implicated in diverse cell processes, only one direct target is known for this kinase, IE62. Thus a major endeavour of my studies was to find novel ORF66 cellular or viral protein targets. As a result, a set of candidate viral proteins were chosen that fit a phosphorylation motif based on IE62 direct targeting for further investigation using *in vitro* kinase assays (Figure 4-1). Using aforementioned MBP fused to viral proteins and GST-66 and GST-66kd, results showed that both VZV ORF4 and ORF9 were direct ORF66 targets *in vitro* (Figure 4-2). Interestingly both of these proteins are viral tegument proteins and both contain a proline at the +2 position following the putative phosphorylated serine/threonine - both characteristics shared with the IE62 protein. ORF 4 is an IE phosphoprotein and major transactivator, post-transcriptional regulator of gene expression, and partner in mRNA export. IE4 is divided into four regions, one which is an arginine rich region subdivided into 3 units -Ra, Rb, & Rc. This argine rich region is important for transactivation properties & protein-protein interactions. Intriguingly, the putative phosphorylation site is located within the Rb region which binds strongly to RNA *in vitro* (151), and is adjacent to IE4 nuclear localization signal. Therefore, it is important that further studies pinpoint the site of IE4 phosphorylation by ORF66 to begin to understand possible functions of this phosphorylation. ORF9 is a tegument protein and displays limited homology to its homologue HSV VP22. This protein is not well characterized but has been reported to bind IE62 in complex with tubulin, possibly as a means of recruitment for virion incorporation (26). Interestingly, my studies with HA tagged ORF9 indicate that ORF9 displays multiple different localizations. This same observation has been reported for VP22 (126). Namely for ORF9 - cytoplasmic accumulations, perinuclear speckling,

rod-shaped filaments were noted. When cells were co-transfected with EGFP66, ORF9 predominantly displayed a cytoplasmic localization (data not shown). This suggests that ORF66 can modulate ORF9 subcellular localization. In VZV infection, ORF9 displayed cytoplasmic, nuclear, and at times rod shaped filaments as well as what appeared to be mitotic chromatin binding, yet it was unclear if there were localization differences in kinase-inactive cells. In VP22, these rod-shaped bundles reflect VP22 binding to microtubules causing their stabilization and in turn bundling. Thus, this implicates ORF66 in altering ORF9 intracellular localization, interactions with microtubules and any downstream effects resulting from that disruption. Challenges were encountered in *in vivo* phospholabeling of transfected cells, since ORF4 and ORF9 are phosphoproteins in addition to the observation that ORF66 seems to increase amounts of these proteins, therefore alternate methods should be considered. However, investigation of these interactions may reveal undescribed viral protein targets for the alphaherpesvirus US3 kinases as well as further understandings of the role of the ORF66 kinase in VZV infection.

ORF66 targets in IE62:

VZV IE62: R-K-R-K-S₆₈₆-Q-P-V

VZV IE62: K-R-R-V-S₇₂₂-E-P-V

Candidate VZV ORF 66 Targets

Membrane protein

No HSV homologue

ORF1: -R-R-K-A-S₆₀-A-Q- a.a.
1-108

Transcriptional

activator

ORF4: -R-R-R-R-P-T₁₄₅-T-P- 1-452

Tegument proteins

ORF9: -R-R-K-T₁₉-T-P- 1-302

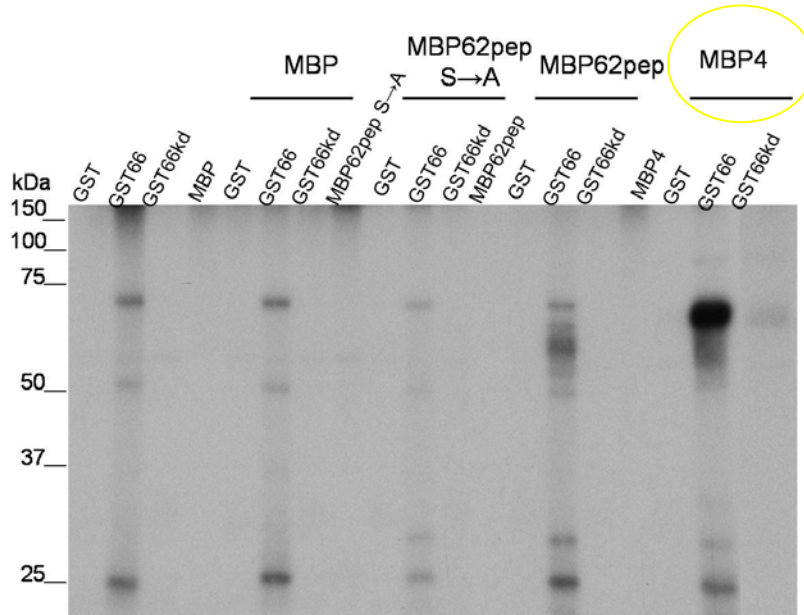
ORF22: -R-R-R-R-R-P-S₃₃₇-W-T- 1-2763

ORF38: -R-R-R-K-K-S₂₄₇-D-H- 1-541

ORF33: -R-R-R-R-V-S₄₈₄-P-S- 1-605

ORF49: -K-R-K-P-S₇₀-G-K- 1-81

Figure 4-1. List of candidate VZV ORF66 targets



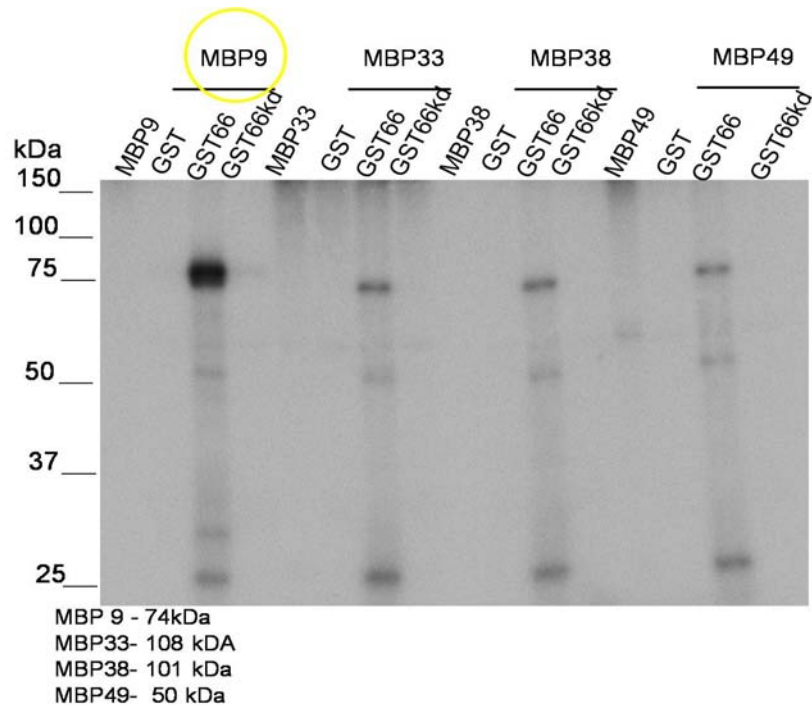


Figure 4-2. VZV ORF66 targets ORF 4 & ORF9 *in vitro*

Autoradiograph showing results of an *in vitro* kinase assay. Maltose binding protein (MBP) ORF9 and ORF4 fusion proteins were incubated alone or in equal amounts with GST, GST66, or GST66kd under optimal ORF66 kinase assay conditions described in section 3.3.9.

Actin.

Viruses interact with cytoskeletal elements at almost every step of the infectious cycle. The cytoskeleton itself is a diffusion barrier that must be overcome for viruses to transport itself within the cell (197). Actin is a globular structural protein that polymerizes into helical actin filaments forming a network within the cell. This dynamic structure provides mechanical support, determines cell shape, and is involved in cell mobility and formation of cell-cell junctions. Viruses often depolymerize actin to alter the diffusion properties of the cytoplasm and facilitate viral egress or induce actin polymerization to propel viruses to adjacent cells (197). Actin has also been implicated in nuclear activities such as transcription, chromatin remodeling

and modeling of the nucleoskeleton (170). Interestingly, HSV, MDV and PRV US3 kinases all manipulate cellular signaling pathways in restructuring actin networks to form projections or network disassembly (See Section 1.4.6.4). In PRV, the US3 kinases actually target PAK1 and PAK2 cellular kinases which in turn have roles in the Rho GTPase signaling pathways involved in actin disassembly and lamellopodia and filopodia formation. This concurs with a common theme as exemplified by US3 relationship with PKA, ORF66 phosphorylation of HDACs, and matrix 3; ORF66/US3 functions in direct phosphorylation of certain targets, but also seems to engage key host proteins for a common downstream effect especially when modulating cellular processes. Results showed that VZV-infected cells disorganized normally stratified filamentous actin (F-actin) filaments 24 hrs p.i., yet when ORF66 was kinase-inactivated actin cytoskeletal networks remained mainly intact (Figure 4-3). ORF66 expressed in the absence of other VZV proteins using Ad.GFP-66 or Ad.GFP-66kd, induced cell rounding and cellular extensions when ORF66 was functional and loss of stratified F-actin, yet ORF66kd expressing cells did not significantly alter overall cell morphology and F-actin filamentous were readily detected (data not shown). These findings strongly suggest that ORF66 does alter cell signaling pathways responsible for the dissolution of actin filaments. Initial studies should be directed at first delineating whether these effects are not solely because of differences in degree of infection between VZV and 66-inactive VZV, or in the case of adenoviruses a phenomenon due to apoptosis or protein overexpression, in addition to a concentration on what components of Rho GTPase pathways are modulated by 66 kinase activity. Single-cell live cell imaging experiments using VZV with fluorescently tagged capsid proteins in a 66 or 66kd background, together with delivered commercially available fluorescent phalloidin or transiently expressed actin-GFP may shed light on whether actin projections are produced in VZV with potential roles for intercellular

spread. Because, VZV seems to place heavy restrictions on production of cell free virions, it is highly probable that the virus would utilize the cytoskeletal network for intercellular spread and hijacking this cellular component is amongst the shared functions of the ORF66/US3 kinase family.

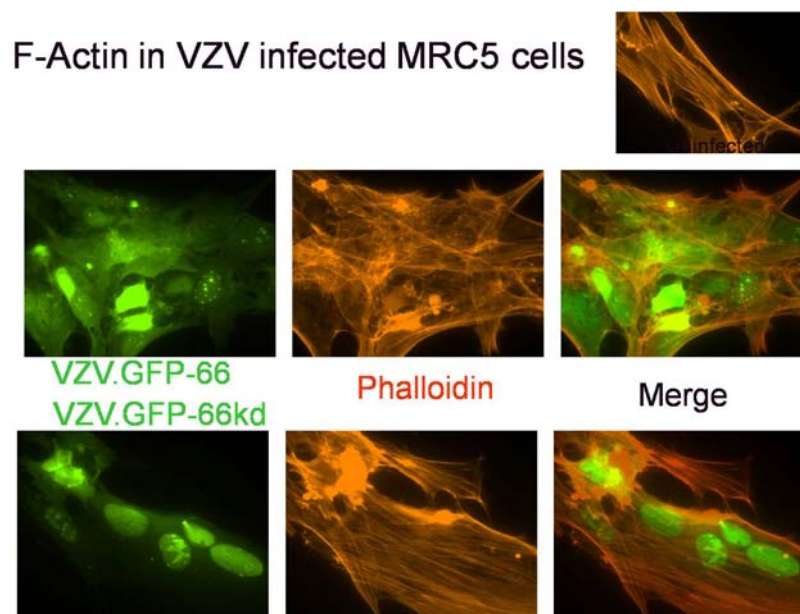


Figure 4-3. VZV ORF66 kinase activity induces actin rearrangement in infected cells

MRC-5 cells were infected with VZV.GFP-66 or VZV.GFP-66kd. Cells were fixed 24hrs p.i and fixed with 4% paraformaldehyde and stained with Alexa Fluor-546 phalloidin to visualize for F-actin (red). ORF66/66kd is visualized by GFP fluorescence (green).

PKA-substrates & MatrIn 3

Our investigation for ORF66 phosphorylation targets using a phosphospecific PKA-substrate as a tool to identify potential candidates fitting an IE62-like motif, lead to identification of MatrIn 3. VZV ORF66 expression did not lead to the phosphorylation of

multiple PKA-substrate proteins as noted for HSV and PRV, yet ORF66 kinase expression did lead to detection of protein bands of approximately 40kDa, 55kDa, and diffuse set of bands of 65-75kDa. Identification of these proteins by LC/MS in the context of VZV infection and adenovirus infection may highlight interesting new ORF66 viral or host targets. One possibility is that these proteins are all part of a signaling pathway that is activated by ORF66, or components of different pathways with PKA as a common upstream activator, although our forskolin studies would indicate that the latter is not the case. Using this antibody in IF studies, p-PKA-substrates were strongly noted in the nucleus in VZV.GFP-66-infected cells as opposed to mostly cytoplasmic accumulation in VZV.GFP-66kd. Although this may represent the matrix target, it may also indicate that ORF66 is targeting other nuclear PKA-substrate proteins (Figure 4-4). Use of this antibody in IF maybe useful in future studies to further investigate ORF66 targets.

A separate observation made during this investigation was that purified GST tagged ORF66 was detected as a PKA-substrate in western blots, but not kinase-inactive ORF66 (Figure 4-5). This suggests that ORF66 is a PKA-substrate or that the antibody may be detecting ORF66 autophosphorylation. Similarly, this antibody was used to reveal the HSV -1 US3 autophosphorylation motif, and this self regulation was needed for some of US3's physiological functions (87, 181). Thus, this tool may also serve to find phosphorylation sites on ORF66 which may impart regulation of the multiple functions of this kinase. Interestingly, the antibody also detected a PKA-substrate band within the gel region for which MBP62p is usually detected when MBP62p or MBP62pDM and GST66 were incubated together. This suggests that the antibody detected a phosphorylated residue on MBP62p other than the ORF66 phosphorylation sites – S686 and S722.

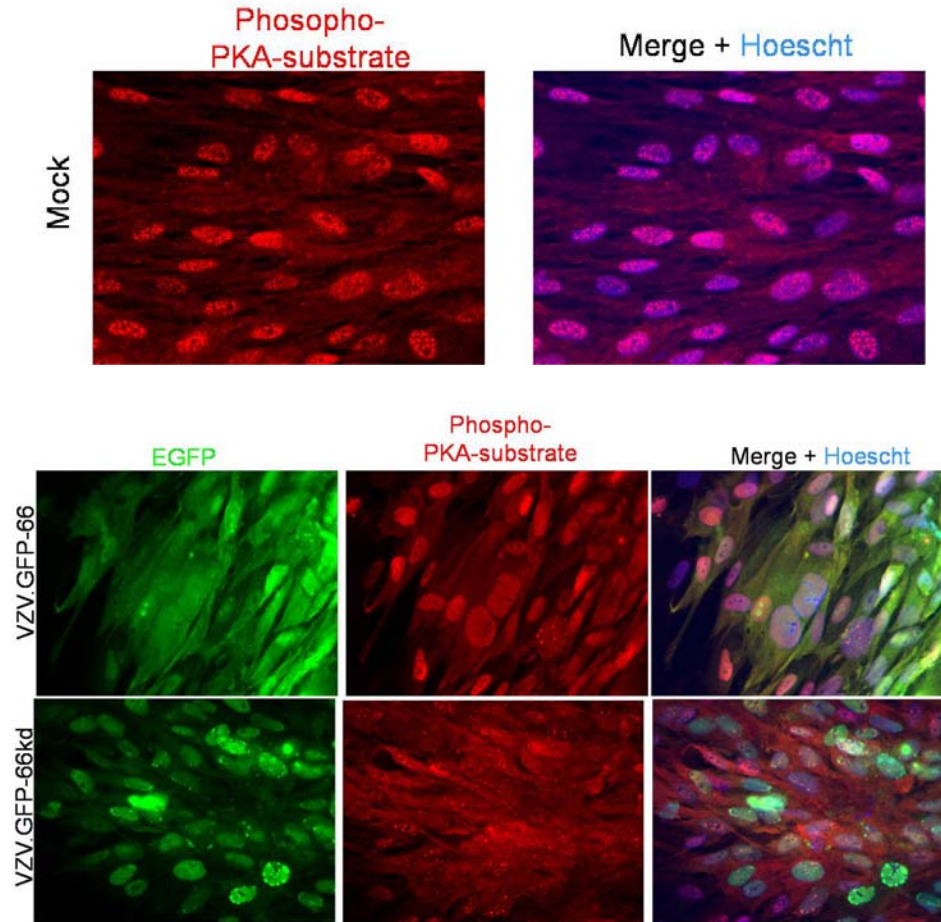


Figure 4-4. VZV ORF66 kinase activity induces greater phosphorylation of nuclear PKA-substrate proteins.

MRC-5 cells were infected with VZV.GFP-66 or VZV.GFP-66kd and fixed 2days p.i. with 4% paraformaldehyde. Cells were then immunostained with rabbit anti-p-PKA-substrate antibody and visualized using Alexa Fluor 546 anti-rabbit and fluorescence microscopy. ORF66 or ORF66kd expression is visualized by GFP fluorescence (green) and nuclei are stained with Hoechst dye (blue)

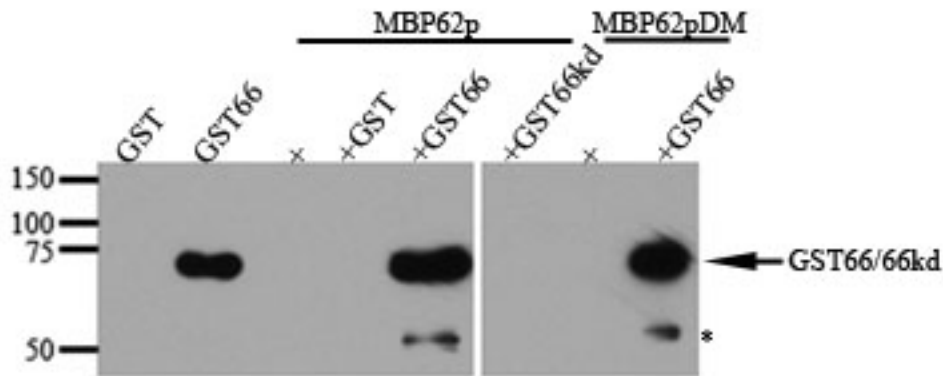


Figure 4-5. GST66 is detected by PKA-substrate antibody.

Purified GST, GST66 or GST66kd were subjected to an *in vitro* kinase assay alone or incubated with MBP62p or MBP62pDM (62p double mutant-S686A, S722A). SDS-PAGE separated proteins were transferred to PVDF membranes and probed with rabbit- α -PKA-substrate and visualized by autoradiography for antibody detected proteins. The star denotes MBP62 or 62-DM peptide.

Lastly, this work has uncovered the nuclear matrix protein, matrin 3, as a novel ORF66 cellular protein phosphorylation target. This is a first report of any virus targeting this component of the nuclear matrix, and reveals a common target for the alphaherpesvirus US3 kinases. The latter point is highly indicative that targeting of this protein is important at a point in the alphaherpesvirus life cycle. Moreover, this work strongly suggests that this induced matrin 3 phosphorylation is involved in regulation of matrin 3 subnuclear localization in VZV-infected cells, or matrin 3 nuclear retainment late into infection in HSV-1 and PRV-infected cells. Although ORF66 and US3 kinase functions are not essential for viral replication in most cell culture, our studies with corneal fibroblasts, and studies in SCID-hu xenografts amongst others (56, 81, 181, 186), demonstrate that ORF66/US3 functions indeed are important for optimal viral growth when models closer to a natural host are used. Hence, future studies should be directed at understanding the role of matrin 3 in VZV infection, potentially by using matrin 3 siRNA. While data demonstrated that the matrin 3 T150 a.a. was the major ORF66/US3 specific

phosphorylation site, there was a small fraction of phosphorylation detected in HA-Matrin-T150A by the PKA-substrate antibody. This indicates that there is still potential for ORF66 at another site(s) on matrin 3 that are not detected by the PKA-substrate antibody due to sensitivity or because the site does not fit the PKA-substrate consensus site. Finding matrin 3 *in vivo* phosphorylation sites in the context of VZV infection versus infection lacking 66 kinase may unveil differential phosphorylation that may have been missed by our current analysis. Additionally, this phosphorylation may serve to increase solubility of the protein, as matrin 3 is a major nuclear matrix protein and this would likely aid in capsid egress from the nucleus. Lamin A/C is phosphorylated at multiple sites by US3 expression *in vitro* which aids in its partial solubilization, though there is only one consensus site on the protein (138). Matrin 3 has also been implicated in a nuclear complex containing p54nrb and PSF that prevent the nuclear export of nuclear hyperedited dsRNAs (45). An interesting question to be pursued is to test whether ORF66 has any functional consequences on the formation of this complex or on the retention of these hyperedited RNAs. If hyperedited dsRNAs occur in VZV infection either made accidentally or by design, ORF66 regulation of this process may serve as a means to prevent defective viral RNAs from being translated or to override a natural cellular response. These studies open up many interesting avenues of investigation for the role of ORF66 in VZV infection. Matrin 3 targeting by ORF66 may represent a large gradient of matrin 3 involvement in VZV pathogenesis, from involvement of a nuclear scaffold needed for VZV replication to potentially clinical consequences such as neuron death in chronic zoster. Overall, our studies contribute to the notion that ORF66 is critical for efficient VZV replication in a cell type dependent manner and unveils a novel ORF66 cellular protein phosphorylation target that is conserved for the alphaherpesvirus families, suggesting an added role of the kinase as a mediator of VZV DNA

replication and transcriptional activities. Discovery of novel viral and host cell targets, as well as understanding the intricacies of each of these phosphorylation events and their functional effects will shed light on the complex and remarkably diverse roles of ORF66 in VZV infection & pathogenesis.

APPENDIX

PUBLICATIONS

1. Einfeld, A.J., M.B. Yee, **A. Erazo**, A. Abendroth, and P.R. Kinchington. 2007. Downregulation of class 1 major histocompatibility complex surface expression by varicella-zoster virus involves open reading frame 66 protein kinase-dependent and -independent mechanisms. *J. Virol* **81**: 9034-49
2. **Erazo, A.**, M.B. Yee, N. Osterrieder, and P.R. Kinchington. 2008. Varicella-zoster virus open reading frame 66 protein kinase is required for efficient viral growth in primary human corneal stromal fibroblast cells. *J. Virol* 82: 7653-65
3. Cockrell S.K., M.E. Sanchez, **A. Erazo**, and F.L. Homa. 2009. Role of the UL25 protein in herpes simplex virus DNA encapsidation. *J. Virol.* 83: 47-57
4. Walters, M.S., **A. Erazo**, P.R. Kinchington, and S. Silverstein. 2009. Histone deacetylases 1 and 2 are phosphorylated at novel sites during varicella-zoster virus infection. *J. Virol.* 83: 11502-13
5. **Erazo, A.** and P.R. Kinchington. 2010. Varicella-Zoster Virus open reading frame 66 protein kinase and its relationship to alphaherpesvirus US3 kinases. *Curr Top Microbiol Immunol. In Press.*
6. **Erazo, A.**, M.B. Yee, and P.R. Kinchington. 2010. The alphaherpesvirus ORF66/US3 kinases direct specific phosphorylation of the nuclear matrix protein, matrin 3. *In Preparation.*

REFERENCES

1. **Abendroth, A., I. Lin, B. Slobedman, H. Ploegh, and A. M. Arvin.** 2001. Varicella-zoster virus retains major histocompatibility complex class I proteins in the Golgi compartment of infected cells. *J Virol* **75**:4878-88.
2. **Ambagala, A. P., and J. I. Cohen.** 2007. Varicella-Zoster virus IE63, a major viral latency protein, is required to inhibit the alpha interferon-induced antiviral response. *J Virol* **81**:7844-51.
3. **Anachkova, B., V. Djeliova, and G. Russev.** 2005. Nuclear matrix support of DNA replication. *J Cell Biochem* **96**:951-61.
4. **Arvin, A. M.** 2001. Varicella-zoster virus: molecular virology and virus-host interactions. *Curr Opin Microbiol* **4**:442-9.
5. **Aubert, M., and J. A. Blaho.** 2001. Modulation of apoptosis during herpes simplex virus infection in human cells. *Microbes Infect* **3**:859-66.
6. **Bechtel, J. T., R. C. Winant, and D. Ganem.** 2005. Host and viral proteins in the virion of Kaposi's sarcoma-associated herpesvirus. *J Virol* **79**:4952-64.
7. **Belgrader, P., R. Dey, and R. Berezney.** 1991. Molecular cloning of matrin 3. A 125-kilodalton protein of the nuclear matrix contains an extensive acidic domain. *J Biol Chem* **266**:9893-9.
8. **Ben-Porat, T., R. A. Veach, M. L. Blankenship, and A. S. Kaplan.** 1984. Differential association with cellular substructures of pseudorabies virus DNA during early and late phases of replication. *Virology* **139**:205-22.
9. **Benetti, L., and B. Roizman.** 2004. Herpes simplex virus protein kinase US3 activates and functionally overlaps protein kinase A to block apoptosis. *Proc Natl Acad Sci U S A* **101**:9411-6.
10. **Benetti, L., and B. Roizman.** 2007. In transduced cells, the US3 protein kinase of herpes simplex virus 1 precludes activation and induction of apoptosis by transfected procaspase 3. *J Virol* **81**:10242-8.
11. **Berezney, R., and D. S. Coffey.** 1975. Nuclear protein matrix: association with newly synthesized DNA. *Science* **189**:291-3.
12. **Berezney, R., K. S. Malyavantham, A. Pliss, S. Bhattacharya, and R. Acharya.** 2005. Spatio-temporal dynamics of genomic organization and function in the mammalian cell nucleus. *Adv Enzyme Regul* **45**:17-26.
13. **Bernert, G., M. Fountoulakis, and G. Lubec.** 2002. Manifold decreased protein levels of matrin 3, reduced motor protein HMP and hIark in fetal Down's syndrome brain. *Proteomics* **2**:1752-7.

14. **Besser, J., M. Ikoma, K. Fabel, M. H. Sommer, L. Zerboni, C. Grose, and A. M. Arvin.** 2004. Differential requirement for cell fusion and virion formation in the pathogenesis of varicella-zoster virus infection in skin and T cells. *J Virol* **78**:13293-305.
15. **Besser, J., M. H. Sommer, L. Zerboni, C. P. Bagowski, H. Ito, J. Moffat, C. C. Ku, and A. M. Arvin.** 2003. Differentiation of varicella-zoster virus ORF47 protein kinase and IE62 protein binding domains and their contributions to replication in human skin xenografts in the SCID-hu mouse. *J Virol* **77**:5964-74.
16. **Bibor-Hardy, V., A. Dagenais, and R. Simard.** 1985. In situ localization of the major capsid protein during lytic infection by herpes simplex virus. *J Gen Virol* **66 (Pt 4)**:897-901.
17. **Bibor-Hardy, V., M. Pouchet, E. St-Pierre, M. Herzberg, and R. Simard.** 1982. The nuclear matrix is involved in herpes simplex virogenesis. *Virology* **121**:296-306.
18. **Bontems, S., E. Di Valentin, L. Baudoux, B. Rentier, C. Sadzot-Delvaux, and J. Piette.** 2002. Phosphorylation of varicella-zoster virus IE63 protein by casein kinases influences its cellular localization and gene regulation activity. *J Biol Chem* **277**:21050-60.
19. **Calle, A., I. Ugrinova, A. L. Epstein, P. Bouvet, J. J. Diaz, and A. Greco.** 2008. Nucleolin is required for an efficient herpes simplex virus type 1 infection. *J Virol* **82**:4762-73.
20. **Calton, C. M., J. A. Randall, M. W. Adkins, and B. W. Banfield.** 2004. The pseudorabies virus serine/threonine kinase Us3 contains mitochondrial, nuclear and membrane localization signals. *Virus Genes* **29**:131-45.
21. **Cartier, A., E. Broberg, T. Komai, M. Henriksson, and M. G. Masucci.** 2003. The herpes simplex virus-1 Us3 protein kinase blocks CD8T cell lysis by preventing the cleavage of Bid by granzyme B. *Cell Death Differ* **10**:1320-8.
22. **Cartier, A., T. Komai, and M. G. Masucci.** 2003. The Us3 protein kinase of herpes simplex virus 1 blocks apoptosis and induces phosphorylation of the Bcl-2 family member Bad. *Exp Cell Res* **291**:242-50.
23. **Chang, Y. E., and B. Roizman.** 1993. The product of the UL31 gene of herpes simplex virus 1 is a nuclear phosphoprotein which partitions with the nuclear matrix. *J Virol* **67**:6348-56.
24. **Che, X., L. Zerboni, M. H. Sommer, and A. M. Arvin.** 2006. Varicella-zoster virus open reading frame 10 is a virulence determinant in skin cells but not in T cells in vivo. *J Virol* **80**:3238-48.
25. **Chen, J. J., Z. Zhu, A. A. Gershon, and M. D. Gershon.** 2004. Mannose 6-phosphate receptor dependence of varicella zoster virus infection in vitro and in the epidermis during varicella and zoster. *Cell* **119**:915-26.
26. **Cilloniz, C., W. Jackson, C. Grose, D. Czechowski, J. Hay, and W. T. Ruyechan.** 2007. The varicella-zoster virus (VZV) ORF9 protein interacts with the IE62 major VZV transactivator. *J Virol* **81**:761-74.
27. **Clarke, P., T. Beer, R. Cohrs, and D. H. Gilden.** 1995. Configuration of latent varicella-zoster virus DNA. *J Virol* **69**:8151-4.
28. **Cliffe, A. R., and D. M. Knipe.** 2008. Herpes simplex virus ICP0 promotes both histone removal and acetylation on viral DNA during lytic infection. *J Virol* **82**:12030-8.
29. **Cocchi, F., M. Lopez, L. Menotti, M. Aoubala, P. Dubreuil, and G. Campadelli-Fiume.** 1998. The V domain of herpesvirus Ig-like receptor (HLgR) contains a major

- functional region in herpes simplex virus-1 entry into cells and interacts physically with the viral glycoprotein D. *Proc Natl Acad Sci U S A* **95**:15700-5.
30. **Cohen, J. I., T. Krogmann, S. Bontems, C. Sadzot-Delvaux, and L. Pesnicak.** 2005. Regions of the varicella-zoster virus open reading frame 63 latency-associated protein important for replication in vitro are also critical for efficient establishment of latency. *J Virol* **79**:5069-77.
 31. **Cohen, J. I., and H. Nguyen.** 1997. Varicella-zoster virus glycoprotein I is essential for growth of virus in Vero cells. *J Virol* **71**:6913-20.
 32. **Cohen, J. I., and K. Seidel.** 1994. Varicella-zoster virus (VZV) open reading frame 10 protein, the homolog of the essential herpes simplex virus protein VP16, is dispensable for VZV replication in vitro. *J Virol* **68**:7850-8.
 33. **Cohen JI, S. S.** 2001. Varicella-Zoster Virus and Its Replication, p. 2707-2729. *In* D. M. K. a. P. M. Howley (ed.), *Fields Virology*, 4th ed. Lippincott Williams & Wilkins, Philadelphia, Pa.
 34. **Cohrs, R. J., and D. H. Gilden.** 2007. Prevalence and abundance of latently transcribed varicella-zoster virus genes in human ganglia. *J Virol* **81**:2950-6.
 35. **Cohrs, R. J., D. H. Gilden, P. R. Kinchington, E. Grinfeld, and P. G. Kennedy.** 2003. Varicella-zoster virus gene 66 transcription and translation in latently infected human Ganglia. *J Virol* **77**:6660-5.
 36. **Cohrs, R. J., M. P. Hurley, and D. H. Gilden.** 2003. Array analysis of viral gene transcription during lytic infection of cells in tissue culture with Varicella-Zoster virus. *J Virol* **77**:11718-32.
 37. **Cohrs, R. J., J. J. Laguardia, and D. Gilden.** 2005. Distribution of latent herpes simplex virus type-1 and varicella zoster virus DNA in human trigeminal Ganglia. *Virus Genes* **31**:223-7.
 38. **Cohrs, R. J., J. Randall, J. Smith, D. H. Gilden, C. Dabrowski, H. van Der Keyl, and R. Tal-Singer.** 2000. Analysis of individual human trigeminal ganglia for latent herpes simplex virus type 1 and varicella-zoster virus nucleic acids using real-time PCR. *J Virol* **74**:11464-71.
 39. **Cole, N. L., and C. Grose.** 2003. Membrane fusion mediated by herpesvirus glycoproteins: the paradigm of varicella-zoster virus. *Rev Med Virol* **13**:207-22.
 40. **Cowan, M. R., P. A. Primm, S. M. Scott, T. J. Abramo, and R. A. Wiebe.** 1994. Serious group A beta-hemolytic streptococcal infections complicating varicella. *Ann Emerg Med* **23**:818-22.
 41. **Daikoku, T., R. Kurachi, T. Tsurumi, and Y. Nishiyama.** 1994. Identification of a target protein of US3 protein kinase of herpes simplex virus type 2. *J Gen Virol* **75 (Pt 8)**:2065-8.
 42. **Daikoku, T., Y. Yamashita, T. Tsurumi, and Y. Nishiyama.** 1995. The US3 protein kinase of herpes simplex virus type 2 is associated with phosphorylation of the UL12 alkaline nuclease in vitro. *Arch Virol* **140**:1637-44.
 43. **Davison, A.** 2000. Molecular evolution of alphaherpesviruses, p. 25-50. *In* A. Arvin, Gershon,A (ed.), *Varicella-Zoster Virus Virology and Clinical Management*. University Press, Cambridge.
 44. **Davison, A. J., and J. E. Scott.** 1986. The complete DNA sequence of varicella-zoster virus. *J Gen Virol* **67 (Pt 9)**:1759-816.

45. **DeCerbo, J., and G. G. Carmichael.** 2005. Retention and repression: fates of hyperedited RNAs in the nucleus. *Curr Opin Cell Biol* **17**:302-8.
46. **Defechereux, P., S. Debrus, L. Baudoux, B. Rentier, and J. Piette.** 1997. Varicella-zoster virus open reading frame 4 encodes an immediate-early protein with posttranscriptional regulatory properties. *J Virol* **71**:7073-9.
47. **del Rio, T., C. J. DeCoste, and L. W. Enquist.** 2005. Actin is a component of the compensation mechanism in pseudorabies virus virions lacking the major tegument protein VP22. *J Virol* **79**:8614-9.
48. **Deruelle, M., K. Geenen, H. J. Nauwynck, and H. W. Favoreel.** 2007. A point mutation in the putative ATP binding site of the pseudorabies virus US3 protein kinase prevents Bad phosphorylation and cell survival following apoptosis induction. *Virus Res* **128**:65-70.
49. **Desloges, N., M. Rahaus, and M. H. Wolff.** 2008. The phosphorylation profile of protein kinase A substrates is modulated during Varicella-zoster virus infection. *Med Microbiol Immunol* **197**:353-60.
50. **Di Valentin, E., S. Bontems, L. Habran, O. Jolois, N. Markine-Goriaynoff, A. Vanderplassen, C. Sadzot-Delvaux, and J. Piette.** 2005. Varicella-zoster virus IE63 protein represses the basal transcription machinery by disorganizing the pre-initiation complex. *Biol Chem* **386**:255-67.
51. **Disney, G. H., and R. D. Everett.** 1990. A herpes simplex virus type 1 recombinant with both copies of the Vmw175 coding sequences replaced by the homologous varicella-zoster virus open reading frame. *J Gen Virol* **71 (Pt 11)**:2681-9.
52. **Eisfeld, A. J., S. E. Turse, S. A. Jackson, E. C. Lerner, and P. R. Kinchington.** 2006. Phosphorylation of the varicella-zoster virus (VZV) major transcriptional regulatory protein IE62 by the VZV open reading frame 66 protein kinase. *J Virol* **80**:1710-23.
53. **Eisfeld, A. J., M. B. Yee, A. Erazo, A. Abendroth, and P. R. Kinchington.** 2007. Downregulation of class I major histocompatibility complex surface expression by varicella-zoster virus involves open reading frame 66 protein kinase-dependent and -independent mechanisms. *J Virol* **81**:9034-49.
54. **Erazo, A., M. B. Yee, N. Osterrieder, and P. R. Kinchington.** 2008. Varicella-zoster virus open reading frame 66 protein kinase is required for efficient viral growth in primary human corneal stromal fibroblast cells. *J Virol* **82**:7653-65.
55. **Farquhar, M. J., H. J. Harris, M. Diskar, S. Jones, C. J. Mee, S. U. Nielsen, C. L. Brimacombe, S. Molina, G. L. Toms, P. Maurel, J. Howl, F. W. Herberg, S. C. van Ijzendoorn, P. Balfe, and J. A. McKeating.** 2008. Protein kinase A-dependent step(s) in hepatitis C virus entry and infectivity. *J Virol* **82**:8797-811.
56. **Favoreel, H. W., G. Van Minnebruggen, D. Adriaensen, and H. J. Nauwynck.** 2005. Cytoskeletal rearrangements and cell extensions induced by the US3 kinase of an alphaherpesvirus are associated with enhanced spread. *Proc Natl Acad Sci U S A* **102**:8990-5.
57. **Flint, S., Enquist LW, Rancaniello V, Skalka AM.** *Principles of Virology.* ASM, Washington DC.
58. **Forghani, B., R. Mahalingam, A. Vafai, J. W. Hurst, and K. W. Dupuis.** 1990. Monoclonal antibody to immediate early protein encoded by varicella-zoster virus gene 62. *Virus Res* **16**:195-210.

59. **Geenen, K., H. W. Favoreel, L. Olsen, L. W. Enquist, and H. J. Nauwynck.** 2005. The pseudorabies virus US3 protein kinase possesses anti-apoptotic activity that protects cells from apoptosis during infection and after treatment with sorbitol or staurosporine. *Virology* **331**:144-50.
60. **Gershon, A. A., D. L. Sherman, Z. Zhu, C. A. Gabel, R. T. Ambron, and M. D. Gershon.** 1994. Intracellular transport of newly synthesized varicella-zoster virus: final envelopment in the trans-Golgi network. *J Virol* **68**:6372-90.
61. **Gershon, M. D., and A. A. Gershon.** 2010. VZV Infection of Keratinocytes: Production of Cell-Free Infectious Virions In Vivo. *Curr Top Microbiol Immunol*.
62. **Gewurz, B. E., E. W. Wang, D. Tortorella, D. J. Schust, and H. L. Ploegh.** 2001. Human cytomegalovirus US2 endoplasmic reticulum-luminal domain dictates association with major histocompatibility complex class I in a locus-specific manner. *J Virol* **75**:5197-204.
63. **Gilden, D.** 2000. Postherpetic neuralgia and other neurologic complications, p. 299-316. *In* A. Arvin, Gershon, A (ed.), *Varicella-Zoster Virus Virology and Clinical Management*. University Press, Cambridge.
64. **Giordano, G., A. M. Sanchez-Perez, C. Montoliu, R. Berezney, K. Malyavantham, L. G. Costa, J. J. Calvete, and V. Felipo.** 2005. Activation of NMDA receptors induces protein kinase A-mediated phosphorylation and degradation of matrin 3. Blocking these effects prevents NMDA-induced neuronal death. *J Neurochem* **94**:808-18.
65. **Gomi, Y., H. Sunamachi, Y. Mori, K. Nagaike, M. Takahashi, and K. Yamanishi.** 2002. Comparison of the complete DNA sequences of the Oka varicella vaccine and its parental virus. *J Virol* **76**:11447-59.
66. **Greenfield, I., J. Nickerson, S. Penman, and M. Stanley.** 1991. Human papillomavirus 16 E7 protein is associated with the nuclear matrix. *Proc Natl Acad Sci U S A* **88**:11217-21.
67. **Grose, C.** 2000. Pathogenesis of primary infection, p. 123-141. *In* A. Arvin (ed.), *Varicella-Zoster Virus Virology & Clinical Management*. University Press, Cambridge.
68. **Grose, C.** 1981. Variation on a theme by Fenner: the pathogenesis of chickenpox. *Pediatrics* **68**:735-7.
69. **Haberland, M., R. L. Montgomery, and E. N. Olson.** 2009. The many roles of histone deacetylases in development and physiology: implications for disease and therapy. *Nat Rev Genet* **10**:32-42.
70. **Hambleton, S., M. D. Gershon, and A. A. Gershon.** 2004. The role of the trans-Golgi network in varicella zoster virus biology. *Cell Mol Life Sci* **61**:3047-56.
71. **Hanks, S. K., and T. Hunter.** 1995. Protein kinases 6. The eukaryotic protein kinase superfamily: kinase (catalytic) domain structure and classification. *Faseb J* **9**:576-96.
72. **Harreman, M. T., T. M. Kline, H. G. Milford, M. B. Harben, A. E. Hodel, and A. H. Corbett.** 2004. Regulation of nuclear import by phosphorylation adjacent to nuclear localization signals. *J Biol Chem* **279**:20613-21.
73. **Heineman, T. C., and J. I. Cohen.** 1995. The varicella-zoster virus (VZV) open reading frame 47 (ORF47) protein kinase is dispensable for viral replication and is not required for phosphorylation of ORF63 protein, the VZV homolog of herpes simplex virus ICP22. *J Virol* **69**:7367-70.
74. **Heineman, T. C., K. Seidel, and J. I. Cohen.** 1996. The varicella-zoster virus ORF66 protein induces kinase activity and is dispensable for viral replication. *J Virol* **70**:7312-7.

75. **Hibino, Y., T. Usui, Y. Morita, N. Hirose, M. Okazaki, N. Sugano, and K. Hiraga.** 2006. Molecular properties and intracellular localization of rat liver nuclear scaffold protein P130. *Biochim Biophys Acta* **1759**:195-207.
76. **Hill, A., P. Jugovic, I. York, G. Russ, J. Bennink, J. Yewdell, H. Ploegh, and D. Johnson.** 1995. Herpes simplex virus turns off the TAP to evade host immunity. *Nature* **375**:411-5.
77. **Hisada-Ishii, S., M. Ebihara, N. Kobayashi, and Y. Kitagawa.** 2007. Bipartite nuclear localization signal of matrin 3 is essential for vertebrate cells. *Biochem Biophys Res Commun* **354**:72-6.
78. **Honess, R. W., and B. Roizman.** 1974. Regulation of herpesvirus macromolecular synthesis. I. Cascade regulation of the synthesis of three groups of viral proteins. *J Virol* **14**:8-19.
79. **Hope-Simpson, R. E.** 1965. The Nature of Herpes Zoster: A Long-Term Study and a New Hypothesis. *Proc R Soc Med* **58**:9-20.
80. **Hu, H., and J. I. Cohen.** 2005. Varicella-zoster virus open reading frame 47 (ORF47) protein is critical for virus replication in dendritic cells and for spread to other cells. *Virology* **337**:304-11.
81. **Imai, T., K. Sagou, J. Arii, and Y. Kawaguchi.** Effects of phosphorylation of herpes simplex virus 1 envelope glycoprotein B by Us3 kinase in vivo and in vitro. *J Virol* **84**:153-62.
82. **Ito, Y., H. Kimura, S. Hara, S. Kido, T. Ozaki, Y. Nishiyama, and T. Morishima.** 2001. Investigation of varicella-zoster virus DNA in lymphocyte subpopulations by quantitative PCR assay. *Microbiol Immunol* **45**:267-9.
83. **Jackson, D. A.** 2003. The principles of nuclear structure. *Chromosome Res* **11**:387-401.
84. **Jacquemont, B., and B. Roizman.** 1975. RNA synthesis in cells infected with herpes simplex virus. X. Properties of viral symmetric transcripts and of double-stranded RNA prepared from them. *J Virol* **15**:707-13.
85. **Jans, D. A., and S. Hubner.** 1996. Regulation of protein transport to the nucleus: central role of phosphorylation. *Physiol Rev* **76**:651-85.
86. **Kato, A., J. Arii, I. Shiratori, H. Akashi, H. Arase, and Y. Kawaguchi.** 2009. Herpes simplex virus 1 protein kinase Us3 phosphorylates viral envelope glycoprotein B and regulates its expression on the cell surface. *J Virol* **83**:250-61.
87. **Kato, A., M. Tanaka, M. Yamamoto, R. Asai, T. Sata, Y. Nishiyama, and Y. Kawaguchi.** 2008. Identification of a physiological phosphorylation site of the herpes simplex virus 1-encoded protein kinase Us3 which regulates its optimal catalytic activity in vitro and influences its function in infected cells. *J Virol* **82**:6172-89.
88. **Kato, A., M. Yamamoto, T. Ohno, H. Kodaira, Y. Nishiyama, and Y. Kawaguchi.** 2005. Identification of proteins phosphorylated directly by the Us3 protein kinase encoded by herpes simplex virus 1. *J Virol* **79**:9325-31.
89. **Kato, A., M. Yamamoto, T. Ohno, M. Tanaka, T. Sata, Y. Nishiyama, and Y. Kawaguchi.** 2006. Herpes simplex virus 1-encoded protein kinase UL13 phosphorylates viral Us3 protein kinase and regulates nuclear localization of viral envelopment factors UL34 and UL31. *J Virol* **80**:1476-86.
90. **Keller, M. J., A. W. Wu, J. I. Andrews, P. W. McGonagill, E. E. Tibesar, and J. L. Meier.** 2007. Reversal of human cytomegalovirus major immediate-early

- enhancer/promoter silencing in quiescently infected cells via the cyclic AMP signaling pathway. *J Virol* **81**:6669-81.
91. **Kelly, B. J., C. Fraefel, A. L. Cunningham, and R. J. Diefenbach.** 2009. Functional roles of the tegument proteins of herpes simplex virus type 1. *Virus Res* **145**:173-86.
 92. **Kennedy, P. G., E. Grinfeld, and J. E. Bell.** 2000. Varicella-zoster virus gene expression in latently infected and explanted human ganglia. *J Virol* **74**:11893-8.
 93. **Kennedy, P. G., E. Grinfeld, and J. W. Gow.** 1998. Latent varicella-zoster virus is located predominantly in neurons in human trigeminal ganglia. *Proc Natl Acad Sci U S A* **95**:4658-62.
 94. **Kent, J. R., W. Kang, C. G. Miller, and N. W. Fraser.** 2003. Herpes simplex virus latency-associated transcript gene function. *J Neurovirol* **9**:285-90.
 95. **Kenyon, T. K., J. I. Cohen, and C. Grose.** 2002. Phosphorylation by the varicella-zoster virus ORF47 protein serine kinase determines whether endocytosed viral gE traffics to the trans-Golgi network or recycles to the cell membrane. *J Virol* **76**:10980-93.
 96. **Kinchington P.R., C. J. I.** 2000. Viral Proteins, p. 74-104. *In* G. A. Arvin A (ed.), *Varicella-Zoster Virus*. Cambridge University Press 2000, Cambridge, United Kingdom.
 97. **Kinchington, P. R., D. Bookey, and S. E. Turse.** 1995. The transcriptional regulatory proteins encoded by varicella-zoster virus open reading frames (ORFs) 4 and 63, but not ORF 61, are associated with purified virus particles. *J Virol* **69**:4274-82.
 98. **Kinchington, P. R., K. Fite, A. Seman, and S. E. Turse.** 2001. Virion association of IE62, the varicella-zoster virus (VZV) major transcriptional regulatory protein, requires expression of the VZV open reading frame 66 protein kinase. *J Virol* **75**:9106-13.
 99. **Kinchington, P. R., K. Fite, and S. E. Turse.** 2000. Nuclear accumulation of IE62, the varicella-zoster virus (VZV) major transcriptional regulatory protein, is inhibited by phosphorylation mediated by the VZV open reading frame 66 protein kinase. *J Virol* **74**:2265-77.
 100. **Kinchington, P. R., J. K. Hougland, A. M. Arvin, W. T. Ruyechan, and J. Hay.** 1992. The varicella-zoster virus immediate-early protein IE62 is a major component of virus particles. *J Virol* **66**:359-66.
 101. **Kinchington, P. R., G. Inchauspe, J. H. Subak-Sharpe, F. Robey, J. Hay, and W. T. Ruyechan.** 1988. Identification and characterization of a varicella-zoster virus DNA-binding protein by using antisera directed against a predicted synthetic oligopeptide. *J Virol* **62**:802-9.
 102. **Kinchington, P. R., and S. E. Turse.** 1998. Regulated nuclear localization of the varicella-zoster virus major regulatory protein, IE62. *J Infect Dis* **178 Suppl 1**:S16-21.
 103. **Klupp, B. G., H. Granzow, and T. C. Mettenleiter.** 2001. Effect of the pseudorabies virus US3 protein on nuclear membrane localization of the UL34 protein and virus egress from the nucleus. *J Gen Virol* **82**:2363-71.
 104. **Koppers-Lalic, D., M. C. Verweij, A. D. Lipinska, Y. Wang, E. Quinten, E. A. Reits, J. Koch, S. Loch, M. Marcondes Rezende, F. Daus, K. Bienkowska-Szewczyk, N. Osterrieder, T. C. Mettenleiter, M. H. Heemskerk, R. Tampe, J. J. Neefjes, S. I. Chowdhury, M. E. Rensing, F. A. Rijsewijk, and E. J. Wiertz.** 2008. Varicellovirus UL 49.5 proteins differentially affect the function of the transporter associated with antigen processing, TAP. *PLoS Pathog* **4**:e1000080.

105. **Koropchak, C. M., S. M. Solem, P. S. Diaz, and A. M. Arvin.** 1989. Investigation of varicella-zoster virus infection of lymphocytes by in situ hybridization. *J Virol* **63**:2392-5.
106. **Ku, C. C., J. Besser, A. Abendroth, C. Grose, and A. M. Arvin.** 2005. Varicella-Zoster virus pathogenesis and immunobiology: new concepts emerging from investigations with the SCIDhu mouse model. *J Virol* **79**:2651-8.
107. **Ku, C. C., J. A. Padilla, C. Grose, E. C. Butcher, and A. M. Arvin.** 2002. Tropism of varicella-zoster virus for human tonsillar CD4(+) T lymphocytes that express activation, memory, and skin homing markers. *J Virol* **76**:11425-33.
108. **Ku, C. C., L. Zerboni, H. Ito, B. S. Graham, M. Wallace, and A. M. Arvin.** 2004. Varicella-zoster virus transfer to skin by T Cells and modulation of viral replication by epidermal cell interferon-alpha. *J Exp Med* **200**:917-25.
109. **Leach, N., S. L. Bjerke, D. K. Christensen, J. M. Bouchard, F. Mou, R. Park, J. Baines, T. Haraguchi, and R. J. Roller.** 2007. Emerin is hyperphosphorylated and redistributed in herpes simplex virus type 1-infected cells in a manner dependent on both UL34 and US3. *J Virol* **81**:10792-803.
110. **Leader, D. P.** 1993. Viral protein kinases and protein phosphatases. *Pharmacol Ther* **59**:343-89.
111. **Leader, D. P., A. D. Deana, F. Marchiori, F. C. Purves, and L. A. Pinna.** 1991. Further definition of the substrate specificity of the alpha-herpesvirus protein kinase and comparison with protein kinases A and C. *Biochim Biophys Acta* **1091**:426-31.
112. **Leisenfelder, S. A., P. R. Kinchington, and J. F. Moffat.** 2008. Cyclin-dependent kinase 1/cyclin B1 phosphorylates varicella-zoster virus IE62 and is incorporated into virions. *J Virol* **82**:12116-25.
113. **Li, H., J. Zhang, A. Kumar, M. Zheng, S. S. Atherton, and F. S. Yu.** 2006. Herpes simplex virus 1 infection induces the expression of proinflammatory cytokines, interferons and TLR7 in human corneal epithelial cells. *Immunology* **117**:167-76.
114. **Li, P. L., T. Wang, K. A. Buckley, A. L. Chenine, S. Popov, and R. M. Ruprecht.** 2005. Phosphorylation of HIV Nef by cAMP-dependent protein kinase. *Virology* **331**:367-74.
115. **Li, Q., M. A. Ali, and J. I. Cohen.** 2006. Insulin degrading enzyme is a cellular receptor mediating varicella-zoster virus infection and cell-to-cell spread. *Cell* **127**:305-16.
116. **Liang, L., and B. Roizman.** 2008. Expression of gamma interferon-dependent genes is blocked independently by virion host shutoff RNase and by US3 protein kinase. *J Virol* **82**:4688-96.
117. **Liesegang, T. J.** 2009. Varicella zoster virus vaccines: effective, but concerns linger. *Can J Ophthalmol* **44**:379-84.
118. **Lungu, O., C. A. Panagiotidis, P. W. Annunziato, A. A. Gershon, and S. J. Silverstein.** 1998. Aberrant intracellular localization of Varicella-Zoster virus regulatory proteins during latency. *Proc Natl Acad Sci U S A* **95**:7080-5.
119. **Lynch, J. M., T. K. Kenyon, C. Grose, J. Hay, and W. T. Ruyechan.** 2002. Physical and functional interaction between the varicella zoster virus IE63 and IE62 proteins. *Virology* **302**:71-82.
120. **Mahalingam, R., M. Wellish, R. Cohrs, S. Debrus, J. Piette, B. Rentier, and D. H. Gilden.** 1996. Expression of protein encoded by varicella-zoster virus open reading

- frame 63 in latently infected human ganglionic neurons. *Proc Natl Acad Sci U S A* **93**:2122-4.
121. **Mainka, C., B. Fuss, H. Geiger, H. Hofelmayr, and M. H. Wolff.** 1998. Characterization of viremia at different stages of varicella-zoster virus infection. *J Med Virol* **56**:91-8.
 122. **Mallory, S., M. Sommer, and A. M. Arvin.** 1997. Mutational analysis of the role of glycoprotein I in varicella-zoster virus replication and its effects on glycoprotein E conformation and trafficking. *J Virol* **71**:8279-88.
 123. **Malyavantham, K. S., S. Bhattacharya, M. Barbeitos, L. Mukherjee, J. Xu, F. O. Fackelmayer, and R. Berezney.** 2008. Identifying functional neighborhoods within the cell nucleus: proximity analysis of early S-phase replicating chromatin domains to sites of transcription, RNA polymerase II, HP1gamma, matrin 3 and SAF-A. *J Cell Biochem* **105**:391-403.
 124. **Maresova, L., T. J. Pasiaka, and C. Grose.** 2001. Varicella-zoster Virus gB and gE coexpression, but not gB or gE alone, leads to abundant fusion and syncytium formation equivalent to those from gH and gL coexpression. *J Virol* **75**:9483-92.
 125. **Marin, M., H. C. Meissner, and J. F. Seward.** 2008. Varicella prevention in the United States: a review of successes and challenges. *Pediatrics* **122**:e744-51.
 126. **Martin, A., P. O'Hare, J. McLauchlan, and G. Elliott.** 2002. Herpes simplex virus tegument protein VP22 contains overlapping domains for cytoplasmic localization, microtubule interaction, and chromatin binding. *J Virol* **76**:4961-70.
 127. **McGeoch, D. J., and A. J. Davison.** 1986. Alphaherpesviruses possess a gene homologous to the protein kinase gene family of eukaryotes and retroviruses. *Nucleic Acids Res* **14**:1765-77.
 128. **McKnight, J. L., M. Doerr, and Y. Zhang.** 1994. An 85-kilodalton herpes simplex virus type 1 alpha trans-induction factor (VP16)-VP13/14 fusion protein retains the transactivation and structural properties of the wild-type molecule during virus infection. *J Virol* **68**:1750-7.
 129. **Michael, K., B. G. Klupp, T. C. Mettenleiter, and A. Karger.** 2006. Composition of pseudorabies virus particles lacking tegument protein US3, UL47, or UL49 or envelope glycoprotein E. *J Virol* **80**:1332-9.
 130. **Miles, D. H., M. D. Willcox, and S. Athmanathan.** 2004. Ocular and neuronal cell apoptosis during HSV-1 infection: a review. *Curr Eye Res* **29**:79-90.
 131. **Moffat, J., H. Ito, M. Sommer, S. Taylor, and A. M. Arvin.** 2002. Glycoprotein I of varicella-zoster virus is required for viral replication in skin and T cells. *J Virol* **76**:8468-71.
 132. **Moffat, J. F., M. D. Stein, H. Kaneshima, and A. M. Arvin.** 1995. Tropism of varicella-zoster virus for human CD4+ and CD8+ T lymphocytes and epidermal cells in SCID-hu mice. *J Virol* **69**:5236-42.
 133. **Moffat, J. F., L. Zerboni, M. H. Sommer, T. C. Heineman, J. I. Cohen, H. Kaneshima, and A. M. Arvin.** 1998. The ORF47 and ORF66 putative protein kinases of varicella-zoster virus determine tropism for human T cells and skin in the SCID-hu mouse. *Proc Natl Acad Sci U S A* **95**:11969-74.
 134. **Montgomery, R. I., M. S. Warner, B. J. Lum, and P. G. Spear.** 1996. Herpes simplex virus-1 entry into cells mediated by a novel member of the TNF/NGF receptor family. *Cell* **87**:427-36.

135. **Mori, I., and Y. Nishiyama.** 2005. Herpes simplex virus and varicella-zoster virus: why do these human alphaherpesviruses behave so differently from one another? *Rev Med Virol* **15**:393-406.
136. **Moriuchi, H., M. Moriuchi, S. E. Straus, and J. I. Cohen.** 1993. Varicella-zoster virus open reading frame 10 protein, the herpes simplex virus VP16 homolog, transactivates herpesvirus immediate-early gene promoters. *J Virol* **67**:2739-46.
137. **Morrow, G., B. Slobedman, A. L. Cunningham, and A. Abendroth.** 2003. Varicella-zoster virus productively infects mature dendritic cells and alters their immune function. *J Virol* **77**:4950-9.
138. **Mou, F., T. Forest, and J. D. Baines.** 2007. US3 of herpes simplex virus type 1 encodes a promiscuous protein kinase that phosphorylates and alters localization of lamin A/C in infected cells. *J Virol* **81**:6459-70.
139. **Mou, F., E. Wills, and J. D. Baines.** 2009. Phosphorylation of the U(L)31 protein of herpes simplex virus 1 by the U(S)3-encoded kinase regulates localization of the nuclear envelopment complex and egress of nucleocapsids. *J Virol* **83**:5181-91.
140. **Mueller, N. H., D. H. Gilden, R. J. Cohrs, R. Mahalingam, and M. A. Nagel.** 2008. Varicella zoster virus infection: clinical features, molecular pathogenesis of disease, and latency. *Neurol Clin* **26**:675-97, viii.
141. **Muller, L. J., L. Pels, and G. F. Vrensen.** 1995. Novel aspects of the ultrastructural organization of human corneal keratocytes. *Invest Ophthalmol Vis Sci* **36**:2557-67.
142. **Muller, W. E., T. Okamoto, P. Reuter, D. Ugarkovic, and H. C. Schroder.** 1990. Functional characterization of Tat protein from human immunodeficiency virus. Evidence that Tat links viral RNAs to nuclear matrix. *J Biol Chem* **265**:3803-8.
143. **Murata, T., F. Goshima, T. Daikoku, H. Takakuwa, and Y. Nishiyama.** 2000. Expression of herpes simplex virus type 2 US3 affects the Cdc42/Rac pathway and attenuates c-Jun N-terminal kinase activation. *Genes Cells* **5**:1017-27.
144. **Murata, T., F. Goshima, Y. Nishizawa, T. Daikoku, H. Takakuwa, K. Ohtsuka, T. Yoshikawa, and Y. Nishiyama.** 2002. Phosphorylation of cytokeratin 17 by herpes simplex virus type 2 US3 protein kinase. *Microbiol Immunol* **46**:707-19.
145. **Mustafa, M. B., P. G. Arduino, and S. R. Porter.** 2009. Varicella zoster virus: review of its management. *J Oral Pathol Med* **38**:673-88.
146. **Nagpal, S., and J. M. Ostrove.** 1991. Characterization of a potent varicella-zoster virus-encoded trans-repressor. *J Virol* **65**:5289-96.
147. **Nakayasu, H., and R. Berezney.** 1991. Nuclear matrins: identification of the major nuclear matrix proteins. *Proc Natl Acad Sci U S A* **88**:10312-6.
148. **Ng, T. I., L. Keenan, P. R. Kinchington, and C. Grose.** 1994. Phosphorylation of varicella-zoster virus open reading frame (ORF) 62 regulatory product by viral ORF 47-associated protein kinase. *J Virol* **68**:1350-9.
149. **Nguyen, M. L., R. M. Kraft, and J. A. Blaho.** 2007. Susceptibility of cancer cells to herpes simplex virus-dependent apoptosis. *J Gen Virol* **88**:1866-75.
150. **Nikkels, A. F., S. Debrus, C. Sadzot-Delvaux, J. Piette, B. Rentier, and G. E. Pierard.** 1995. Immunohistochemical identification of varicella-zoster virus gene 63-encoded protein (IE63) and late (gE) protein on smears and cutaneous biopsies: implications for diagnostic use. *J Med Virol* **47**:342-7.

151. **Ote, I., M. Lebrun, P. Vandevenne, S. Bontems, C. Medina-Palazon, E. Manet, J. Piette, and C. Sadzot-Delvaux.** 2009. Varicella-zoster virus IE4 protein interacts with SR proteins and exports mRNAs through the TAP/NXF1 pathway. *PLoS One* **4**:e7882.
152. **Overton, H. A., D. J. McMillan, L. S. Klavinskis, L. Hope, A. J. Ritchie, and P. Wong-kai-in.** 1992. Herpes simplex virus type 1 gene UL13 encodes a phosphoprotein that is a component of the virion. *Virology* **190**:184-92.
153. **Oxman, M. N.** 2009. Herpes zoster pathogenesis and cell-mediated immunity and immunosenescence. *J Am Osteopath Assoc* **109**:S13-7.
154. **Oxman, M. N., M. J. Levin, G. R. Johnson, K. E. Schmader, S. E. Straus, L. D. Gelb, R. D. Arbeit, M. S. Simberkoff, A. A. Gershon, L. E. Davis, A. Weinberg, K. D. Boardman, H. M. Williams, J. H. Zhang, P. N. Peduzzi, C. E. Beisel, V. A. Morrison, J. C. Guatelli, P. A. Brooks, C. A. Kauffman, C. T. Pachucki, K. M. Neuzil, R. F. Betts, P. F. Wright, M. R. Griffin, P. Brunell, N. E. Soto, A. R. Marques, S. K. Keay, R. P. Goodman, D. J. Cotton, J. W. Gnann, Jr., J. Loutit, M. Holodniy, W. A. Keitel, G. E. Crawford, S. S. Yeh, Z. Lobo, J. F. Toney, R. N. Greenberg, P. M. Keller, R. Harbecke, A. R. Hayward, M. R. Irwin, T. C. Kyriakides, C. Y. Chan, I. S. Chan, W. W. Wang, P. W. Annunziato, and J. L. Silber.** 2005. A vaccine to prevent herpes zoster and postherpetic neuralgia in older adults. *N Engl J Med* **352**:2271-84.
155. **Pavan-Langston, D.** 2000. Ophthalmic zoster, p. 276-298. *In* A. Arvin and A. Gershon (ed.), *Varicella-Zoster Virus: virology and clinical management*. Cambridge University Press, Cambridge, UK.
156. **Pavan-Langston, D.** 2000. Ophthalmic zoster, p. 276-298. *In* A. M. a. G. Arvin, A (ed.), *Varicella-Zoster Virus Virology and Clinical Management*. Cambridge University Press, Cambridge, UK.
157. **Perera, L. P., J. D. Mosca, W. T. Ruyechan, G. S. Hayward, S. E. Straus, and J. Hay.** 1993. A major transactivator of varicella-zoster virus, the immediate-early protein IE62, contains a potent N-terminal activation domain. *J Virol* **67**:4474-83.
158. **Perera, L. P., J. D. Mosca, M. Sadeghi-Zadeh, W. T. Ruyechan, and J. Hay.** 1992. The varicella-zoster virus immediate early protein, IE62, can positively regulate its cognate promoter. *Virology* **191**:346-54.
159. **Pevenstein, S. R., R. K. Williams, D. McChesney, E. K. Mont, J. E. Smialek, and S. E. Straus.** 1999. Quantitation of latent varicella-zoster virus and herpes simplex virus genomes in human trigeminal ganglia. *J Virol* **73**:10514-8.
160. **Pflum, M. K., J. K. Tong, W. S. Lane, and S. L. Schreiber.** 2001. Histone deacetylase 1 phosphorylation promotes enzymatic activity and complex formation. *J Biol Chem* **276**:47733-41.
161. **Poon, A. P., L. Benetti, and B. Roizman.** 2006. U(S)3 and U(S)3.5 protein kinases of herpes simplex virus 1 differ with respect to their functions in blocking apoptosis and in virion maturation and egress. *J Virol* **80**:3752-64.
162. **Poon, A. P., H. Gu, and B. Roizman.** 2006. ICP0 and the US3 protein kinase of herpes simplex virus 1 independently block histone deacetylation to enable gene expression. *Proc Natl Acad Sci U S A* **103**:9993-8.
163. **Poon, A. P., Y. Liang, and B. Roizman.** 2003. Herpes simplex virus 1 gene expression is accelerated by inhibitors of histone deacetylases in rabbit skin cells infected with a mutant carrying a cDNA copy of the infected-cell protein no. 0. *J Virol* **77**:12671-8.

164. **Poon, A. P., and B. Roizman.** 2005. Herpes simplex virus 1 ICP22 regulates the accumulation of a shorter mRNA and of a truncated US3 protein kinase that exhibits altered functions. *J Virol* **79**:8470-9.
165. **Poon, A. P., and B. Roizman.** 2007. Mapping of key functions of the herpes simplex virus 1 U(S)3 protein kinase: the U(S)3 protein can form functional heteromultimeric structures derived from overlapping truncated polypeptides. *J Virol* **81**:1980-9.
166. **Punda-Polic, V., W. J. O'Brien, and J. L. Taylor.** 1999. Synergistic anti-varicella-zoster virus activity of interferon-alpha 2a and acyclovir in corneal cells. *Zentralbl Bakteriol* **289**:203-10.
167. **Purves, F. C., A. D. Deana, F. Marchiori, D. P. Leader, and L. A. Pinna.** 1986. The substrate specificity of the protein kinase induced in cells infected with herpesviruses: studies with synthetic substrates [corrected] indicate structural requirements distinct from other protein kinases. *Biochim Biophys Acta* **889**:208-15.
168. **Purves, F. C., W. O. Ogle, and B. Roizman.** 1993. Processing of the herpes simplex virus regulatory protein alpha 22 mediated by the UL13 protein kinase determines the accumulation of a subset of alpha and gamma mRNAs and proteins in infected cells. *Proc Natl Acad Sci U S A* **90**:6701-5.
169. **Purves, F. C., D. Spector, and B. Roizman.** 1991. The herpes simplex virus 1 protein kinase encoded by the US3 gene mediates postranslational modification of the phosphoprotein encoded by the UL34 gene. *J Virol* **65**:5757-64.
170. **Radtke, K., K. Dohner, and B. Sodeik.** 2006. Viral interactions with the cytoskeleton: a hitchhiker's guide to the cell. *Cell Microbiol* **8**:387-400.
171. **Rahaus, M., N. Desloges, and M. H. Wolff.** 2007. Varicella-zoster virus requires a functional PI3K/Akt/GSK-3alpha/beta signaling cascade for efficient replication. *Cell Signal* **19**:312-20.
172. **Ramachandran, S., J. E. Knickelbein, C. Ferko, R. L. Hendricks, and P. R. Kinchington.** 2008. Development and pathogenic evaluation of recombinant herpes simplex virus type 1 expressing two fluorescent reporter genes from different lytic promoters. *Virology* **378**:254-64.
173. **Reddy, S. M., E. Cox, I. Iofin, W. Soong, and J. I. Cohen.** 1998. Varicella-zoster virus (VZV) ORF32 encodes a phosphoprotein that is posttranslationally modified by the VZV ORF47 protein kinase. *J Virol* **72**:8083-8.
174. **Reichelt, M., J. Brady, and A. M. Arvin.** 2009. The replication cycle of varicella-zoster virus: analysis of the kinetics of viral protein expression, genome synthesis, and virion assembly at the single-cell level. *J Virol* **83**:3904-18.
175. **Reynolds, A. E., B. J. Ryckman, J. D. Baines, Y. Zhou, L. Liang, and R. J. Roller.** 2001. U(L)31 and U(L)34 proteins of herpes simplex virus type 1 form a complex that accumulates at the nuclear rim and is required for envelopment of nucleocapsids. *J Virol* **75**:8803-17.
176. **Reynolds, A. E., E. G. Wills, R. J. Roller, B. J. Ryckman, and J. D. Baines.** 2002. Ultrastructural localization of the herpes simplex virus type 1 UL31, UL34, and US3 proteins suggests specific roles in primary envelopment and egress of nucleocapsids. *J Virol* **76**:8939-52.
177. **Ruyechan, W.** 2000. DNA Replication, p. 51-73. *In* A. Arvin, Gershon, A (ed.), *Varicella-Zoster Virus Virology and Clinical Management*. University Press, Cambridge.

178. **Ruyechan, W. T., H. Peng, M. Yang, and J. Hay.** 2003. Cellular factors and IE62 activation of VZV promoters. *J Med Virol* **70 Suppl 1**:S90-4.
179. **Ryckman, B. J., and R. J. Roller.** 2004. Herpes simplex virus type 1 primary envelopment: UL34 protein modification and the US3-UL34 catalytic relationship. *J Virol* **78**:399-412.
180. **Sadaoka, T., H. Yoshii, T. Imazawa, K. Yamanishi, and Y. Mori.** 2007. Deletion in open reading frame 49 of varicella-zoster virus reduces virus growth in human malignant melanoma cells but not in human embryonic fibroblasts. *J Virol* **81**:12654-65.
181. **Sagou, K., T. Imai, H. Sagara, M. Uema, and Y. Kawaguchi.** 2009. Regulation of the Catalytic Activity of Herpes Simplex Virus 1 Protein Kinase Us3 by Autophosphorylation and Its Role in Pathogenesis. *J Virol* **83**:5773-5783.
182. **Sanchez, V., P. C. Angeletti, J. A. Engler, and W. J. Britt.** 1998. Localization of human cytomegalovirus structural proteins to the nuclear matrix of infected human fibroblasts. *J Virol* **72**:3321-9.
183. **Sato, H., L. D. Callanan, L. Pesnicak, T. Krogmann, and J. I. Cohen.** 2002. Varicella-zoster virus (VZV) ORF17 protein induces RNA cleavage and is critical for replication of VZV at 37 degrees C but not 33 degrees C. *J Virol* **76**:11012-23.
184. **Sato, H., L. Pesnicak, and J. I. Cohen.** 2003. Varicella-zoster virus ORF47 protein kinase, which is required for replication in human T cells, and ORF66 protein kinase, which is expressed during latency, are dispensable for establishment of latency. *J Virol* **77**:11180-5.
185. **Schaap-Nutt, A., M. Sommer, X. Che, L. Zerboni, and A. M. Arvin.** 2006. ORF66 Protein Kinase Function Is Required for T-Cell Tropism of Varicella-Zoster Virus In Vivo. *J Virol* **80**:11806-16.
186. **Schaap, A., J. F. Fortin, M. Sommer, L. Zerboni, S. Stamatis, C. C. Ku, G. P. Nolan, and A. M. Arvin.** 2005. T-cell tropism and the role of ORF66 protein in pathogenesis of varicella-zoster virus infection. *J Virol* **79**:12921-33.
187. **Schirmbeck, R., and W. Deppert.** 1987. Specific interaction of simian virus 40 large T antigen with cellular chromatin and nuclear matrix during the course of infection. *J Virol* **61**:3561-9.
188. **Schumacher, D., C. McKinney, B. B. Kaufer, and N. Osterrieder.** 2008. Enzymatically inactive U(S)3 protein kinase of Marek's disease virus (MDV) is capable of depolymerizing F-actin but results in accumulation of virions in perinuclear invaginations and reduced virus growth. *Virology* **375**:37-47.
189. **Schumacher, D., B. K. Tischer, S. Trapp, and N. Osterrieder.** 2005. The protein encoded by the US3 orthologue of Marek's disease virus is required for efficient development of perinuclear virions and involved in actin stress fiber breakdown. *J Virol* **79**:3987-97.
190. **Schwer, B., and E. Verdin.** 2008. Conserved metabolic regulatory functions of sirtuins. *Cell Metab* **7**:104-12.
191. **Sedlackova, L., and S. A. Rice.** 2008. Herpes simplex virus type 1 immediate-early protein ICP27 is required for efficient incorporation of ICP0 and ICP4 into virions. *J Virol* **82**:268-77.
192. **Senderek, J., S. M. Garvey, M. Krieger, V. Guergueltcheva, A. Urtizberea, A. Roos, M. Elbracht, C. Stendel, I. Tournev, V. Mihailova, H. Feit, J. Tramonte, P. Hedera, K. Crooks, C. Bergmann, S. Rudnik-Schoneborn, K. Zerres, H. Lochmuller, E.**

- Seboun, J. Weis, J. S. Beckmann, M. A. Hauser, and C. E. Jackson.** 2009. Autosomal-dominant distal myopathy associated with a recurrent missense mutation in the gene encoding the nuclear matrix protein, matrin 3. *Am J Hum Genet* **84**:511-8.
193. **Shabb, J. B.** 2001. Physiological substrates of cAMP-dependent protein kinase. *Chem Rev* **101**:2381-411.
194. **Silva, L., A. Cliffe, L. Chang, and D. M. Knipe.** 2008. Role for A-type lamins in herpesviral DNA targeting and heterochromatin modulation. *PLoS Pathog* **4**:e1000071.
195. **Skalhegg, B. S., and K. Tasken.** 2000. Specificity in the cAMP/PKA signaling pathway. Differential expression, regulation, and subcellular localization of subunits of PKA. *Front Biosci* **5**:D678-93.
196. **Smith-Donald, B. A., and B. Roizman.** 2008. The interaction of herpes simplex virus 1 regulatory protein ICP22 with the cdc25C phosphatase is enabled in vitro by viral protein kinases US3 and UL13. *J Virol* **82**:4533-43.
197. **Smith, G. A., and L. W. Enquist.** 2002. Break ins and break outs: viral interactions with the cytoskeleton of Mammalian cells. *Annu Rev Cell Dev Biol* **18**:135-61.
198. **Smith, R. F., and T. F. Smith.** 1989. Identification of new protein kinase-related genes in three herpesviruses, herpes simplex virus, varicella-zoster virus, and Epstein-Barr virus. *J Virol* **63**:450-5.
199. **Soong, W., J. C. Schultz, A. C. Patera, M. H. Sommer, and J. I. Cohen.** 2000. Infection of human T lymphocytes with varicella-zoster virus: an analysis with viral mutants and clinical isolates. *J Virol* **74**:1864-70.
200. **Spengler, M., N. Niesen, C. Grose, W. T. Ruyechan, and J. Hay.** 2001. Interactions among structural proteins of varicella zoster virus. *Arch Virol Suppl*:71-9.
201. **Sreenath, K., L. Pavithra, S. Singh, S. Sinha, P. K. Dash, N. B. Siddappa, U. Ranga, D. Mitra, and S. Chattopadhyay.** 2010. Nuclear matrix protein SMAR1 represses HIV-1 LTR mediated transcription through chromatin remodeling. *Virology* **400**:76-85.
202. **Stevenson, D., K. L. Colman, and A. J. Davison.** 1994. Characterization of the putative protein kinases specified by varicella-zoster virus genes 47 and 66. *J Gen Virol* **75** (Pt 2):317-26.
203. **Suomalainen, M., M. Y. Nakano, K. Boucke, S. Keller, and U. F. Greber.** 2001. Adenovirus-activated PKA and p38/MAPK pathways boost microtubule-mediated nuclear targeting of virus. *EMBO J* **20**:1310-9.
204. **Tischer, B. K., B. B. Kaufer, M. Sommer, F. Wussow, A. M. Arvin, and N. Osterrieder.** 2007. A Self-Excisable Infectious Bacterial Artificial Chromosome Clone of Varicella-Zoster Virus Allows Analysis of the Essential Tegument Protein Encoded by ORF9. *J Virol* **81**:13200-13208.
205. **Tischer, B. K., J. von Einem, B. Kaufer, and N. Osterrieder.** 2006. Two-step red-mediated recombination for versatile high-efficiency markerless DNA manipulation in *Escherichia coli*. *Biotechniques* **40**:191-7.
206. **Van den Broeke, C., M. Deruelle, H. J. Nauwynck, K. E. Coller, G. A. Smith, J. Van Doorselaere, and H. W. Favoreel.** 2009. The kinase activity of pseudorabies virus US3 is required for modulation of the actin cytoskeleton. *Virology* **385**:155-60.
207. **Van den Broeke, C., M. Radu, M. Deruelle, H. Nauwynck, C. Hofmann, Z. M. Jaffer, J. Chernoff, and H. W. Favoreel.** 2009. Alphaherpesvirus US3-mediated reorganization of the actin cytoskeleton is mediated by group A p21-activated kinases. *Proc Natl Acad Sci U S A*.

208. **Van Minnebruggen, G., H. W. Favoreel, L. Jacobs, and H. J. Nauwynck.** 2003. Pseudorabies virus US3 protein kinase mediates actin stress fiber breakdown. *J Virol* **77**:9074-80.
209. **van Zijl, M., H. van der Gulden, N. de Wind, A. Gielkens, and A. Berns.** 1990. Identification of two genes in the unique short region of pseudorabies virus; comparison with herpes simplex virus and varicella-zoster virus. *J Gen Virol* **71 (Pt 8)**:1747-55.
210. **Walters, M. S., A. Erazo, P. R. Kinchington, and S. Silverstein.** 2009. Histone deacetylases 1 and 2 are phosphorylated at novel sites during varicella-zoster virus infection. *J Virol* **83**:11502-13.
211. **Wang, L., M. Sommer, J. Rajamani, and A. M. Arvin.** 2009. Regulation of the ORF61 promoter and ORF61 functions in varicella-zoster virus replication and pathogenesis. *J Virol* **83**:7560-72.
212. **Wang, Z., M. D. Gershon, O. Lungu, C. A. Panagiotidis, Z. Zhu, Y. Hao, and A. A. Gershon.** 1998. Intracellular transport of varicella-zoster glycoproteins. *J Infect Dis* **178 Suppl 1**:S7-12.
213. **Wang, Z. X., and J. W. Wu.** 2002. Autophosphorylation kinetics of protein kinases. *Biochem J* **368**:947-52.
214. **Weaver, B. A.** 2009. Herpes zoster overview: natural history and incidence. *J Am Osteopath Assoc* **109**:S2-6.
215. **Weller, T. H., and H. M. Witton.** 1958. The etiologic agents of varicella and herpes zoster; serologic studies with the viruses as propagated in vitro. *J Exp Med* **108**:869-90.
216. **Wenkel, H., C. Rummelt, V. Rummelt, G. Jahn, B. Fleckenstein, and G. O. Naumann.** 1993. Detection of varicella zoster virus DNA and viral antigen in human cornea after herpes zoster ophthalmicus. *Cornea* **12**:131-7.
217. **West-Mays, J. A., and D. J. Dwivedi.** 2006. The keratocyte: corneal stromal cell with variable repair phenotypes. *Int J Biochem Cell Biol* **38**:1625-31.
218. **White, K., H. Peng, J. Hay, and W. T. Ruyechan.** 2010. Role of the IE62 consensus binding site in transactivation by the varicella-zoster virus IE62 protein. *J Virol* **84**:3767-79.
219. **White, T. M., and D. H. Gilden.** 2003. Varicella virus-mono-nuclear cell interaction. *Adv Virus Res* **62**:1-17.
220. **Wilson, S. E.** 2000. Role of apoptosis in wound healing in the cornea. *Cornea* **19**:S7-12.
221. **Wisner, T. W., C. C. Wright, A. Kato, Y. Kawaguchi, F. Mou, J. D. Baines, R. J. Roller, and D. C. Johnson.** 2009. Herpesvirus gB-induced fusion between the virion envelope and outer nuclear membrane during virus egress is regulated by the viral US3 kinase. *J Virol* **83**:3115-26.
222. **Xia, K., D. M. Knipe, and N. A. DeLuca.** 1996. Role of protein kinase A and the serine-rich region of herpes simplex virus type 1 ICP4 in viral replication. *J Virol* **70**:1050-60.
223. **Yamada, H., T. Daikoku, Y. Yamashita, Y. M. Jiang, T. Tsurumi, and Y. Nishiyama.** 1997. The product of the US10 gene of herpes simplex virus type 1 is a capsid/tegument-associated phosphoprotein which copurifies with the nuclear matrix. *J Gen Virol* **78 (Pt 11)**:2923-31.
224. **Yamagishi, Y., T. Sadaoka, H. Yoshii, P. Somboonthum, T. Imazawa, K. Nagaike, K. Ozono, K. Yamanishi, and Y. Mori.** 2008. Varicella-zoster virus glycoprotein M homolog is glycosylated, is expressed on the viral envelope, and functions in virus cell-to-cell spread. *J Virol* **82**:795-804.

225. **Yamamoto, S., A. Eletsy, T. Szyperski, J. Hay, and W. T. Ruyechan.** 2009. Analysis of the varicella-zoster virus IE62 N-terminal acidic transactivating domain and its interaction with the human mediator complex. *J Virol* **83**:6300-5.
226. **Yamauchi, Y., K. Kiriya, H. Kimura, and Y. Nishiyama.** 2008. Herpes simplex virus induces extensive modification and dynamic relocalisation of the nuclear mitotic apparatus (NuMA) protein in interphase cells. *J Cell Sci* **121**:2087-96.
227. **Yang, M., J. Hay, and W. T. Ruyechan.** 2008. Varicella-zoster virus IE62 protein utilizes the human mediator complex in promoter activation. *J Virol* **82**:12154-63.
228. **Yang, M., H. Peng, J. Hay, and W. T. Ruyechan.** 2006. Promoter activation by the varicella-zoster virus major transactivator IE62 and the cellular transcription factor USF. *J Virol* **80**:7339-53.
229. **Zeitz, M. J., K. S. Malyavantham, B. Seifert, and R. Berezney.** 2009. Matrin 3: Chromosomal distribution and protein interactions. *J Cell Biochem*.
230. **Zerboni, L., C. C. Ku, C. D. Jones, J. L. Zehnder, and A. M. Arvin.** 2005. Varicella-zoster virus infection of human dorsal root ganglia in vivo. *Proc Natl Acad Sci U S A* **102**:6490-5.
231. **Zhang, Z., and G. G. Carmichael.** 2001. The fate of dsRNA in the nucleus: a p54(nrb)-containing complex mediates the nuclear retention of promiscuously A-to-I edited RNAs. *Cell* **106**:465-75.
232. **Zhu, Z., M. D. Gershon, R. Ambron, C. Gabel, and A. A. Gershon.** 1995. Infection of cells by varicella zoster virus: inhibition of viral entry by mannose 6-phosphate and heparin. *Proc Natl Acad Sci U S A* **92**:3546-50.